COMPOUND FLOOD EVENTS IN NORTHERN AND CENTRAL EUROPE IN THE PAST AND FUTURE

PHILIPP MAXIMILIAN HEINRICH

Dissertation
zur Erlangung des Doktorgrades
an der Fakultät für Mathematik, Informatik und Naturwissenschaften
Fachbereich Erdsystemwissenschaften
der Universität Hamburg

2024

Fachbereich Erdsystemwissenschaften
Gutachter/innen der Dissertation: Prof. Dr. Corinna Schrum
Dr. Stefan Hagemann

Datum der Disputation: 12.11.2024

The important thing is the unbreakable spirit.

— Kim Hyuk-kyu

This document was typeset using the typographical look-and-feel `classicthesis` developed by André Miede and Ivo Pletikosić. The style was inspired by Robert Bringhurst's seminal book on typography *"The Elements of Typographic Style"*. `classicthesis` is available for both LaTeX and LyX:

https://bitbucket.org/amiede/classicthesis/

ABSTRACT

Globally, coastal regions face the persistent threat of flooding, which ranks among the most common, deadly, and costly natural disasters. In low-lying coastal areas, floods can emerge from several drivers like waves, tides, storm surges, strong precipitation, and high river discharge. The simultaneous occurrence of two or more flood drivers can lead to compound flooding, which amplifies the destructive power of the floods beyond what the events could normally cause separately. Although compound flood events pose a significant threat to the coastal area and its inhabitants, they are not well researched. Very little is known about the causes of these events, their frequency, and the overall damage they can cause. While many studies on compound flood events focus on smaller local regions, there is a notable gap in research at a broader scale for northern and central Europe. Improving our understanding of these compound flood events could greatly benefit coastal protection by providing better risk assessment. The urgency of researching the development of compound flood events is heightened by global warming and the resulting impact on coastal protection infrastructure. In this thesis, I therefore investigate if there are meteorological drivers for compound flood events in northern and central Europe, how the frequency of these events changes under climate change, and how changes to discharge, storm surges, and sea level rise contribute to it.

I begin by examining the simultaneous occurrence of extreme discharge and high storm surges in the North and Baltic Sea catchments in northern and central Europe. To test for dependency between the drivers I use a Monte Carlo-based approach. This is the first time this method has been used in a continental scale study, whereas previous studies have used copulas, which introduce a considerable amount of uncertainty. I show that the west-facing coasts have historically experienced a higher number of compound flood events than expected by chance alone, suggesting the existence of a common meteorological driver favouring concurrent extremes.

Following up on these findings, I demonstrate that the vast majority of these compound flood events on the west-facing coasts of the North and Baltic Sea occur during a particular weather pattern. I present a new neural network that automatically classifies this weather pattern, which is then used as a proxy for compound flood events. The neural network achieves a higher accuracy than the two pre-existing studies on the classification of this weather pattern. By analysing several global climate models and climate scenarios, I find that the models project a higher frequency of this specific weather pattern in winter, indicating a higher likelihood of compound flood events towards the end of the current century.

Finally, I analyse the data from two global climate models in greater detail to better understand what additional factors contribute to changes in the number of compound flood events under climate change. I demonstrate that the rising sea level is the primary factor for future increases in the number of compound flood events, but that the influence of discharge changes should not be neglected.

Furthermore, I show that there will be a strong increase in compound flood events, even if global warming is kept in line with the Paris Agreement.

Overall, in this thesis I highlight the link between large-scale weather patterns and compound flood events for the North and Baltic Seas, and highlight the higher frequency of compound flood events towards the end of the current century, caused by anthropogenic climate change. The results of this thesis do not only contribute to a better scientific understanding of compound flood events in northern and central Europe, but are also important to inform decision-makers about them so that these events are taken into account when planning future coastal protection measures under climate change.

INHALTSANGABE

Weltweit sind Küstenregionen immer wieder von Hochwasserereignissen bedroht, die zu den häufigsten, tödlichsten und kostenträchtigsten Naturkatastrophen zählen. In niedrig gelegenen Küstengebieten können Hochwasser durch verschiedene Ursachen wie Wellen, Gezeiten, Sturmfluten, starke Niederschläge und hohe Flussabflüsse ausgelöst werden. Das gleichzeitige Auftreten von zwei oder mehr Hochwasserursachen kann zu einem kombinierten Hochwasserereignis führen, das die zerstörerische Kraft des Hochwassers über das hinaus verstärkt, was die Ereignisse normalerweise einzeln verursachen. Obwohl kombinierte Hochwasserereignisse eine erhebliche Bedrohung für das Küstengebiet und seine Bewohner darstellen, sind sie nicht gut erforscht. Es ist nur sehr wenig über die Ursachen dieser Ereignisse, ihre Häufigkeit, und die Gesamtschäden, die sie verursachen können, bekannt. Während sich viele Studien auf kleinere lokale Regionen konzentrieren, gibt es auf größerer Ebene eine beachtliche Forschungslücke für das nördliche und mittlere Europa. Ein besseres Verständnis dieser kombinierten Hochwasserereignisse kann dem Küstenschutz durch eine bessere Risikobewertung zugute kommen. Die Dringlichkeit der Erforschung der Entwicklung von kombinierten Hochwasserereignissen wird durch die globale Erwärmung und die daraus resultierenden Auswirkungen auf die Küstenschutzinfrastruktur noch verstärkt. In dieser Arbeit untersuche ich daher, ob es meteorologische Ursachen für kombinierte Hochwasserereignisse im nördlichen und zentralen Europa gibt, wie sich die Häufigkeit dieser Ereignisse im Zuge des Klimawandels verändert und wie Änderungen des Abflusses, der Sturmfluten sowie des Meeresspiegelanstiegs dazu beitragen.

Ich beginne mit der Untersuchung des gleichzeitigen Auftretens von extremen Abflussmengen und hohen Sturmfluten in den Einzugsgebieten der Nord- und Ostsee im nördlichen und zentralen Europa. Um die Abhängigkeit zwischen den Treibern zu testen, verwende ich einen Monte-Carlo basierten Ansatz. Dies ist das erste Mal, dass diese Methode in einer kontinentalen Studie verwendet wurde, während in früheren Studien Copulas verwendet wurden, die eine erhebliche Unsicherheit mit sich bringen. Ich zeige, dass an den westlichen Küsten in der Vergangenheit mehr kombinierte Hochwasserereignisse aufgetreten sind, als rein zufällig zu erwarten wären, was auf die Existenz eines gemeinsamen meteorologischen Auslösers hindeutet, der das gleichzeitige Auftreten von Extremen begünstigt.

Im Anschluss an diese Ergebnisse belege ich, dass die überwiegende Mehrheit dieser kombinierten Hochwasserereignisse an den Westküsten der Nord- und Ostsee während eines bestimmten Wettermusters auftritt. Ich stelle ein neues neuronales Netz vor, das dieses Wettermuster automatisch klassifiziert, welches dann als Proxy für kombinierte Hochwasserereignisse verwendet wird. Das neuronale Netz erreicht eine höhere Genauigkeit als die beiden bereits existierenden Studien zur Klassifizierung dieses Wettermusters. Durch die Analyse mehrerer globaler Klimamodelle und Klimaszenarien stelle ich fest, dass die Modelle eine höhere Häufigkeit dieses spezifischen Wettermusters im Winter vorhersagen, was auf eine

höhere Wahrscheinlichkeit von kombinierten Hochwasserereignissen zum Ende des aktuellen Jahrhunderts hinweist.

Schließlich analysiere ich die Daten zweier globaler Klimamodelle genauer, um besser zu verstehen, welche zusätzlichen Faktoren zu den Veränderungen in der Anzahl der kombinierten Hochwasserereignisse unter dem Klimawandel beitragen. Ich demonstriere, dass der Anstieg des Meeresspiegels der wichtigste Faktor für den künftigen Anstieg der Anzahl der kombinierten Hochwasserereignisse ist, dass aber auch der Einfluss von Abflussänderungen nicht vernachlässigt werden darf. Darüber hinaus verdeutliche ich, dass es zu einer starken Zunahme von Hochwasserereignissen kommen wird, selbst wenn die globale Erwärmung im Einklang mit dem Pariser Abkommen steht.

Insgesamt zeige ich in dieser Arbeit den Zusammenhang zwischen großräumigen Wettermustern und kombinierten Hochwasserereignissen für die Nord- und Ostsee auf und verdeutliche die höhere Häufigkeit kombinierter Hochwasserereignisse gegen Ende des laufenden Jahrhunderts, die durch den anthropogenen Klimawandel verursacht wird. Die Ergebnisse dieser Arbeit tragen nicht nur zu einem besseren wissenschaftlichen Verständnis von kombinierten Hochwasserereignissen im nördlichen und zentralen Europa bei, sondern sind auch wichtig, um Entscheidungsträger über sie zu informieren, damit diese Ereignisse bei der Planung zukünftiger Küstenschutzmaßnahmen unter Klimawandel berücksichtigt werden.

PUBLICATIONS RELATED TO THIS DISSERTATION

Chapter 2

Heinrich, P., Hagemann, S., Weisse, R., Schrum, C., Daewel, U., and Gaslikova, L. (2023). 'Compound flood events: analysing the joint occurrence of extreme river discharge events and storm surges in northern and central Europe.' In: *Natural Hazards and Earth System Sciences* 23.5, pp. 1967-1985. DOI: 10.5194/nhess-23-1967-2023.

Chapter 3

Heinrich, P., Hagemann, S., and Weisse, R. (2024). 'Automated Classification of Atmospheric Circulation Types for Compound Flood Risk Assessment: CMIP6 Model Analysis Utilising a Deep Learning Ensemble' Submitted to: *Theoretical and Applied Climatology*. DOI: 10.21203/rs.3.rs-4017900/v1.

The neural networks developed and presented in this chapter have been published as:

Heinrich, P. 'Convolutional Neural Meteorology Network (CNMN)'. Zenodo, 11 April 2024. DOI: 10.5281/zenodo.10959808.

Chapter 4

Heinrich, P., Hagemann, S., Weisse, R., and Gaslikova, L. (2023). 'Changes in compound flood event frequency in northern and central Europe under climate change.' In: *Frontiers in Climate* 5, p. 1227613. DOI: 10.3389/fclim.2023.1227613.

In addition to the three first-author papers, I contributed to the following publication as a co-author:

Weisse, R., Gaslikova, L., Hagemann, S., **Heinrich, P.**, Berkenbrink, C., Chen, J., Bormann, H., Kebschull, J., Ley, A., Massmann, G., Greskowiak, J., Thissen, L., Karrasch, L., Schoppe, A., Ratter, B., and Wessels, A. (2024). 'Zusammenwirken von Naturgefahren im Klimawandel ist für die Nordseeküste zunehmend eine Herausforderung' In: *Wasser und Abfall* 26.5, pp. 38-45. DOI: 10.1007/s35152-024-1854-y.

ACKNOWLEDGMENTS

First of all, I would like to thank Stefan Hagemann and Ralf Weisse for their supervision. You were always there to discuss science, listen to my concerns, and give me advice. I appreciate that you always took time for our weekly meetings and whenever else I had questions in between. I could not have asked for better mentors. This made my Ph.D. a very pleasant experience.

Furthermore, I want to thank Corinna Schrum for always keeping an eye on me and making sure that things were going in the right direction.

Additionally, I want to express my gratitude towards Beate Geyer for acting like an additional supervisor by always being available to answer my hundreds of questions. You were always very busy but still found the time to help me.

Then there are all the other members of KSR who have made my more than three years at this institute a great experience. It has been a pleasure to work with you. I would especially like to thank Alberto Elizalde for taking the time to read this dissertation and give me feedback.

I want also to thank my colleagues Hoa, Jiayue, Lucas, Mengyao, Pooja, and Veronika for their wonderful company they gave me during my time at the institute. It has been great to learn so much from you, both professionally and personally.

I would also like to thank Lisa Matzer for all her support and friendship during all this time. It was a pleasure to meet you in person during the EGU conference in 2023.

I would like to thank Lin Lin for her friendship and support over the last years. Thank you for cheering me up whenever I needed it, even when you were on the other side of the planet.

I would also like to thank Regina for the countless years of friendship. You are always in good spirits and it is always a pleasure to spend time with you.

My deepest gratitude goes to my family. It has been a very long journey from my first day at school to the end of my Ph.D. Your unwavering support has been invaluable and it has always been great to know that you have my back. I cannot thank you enough for everything you have done for me.

Last but not least, I would like to thank Laurina. There are a million things I would like to say, but to keep it short: Thank you for everything.

This research was financed with funding provided by the German Federal Ministry of Education and Research (BMBF; Förderkennzeichen 01LR2003A). Furthermore, this research is a contribution to 'Wasser an den Küsten Ostfrieslands' (WAKOS) and the PoFIV program of the Helmholtz Association.

LIST OF FIGURES

LIST OF TABLES

ACRONYMS

AR6 Sixth Assessment Report concerning climate change by the Intergovernmental Panel on Climate Change

CCLM Regional climate model COSMO-CLM

CFE Compound flood event

CMIP6 Coupled Model Intercomparison Project Phase 6

CNMN Convolutional Neural Meteorology Network

CORDEX COordinated Regional climate Downscaling Experiment

DKRZ Deutsches Klimarechenzentrum/German Climate Computing Centre

DWD Deutscher Wetterdienst/German Weather Service

ECA&D European Climate Assessment & Dataset

ECMWF European Centre for Medium-Range Weather Forecasts

ECOSMO ECOSystem Mode

ESGF Earth System Grid Federation

ESM Earth System Model

GCM Global climate model

GDP Gross domestic product

GERICS Climate Service Center Germany

GIA Glacial isostatic adjustment

GWL Großwetterlage

HD Hydrological discharge model

IPCC Intergovernmental Panel on Climate Change

IOW Isle of Wight

MPI Max Planck Institute for Meteorology

MPI-GE Grand Ensemble of the Max Planck Institute for Meteorology

NCAR National Center for Atmospheric Research

NCEP National Centers for Environmental Prediction

PET Potential evapotranspiration

POT Peaks over Threshold

ResNet Residual Neural Network

RCM Regional climate model

RCP Representative Concentration Pathway

SREX Special Report for Managing the Risks of Extreme Events and Disasters to Advance Climate Change Adaptation

SSP Shared Socioeconomic Pathway

TRIM Tidal, Residual, and Intertidal Mudflat Model

WAKOS Wasser an den Küsten Ostfrieslands/Water on the coasts of East Frisia

WMO World Meteorological Organization

CONTENTS

1 INTRODUCTION

As one of the most frequent, costly, and deadly natural disasters worldwide, floods pose a major threat to people living in coastal areas of the North and Baltic Seas. The European climate risk assessment (European Environment Agency, 2024) reported that during the past 30 years almost 5.5 million people were affected by floods in Europe, causing nearly 3000 deaths and more than € 170 billion in damages. With many major economic centres in the coastal areas of northern and central Europe, there is a lot of vital infrastructure that can be severely affected by floods, including access to drinking water, digital communication, energy, and transportation (Pant et al., 2018). Flooded roads, for example, prevent emergency services like ambulance and firefighters from accessing the area (Arrighi et al., 2019) while a power outage complicates the communication and coordination of rescue operations in the flooded areas.

In low-lying coastal areas, there are several drivers of different origins that can cause coastal flooding (Wolf, 2009). If the soil is saturated due to high volumes of precipitation it leads to the resulting excess water flowing over the land surface (pluvial). In addition, heavy rainfall or snowmelt can cause the river discharge to surpass the capacity of the river channel and flood the adjacent area (fluvial). Furthermore, additional drivers of oceanographic origin can contribute to flooding. These include astronomical tides, waves, and storm surges in which strong winds rise the sea level (Hendry, 2021). The intricate interplay of spatial and temporal dynamics between these drivers leads to a diverse range of flood events affecting the coastal areas (Couasnon, 2023).

The simultaneous occurrence of two or more of these drivers, so-called compound flood events, can cause them to amplify each other and pose a much greater threat than the individual drivers would under normal circumstances (de Ruiter et al., 2020). At present, there are only definitions for compound events in general, which can be caused by other drivers such as extreme heat and drought. However, these definitions also apply to compound flood events. One often used definition comes from the Intergovernmental Panel on Climate Change (Seneviratne et al., 2012): '(1) two or more extreme events occurring simultaneously or successively, (2) combinations of extreme events with underlying conditions that amplify the impact of the events, or (3) combinations of events that are not themselves extremes but lead to an extreme event or impact when combined. The contributing events can be of similar (clustered multiple events) or different type(s)'. A more generalised definition was proposed by Zscheischler et al. (2018) who defined them as 'the combination of multiple drivers and/or hazards that contributes to societal or environmental risk', which recent studies started to adopt. Compound events were formerly part of the umbrella term 'multi-hazard', which included all kinds of different hazards, whereas nowadays the term 'compound events' is mostly used for weather and climate related hazards (Tilloy et al., 2019).

Compound flood events are not as well understood as the individual drivers that can cause them (Hendry, 2021). Although compound flood events have been known about for many years, they are still often neglected in risk assessment, leading to an underestimation of potential risks (Kruczkiewicz et al., 2022). Most flood risk reduction strategies focus on reducing the impact of a single driver, leaving them vulnerable to compound flooding caused by the interaction of multiple drivers (Ward et al., 2020). An example of this is the compound flood event that hit Lymington in southern England in 1999. Lymington had been flooded ten years earlier in 1989, when a storm surge breached the flood defences. The water inundated the railway as well as several electricity substations (Davison et al., 1993). As a result of the flood, the city improved its coastal defences and added a tidal gate for the Lymington River. The tidal gate was opened during low tide, releasing the water from the river, while being closed during high tide to prevent the sea water from pushing inland. However, in December 1999 a heavy storm raised the coastal water levels and prevented the river drainage for an extended period (Ruocco et al., 2011). This, combined with heavy rainfall in the area, caused flooding in the river upstream (see Fig. 1.1), leading to water depth of over 1 m in parts of the town (O'Connell, 2000). As a result of this compound flood event, £3.5

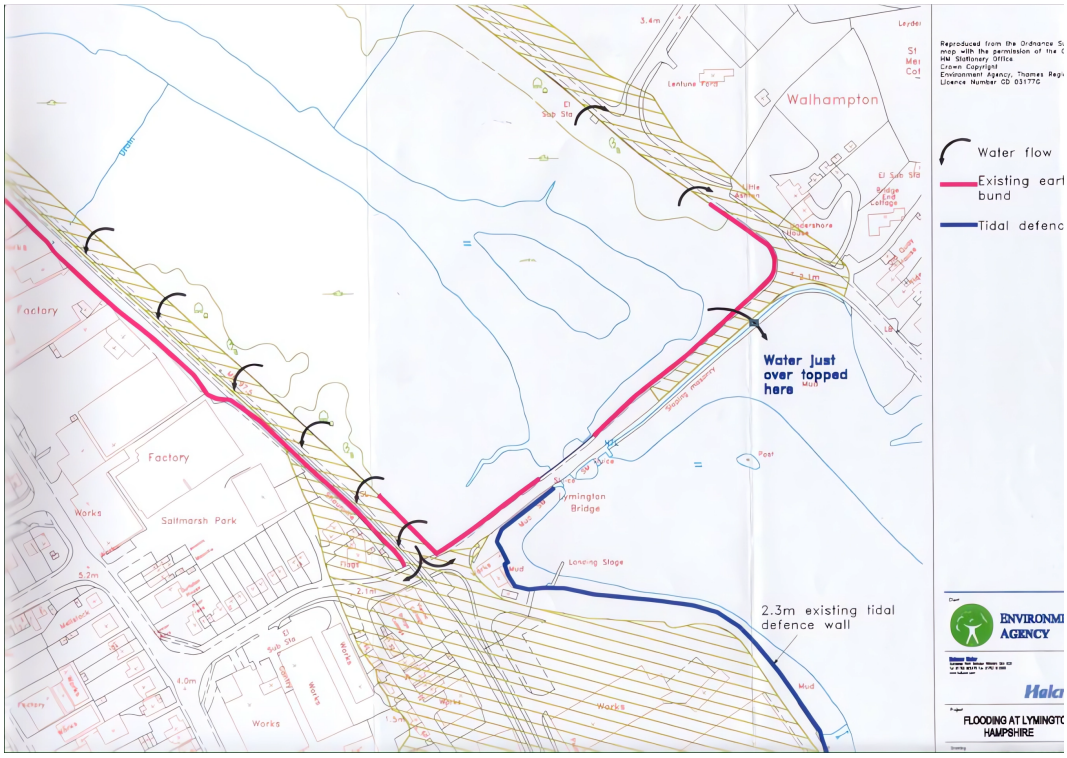

Figure 1.1: Official document by the British Environment Agency detailing the flooding of Lymington in December 1999 due to a compound event. Source: Tim Kermode, Environment Agency. The presentation containing this image can be found in Appendix A. Licence: Contains public sector information licensed under the Open Government Licence v3.0.

million were spent in 2007 to install flood gates, raise road levels, and add sheet piling between the river and the railway line to reduce the risk of future flooding

(Jolliffe, 2007). This example highlights the need of taking compound flood events into account for proper risk assessment.

Due to their importance and dangers, compound floods have attracted increasing interest from the scientific community over the past decade and have been declared a Grand Challenge by the World Climate Research Programme (Zhang et al., 2014). Studies have been conducted at a wide range of scales and locations. Couasnon et al. (2020) found hotspots for compound flood events caused by discharge and storm surge in several regions, including Vietnam, Madagascar, and Taiwan. Eilander et al. (2020) utilised a river routing model to assess the impact of storm surges on riverine flood hazard in deltas on a global scale. They found that in nearly 20% of the more than 3,000 rivers they studied, compound flood events were the dominant cause for flooding. On a smaller scale, there have been local studies such as Ai et al. (2018) for the coastal province of Jiangsu in China, Khatun et al. (2022) for the Upper Mahanadi River basin in India, and Kupfer et al. (2022) for the Breede Estuary in South Africa. In addition, there have been many studies of hurricanes and typhoons. The simultaneous occurrence of extreme winds and excessive rainfall caused by these tropical cyclones often leads to compound flood events. Examples include Cyclone Sidr in Bangladesh in 2007 (Ikeuchi et al., 2017), Hurricane Harvey in the United States in 2017 (Huang et al., 2021), and Typhoon Usagi in Vietnam in 2018 (Rodrigues do Amaral et al., 2023). The focus is often on a better understanding of the flood processes to improve forecasts as well as aiding disaster planning and mitigation efforts. These studies mostly focus on Asia and the United States, as tropical cyclones do not affect Europe.

It is nearly impossible to directly compare different studies on compound flood events, as they analyse different regions and use different data, methods, time periods, variables, and more. For example, Dykstra & Dzwonkowski (2021) used observed precipitation and discharge data from 1930-2019, while Khanal et al. (2019a) worked with modelled storm surge and discharge data for 1950-2000. Local studies in Europe have been conducted, for example, by De Bruijn et al. (2014) for the Rhine estuary in the Netherlands, Banfi & De Michele (2022) for Lake Como in Italy, and Olbert et al. (2023) for Cork City in Ireland. Furthermore, there is no established standard for what is considered 'extreme' in the first place. Some studies utilise block-maxima, such as Galiatsatou et al. (2016), where they most of the time use the annual maximum, while others, such as Ben Daoued et al. (2020), use the peak-over-threshold approach, often applying percentiles to set the threshold. The general consensus of most studies is that the co-occurrence of multiple flood drivers is crucial for a robust risk assessment due to their destructive nature and neglecting it could be fatal. Furthermore, several studies, like e.g. Bray & McCuen (2014), have reported dependencies between flood drivers, suggesting that they may occur more frequently than expected by chance alone.

Very few studies have investigated compound flood events in Europe on a continental scale. Examples include Paprotny et al. (2020), who showed that hydrodynamic models are capable of identifying real-world compound flood events, while Ganguli & Merz (2019) found contrasting patterns in the severity of compound flood events depending on the latitude of the gauge. Bevacqua et al. (2019) investigated compound flood events caused by discharge and precipitation in

Europe but focused mostly on changes under climate change and not dependencies in the present. Although Europe is included in global studies such as those conducted by Lai et al. (2021) and Ridder et al. (2020), they are often limited by their resolution and do not examine each individual region in more detail, as their domain is the entire planet.

One downside of many studies is their reliance on joint probability distribution models, so-called copulas, and tail dependence, which investigates if extremes are correlated (Hao et al., 2018). Both methods are affected by the limited availability of data, which introduces significant uncertainty (Serinaldi, 2013). Especially the usage of tail dependence has been criticised, with Serinaldi et al. (2015) calling the results 'highly questionable and should be carefully reconsidered'. These problems can be avoided by utilising, for example, a Monte Carlo-based approach, as previously done by Poschlod et al. (2020) for rain-on-snow events in Norway. This method shuffles two data sets to make them temporal independent. The resulting 'new' data sets are then examined for the number of compound extreme events. This process is repeated thousands of times to allow us to assess the likelihood of the number of compound events occurring in the original datasets also occurring in the time-independent version. This provides us with information about whether there might be a dependency between the drivers. A more detailed explanation of the method is given in Chapter 2.2.

So far, no study has investigated possible driver dependencies for Europe without the use of copulas, despite the large amount of uncertainty they introduce. If it can be shown that compound flood events in northern and central Europe occur more frequently than by pure chance, it indicates a common meteorological driver, which could then be used in further steps to deepen our understanding of compound flood events. Furthermore, it can be investigated if spatial patterns emerge which show regions that are exposed to a higher risk of compound flood events. By using the aforementioned Monte Carlo-based approach, I aim to answer the first research question:

1. **Do compound flood events in northern and central Europe occur randomly?**

The next question I will address in this dissertation is related to changes in the frequency of compound flood events under anthropogenic climate change. Climate change is probably the greatest challenge humanity has ever faced. Many countries are experiencing an increase in compound heat and drought events, while the number of extreme precipitation events is increasing at the same time (AghaKouchak et al., 2020). Climate change naturally poses a challenge to coastal protection and the marine ecosystem. Coastal zones are particularly vulnerable to sea level rise and storm activity (Wong et al., 2014). The United Nations Office for Disaster Risk Reduction (2020) reports that the number of major flood events has more than doubled in the last 20 years (2000-2020) when compared to 1980-2000. This is becoming an even more pressing issue as Europe's population living in low-lying coastal areas, i.e. near the coast and less than 10 m above sea level, is expected to increase from 50 million in 2000 to 56 million in 2060 (Neumann et al., 2015). It is therefore important to adapt coastal protection strategies, for example by raising dikes and levees or building designated flood shelters (Kreibich et al., 2015).

The increased risk to human life comes on top of the high economic costs of this hazard under anthropogenic climate change. Without additional investment in coastal adaptation, the estimated annual damage of €1.25 billion is projected to increase dramatically by the end of the current century, ranging from €93 billion up to €961 billion (Vousdoukas et al., 2018a). A recent study by Cortés Arbués et al. (2024) reported that some coastal regions could lose 10-21% of their gross domestic product (GDP) as a result of rising sea level, causing more damage and an eventual relocation of investments away from the coast further inland. Vousdoukas et al. (2020b) found that elevating dykes in an economically efficient way for a third of Europe's coastline could mitigate at least 83% of the flood damage. Despite these results, McEvoy et al. (2021) noted that some European countries are planning their coastal protection for only 20 cm of sea level rise, while others follow adaptive strategies for up to 2 m.

For future-proof coastal protection, it is essential to consider compound flood events (Leonard et al., 2014). The overall number of studies that have investigated changes in the frequency and intensity of compound flood events in Europe under climate change is limited. On a global scale, Bevacqua et al. (2020) and Ridder et al. (2022) have investigated compound flood events under climate change, but not in greater detail for Europe. On a smaller local scale, there are, for example, studies by Sayol & Marcos (2018) for the Ebro Delta (Spain), Del-Rosal-Salido et al. (2021) for the Guadalete estuary (Spain), Visser-Quinn et al. (2019) for Great Britain, and Čepienė et al. (2022) for the city of Klaipėda in Lithuania. All studies project an increase in the number of compound flood events and point out the importance of proper adaptation. Bevacqua et al. (2019) and Ganguli et al. (2020) are the only studies that have analysed changes in compound flood events on a continental scale for Europe. These studies considered different time frames, different drivers, and came to rather different conclusions. Ganguli et al. (2020) looked at changes for 2040-2069 and reported a lower risk of compound flood events in the projected scenario due to a lower dependence between storm surges and river discharge extremes, but an increase in compound flood events at ∼30% of the sites when taking sea level rise into account. Bevacqua et al. (2019), on the other hand, considered precipitation and sea level for the period of 2070-2099, where they projected a strong increase in compound flood events due to the warmer atmosphere allowing storms to carry more moisture, in addition to sea level rise.

Some studies have investigated whether there is a relationship between specific weather patterns and the occurrence of compound flood events for current climate. For example, Hendry et al. (2019) found that the compound events on the west coast of Great Britain have a different meteorological background than those on the east coast. Moreover, Ridder et al. (2018) showed that atmospheric rivers, which are associated with high near-surface winds and heavy precipitation, play an important role in compound flood events along the Dutch coast. Similarly, Camus et al. (2022) examined weather patterns that contribute to compound flood events along the North Atlantic coastlines. They found that the coastal hotspots for these compound events align with the main storm tracks along the North Atlantic Ocean.

If it is possible to establish a connection between the occurrence of compound flood events and large-scale weather patterns, they could serve as a proxy for

future changes in the frequency of these events. This would allow the analysis of global climate model ensembles without the need for an additional downscaling step, which is often required for climate change impact assessments to simulate, for example, discharge, and tide-surge. The weather patterns on the other hand can be inferred directly from the global climate model data, as a result saving time, computational resources, and manpower. One of the most widely used weather classification systems in Europe is the Großwetterlagen catalogue of Hess & Brezowsky (1969). It is based on observational data and dates back to 1881 while being updated to this day by the German Weather Service (DWD). The advantage of this classification system is that these circulation types can be associated with consistent and typical local weather conditions (Wapler & James, 2015), in contrast to arbitrary clusters of weather data. However, its application to climate model data is hampered by the fact that the classification is entirely subjective. So far, two studies have worked on an automatic objective approach. James (2007) proposed a method based on composite plots where each day is classified based on its highest correlation. With the widespread use of neural networks in the last decade, they have also become part of meteorological tasks. Convolutional neural networks are particularly effective at finding patterns in images or recognising objects. This allows them to classify weather patterns because, at a basic level, classifying weather patterns is identical to other image classification tasks, such as determining whether an image depicts an aeroplane or a dog. Convolutional neural networks are made up of different building blocks, using layers of convolutions, pooling operations, and fully connected layers (Yamashita et al., 2018). A convolutional neural network that had previously been used by Liu et al. (2016) for the detection of extreme weather was adapted by Mittermeier et al. (2022) for the classification of Großwetterlagen. Although their convolutional neural network improved the classification skills over the previous work by James (2007), it is far from perfect.

To date, there has been no analysis of changes in the frequency of Großwetterlagen for an ensemble of different global climate models. Only Mittermeier et al. (2022) analysed a single-model initial-condition large ensemble for a single climate change scenario. They found statistically significant changes in the frequency of about two thirds of the Großwetterlagen. However, it is unclear whether other climate change scenarios and global climate models show similar changes. In particular, an ensemble of global climate models and different climate change scenarios could reduce the uncertainty of the results.

With this in mind, it outlines a methodology to improve our understanding: First, establish a link between the occurrence of compound flood events in Europe and Großwetterlagen. Second, develop my own convolutional neural network with improved classification capabilities. Third, apply the convolutional neural network to several global climate models and climate change scenarios from the Coupled Model Intercomparison Project Phase 6 (CMIP6). Fourth, analyse the resulting classification for changes in frequency, which in turn could imply changes in the frequency of compound flood events. With this procedure I aim to answer the question:

2. **Are there Großwetterlagen that favour the development of compound flood events and how is their frequency changing due to climate change?**

The utilisation of Großwetterlagen as a proxy in a global climate model ensemble may be able to provide insight into future changes in the frequency of weather patterns that benefit the occurrence of compound flood events, but it cannot paint the whole picture required for coastal protection. While it may provide insight into some of the drivers, it does not take sea level rise into account as it is not related to Großwetterlagen. It is important to have a good understanding of how the different drivers contributing to compound flooding will change in the future to provide the best protection. As mentioned above, the only two studies conducted at the European scale operate at different timescales, use copulas, and come to contradictory results. This results in a glaring knowledge gap in our understanding of future changes in compound flood events in Europe. For this reason, I investigate changes to sea level rise, discharge, and storm surge levels in two regional climate models in greater detail to answer the third question:

3. **What influence will different factors have on the frequency of compound flood events in the future?**

The objective of this dissertation is to contribute to a better understanding of compound flood events in northern and central Europe for the past and future, guided by the previously posed research questions. It contains three independent scientific chapters (Chapters 2 to 4), each of which constitutes a complete publication in its own right. As a result, some brief repetitions are inevitable, but useful for readers interested only in a particular chapter. In addition, each chapter contains a short summary of its content at the beginning.

In Chapter 2, I aim to answer the first research question by investigating whether compound flood events caused by discharge and storm surges occur more frequently than by pure chance in northern and central Europe. For this, I utilise an approach based on Monte Carlo simulations. It is shown that rivers on west-facing coastlines tend to exhibit more compound flood events than expected by random chance alone. With this pointing towards a common driver, I confirm that the majority of these events are caused by the Großwetterlage Cyclonic Westerly. In addition, I demonstrate that rivers with larger catchments tend to have a lower number of compound flood events compared to smaller river catchments.

Motivated by these findings, Chapter 3 aims to improve the automatic classification of Großwetterlagen and answer the second part of the second research question. For this, I develop a neural network that outperforms previous studies. I also test several additional variables to investigate whether they improve the classification capabilities of the network. The network is then utilised to analyse changes to Cyclonic Westerly under climate change at the end of the current century for 31 different global climate models from the Coupled Model Intercomparison Project Phase 6. The results show that the number of days with Cyclonic Westerly increases during the winter half-year but decreases during the summer season. The higher frequency of Cyclonic Westerly during the main season of compound flood events indicates that the conditions for such events are more likely to be met under climate change.

To further investigate how different factors influence the frequency of compound flood events under climate change, I analyse downscaled data sets from two global climate models in Chapter 4. To answer the third research question, I then look at

the concurrent appearance of discharge and storm surges for 2070-2099 in northern and central Europe, taking sea level rise into account. The results show that there will be a massive increase in the frequency of compound flood events for the majority of locations. The primary source for this increase comes from the ongoing sea level rise, but the changes in discharge cannot be neglected.

In Chapter 5, I summarise the results of all three research questions and give final remarks on compound flood events and their future changes under anthropogenic climate change. The chapter concludes with the implications of the findings presented in this dissertation and an outlook on future research ideas.

In addition, Appendix A contains official documents related to the flooding of Lymington in 1999 for preservation purposes.

2

COMPOUND FLOOD EVENTS: ANALYSING THE JOINT OCCURRENCE OF EXTREME RIVER DISCHARGE EVENTS AND STORM SURGES IN NORTHERN AND CENTRAL EUROPE

CHAPTER SUMMARY

The simultaneous occurrence of extreme events gained more and more attention from scientific research in the last couple of years. Compared to the occurrence of single extreme events, co-occurring or compound extremes may substantially increase risks. To adequately address such risks, improving our understanding of compound flood events in Europe is necessary and requires reliable estimates of their probability of occurrence together with potential future changes. In this study compound flood events in northern and central Europe were studied using a Monte Carlo-based approach that avoids the use of copulas. Second, we investigate if the number of observed compound extreme events is within the expected range of two standard deviations of randomly occurring compound events. This includes variations of several parameters to test the stability of the identified patterns. Finally, we analyse if the observed compound extreme events had a common large-scale meteorological driver. The results of our investigation show that rivers along the west-facing coasts of Europe experienced a higher amount of compound flood events than expected by pure chance. In these regions, the vast majority of the observed compound flood events seem to be related to the Großwetterlage Cyclonic Westerly.

2.1 INTRODUCTION

Coastal flooding is one of the most frequent, expensive, and fatal natural disasters. In the US alone, it dealt $199 billion in flood damages from 1988 to 2017 according to Davenport et al. (2021). For Europe, Vousdoukas et al. (2018a) projected an increase in annual costs caused by coastal floods of up to $1 trillion in 2100 for Representative Concentration Pathway 8.5 (RCP8.5). Furthermore, more than 600 million people live in coastal areas that are less than 10 m above sea level and less than 100 kilometres from the shore (McGranahan et al., 2007). Drivers for floods are storm surges, waves, tides, precipitation, and high river discharge (Paprotny et al., 2020). The area of the river in which two or more of these drivers influence the water level are called transition zones (Bilskie & Hagen, 2018). Additionally, floods can also be the result of failures of critical infrastructure like hydropower dams or flood defences (ECHO, 2021).

The IPCC special report on *Managing the Risks of Extreme Events and Disasters to Advance Climate Change Adaptation* (SREX) defined compound events as '(1) two or more extreme events occurring simultaneously or successively, (2) combinations of extreme events with underlying conditions that amplify the impact of the events,

or (3) combinations of events that are not themselves extremes but lead to an extreme event or impact when combined. The contributing events can be of similar (clustered multiple events) or different type(s)' (Seneviratne et al., 2012). A more general definition was proposed by Leonard et al. (2014), who defined it as 'an extreme impact that depends on multiple statistically dependent variables or events'. This study focuses on compound flood events that occur when large runoff from, for example, heavy precipitation, leading to extreme river discharge, is combined with high sea level (storm surge). Because it is not possible to take local properties like topography into account, we will denote these 'potential compound flood events' as 'compound flood events' in the following text for the sake of readability.

The occurrence of extreme discharge and storm surge events either simultaneously or in close succession can lead to severe damage, which greatly exceeds the damage those events would cause separately (de Ruiter et al., 2020; Xu et al., 2022). Several studies conducted over previous years have shown the importance and catastrophic nature of compound flood events for various locations. One example is the flooding of Jacksonville (Florida) where the surge caused by the strong winds of Hurricane Irma stalled the fluvial discharge (Juarez et al., 2022). Considering data from 1901-2014 and gauges from northwestern Europe Ganguli & Merz (2019) found opposing trends in the magnitude of compound flood events depending on the latitude of the gauge. They reported increases at midlatitudes (47° N to 60° N) and decreases for gauges at high latitude (>60° N). Svensson & Jones (2002) analysed the dependence of high sea surge, river flow, and precipitation in the UK. They found a higher number of compound flood events on the western coast than on the eastern coast, while Paprotny et al. (2020) demonstrated that hydrodynamic models are capable of identifying real-world compound flood events in northwestern Europe. Many studies found that the assumption of independence between drivers leads to an underestimation of the occurrence rate of compound events.

In addition to the large-scale studies mentioned above, a large number of studies exist that focus on smaller regions. Examples are the studies of van den Hurk et al. (2015) and Santos et al. (2021b), which both analysed a near flood event in the Netherlands in January 2012, which was caused by a combination of extreme weather conditions. Additionally, there have been studies modelling compound flood events in rivers on a local scale such as for the Zengwen River basin in Taiwan by Chen & Liu (2014), the Shoalhaven River in Australia by Kumbier et al. (2018), and the Min River in China by Lian et al. (2013).

A direct comparison between different studies is hampered by the use of different approaches, data, analysis periods, and other factors. There are currently no established standards for detecting extreme events. For example, the thresholds for extreme events were calculated by utilising the return period (Bevacqua et al., 2019), utilising a certain number of events per year (Ganguli et al., 2020; Hendry et al., 2019), or utilising a percentile approach (Paprotny et al., 2018b). Other studies chose block maxima to detect extreme events (Engeland et al., 2004). The exact parameters are chosen nearly arbitrarily by the authors, with the only common goal being a low number of events so that they can be declared as 'extreme'. Nonetheless, there have been some studies that investigated the sensitivity of their results. Zheng et al. (2014) compared three classes of statistical methods and found

that the point process method overestimated the dependence of extremes while the conditional method underestimated it. In a similar vein, Jane et al. (2022) assessed that their estimates of the potential for compound events were highly sensitive to the statistical model setup. Basically, all studies found a correlation between drivers to a certain extent.

The influence of climate change on the frequency of compound flood events in Europe has been investigated by different studies. The increasing sea level due to climate change and higher occurrence of strong precipitation pose an increasing threat to important economic centres around the world and the people living there (De Sherbinin et al., 2007). Feyen et al. (2020) projected that in the event of a high-emissions scenario, the damages caused by floods would represent a considerable proportion of some countries' national gross domestic product (GDP) at the end of the century. Studies that investigated the effect of climate change on compound flood events focused on various regions of interest, for example, Bevacqua et al. (2019) on all of Europe, Poschlod et al. (2020) on Norway, Bermúdez et al. (2021) on the rivers Mandeo and Mendo in Spain, and Ganguli et al. (2020) on northwestern Europe. Bevacqua et al. (2019, 2020) reported a strong increase in the occurrence rate of compound flooding events for the future, especially for northern Europe, mainly due to the stronger precipitation as the result of a warmer atmosphere carrying more moisture. Contrarily, Ganguli et al. (2020) reported a lower risk of compound flooding due to a lower dependence between surges and river discharge peaks.

Many studies utilised multivariate extreme value theory and copulas to describe the data distribution of two or more time series and investigate the dependence between extreme events (Hao et al., 2018). In climate research, the amount of available data points is often very small, with many studies operating at merely 30 extreme events. This can cause large uncertainties when trying to evaluate the tail dependence of the distribution (Joe, 2014; Serinaldi, 2013). An alternative approach is based on Monte Carlo simulations where the dependence between joint extremes is studied by randomly rearranging one of the time series. Given our small sample size, in the following we used such an approach to avoid the uncertainties associated with the use of copulas in small samples.

In the present study, we analyse compound flood events by focusing on the question of whether they occur more often than by pure coincidence. Utilising several available large-scale data sets allowed us to conduct this analysis for northern and central Europe, instead of focusing on a single river. Furthermore, we wanted to investigate if spatial patterns occur and if they are caused by one common meteorological driver. To achieve this, we implemented a simple statistical method that avoids the application of copulas. For this, we randomised our data sets in a bootstrap process and investigated the number of compound extreme events in them, which resulted in a probability distribution in case of independence. Rivers with a number of observed compound extreme events outside of the 95.4% confidence interval of two standard deviations might have a common large-scale driver. Similar studies have so far only been carried out by van den Hurk et al. (2015) for the Lauwersmeer in the Netherlands and by Poschlod et al. (2020) for Norway (in this case covering rain-on-snow events). To our knowledge, this will be the first

recent publication investigating compound flooding in northern Europe without the use of copulas. For this, we utilised discharge and sea level data sets that were simulated based on reanalysis and hindcast data. Moreover, we investigated the robustness of the spatial patterns in our results by modifying various parameters of our method, like the thresholds for determining extreme events. Additionally, we investigated potential correlations between a river's catchment size and the number of compound flood events that occur. Finally, we examined possible drivers that could cause the occurrence of compound flood events.

2.2 METHODS

The first step in determining extreme events is to define which events are considered to be extreme. There are ways to use automatic threshold approaches for detecting extreme events, like goodness-of-fit p-value (Solari et al., 2017) or the characteristics of extrapolated significant wave heights (Liang et al., 2019), but they struggle due to the diverse characteristics in the time series of drivers that cause coastal floods (Camus et al., 2021). River-specific thresholds are only feasible for case studies that can take the local properties, like flood protection or elevation of the surrounding area, into account. Therefore a more general approach is needed that is applicable to all rivers. As described in Chapter 2.1, there is so far no standardised method that is generally used. Quite the contrary, every study uses its own modus operandi, each having individual reasoning for their choice.

One option is utilising block maxima for extreme event detection (Gumbel, 1958), which provides a well-spaced distribution of extreme events, e.g. one event per year, meaning one annual maximum event. However, it can miss out on events with high values, in case several events happen in the same year (Santos et al., 2021a), while also labelling lower values as extreme in years without any major events.

We, therefore, chose the peaks-over-threshold (Pickands III, 1975) method to select extreme events by using percentiles, like in the works of Ridder et al. (2018), Ward et al. (2018), Fang et al. (2021), Lai et al. (2021), and Brunner & Slater (2022). While using the peaks-over-threshold method, it is important to ensure the independence of the events. It has to be prevented that, for example, a single day that slightly drops under the thresholds creates two separate events (Harley, 2017). A critical element in the analysis is the definition of a de-clustering window such that subsequent events can be considered independent. A frequently used window size is based, for example, on the typical duration of storms in the area (e.g. Camus et al. (2021) and Harley (2017)). Here, we chose a de-clustering time of three days as used in other studies spanning larger domains (e.g., Bevacqua et al. (2019), Haigh et al. (2016) and Ward et al. (2018)).

Extreme events should be rare by definition, regardless of the river size, therefore only occurring scarcely throughout the year. This especially prevents the accidental analysis of events that are normally not considered extreme. On the other hand, the choice of our threshold needed to take the limited data availability into account. Hence, we were forced to choose our thresholds low enough to ensure that enough points were available for robust statistical analysis. The number of extreme discharge events can vary strongly depending on the river itself. Large rivers like the

Elbe show the tendency of having very long extreme events that can last for several weeks, therefore resulting in a lower number of independent extreme events for a specified quantile threshold. Smaller rivers, however, have usually rather short extreme events, and consequently a larger number of independent extremes for the same quantile threshold. While this specific approach might result in nominally different numbers of extreme events for each river, it ensures that for each river the same amount of data points exceed the threshold. Sea level also exhibits variations in event duration, albeit to a lesser extent. For the discharge of rivers we chose the 90^{th} percentile Q_{90} and for the sea level the 99^{th} percentile S_{99}.

To test the influence of the extreme event definition on possible patterns, we additionally implemented an automatic threshold tuning that modifies the percentiles and the subsequent thresholds in such a way that they result in an average of two extreme events per year. This was done to test in Chapter 2.4.2 if our results remain stable under much stricter definitions of extreme events. Moreover, the threshold tuning results in an average return period of 0.5 years for extreme discharge and sea level events since the return period can be defined as

$$RP = \frac{L}{E} \tag{2.1}$$

where RP denotes the return period, L the duration of the data set in years, and E the number of extreme events.

Another factor we had to take into account is the so-called *lag*, which characterises the temporal delay between variables reacting to the same meteorological event. Such lag can occur for example, if a storm approaches a coast it generates increased sea level due to stronger winds, before travelling inland where it causes higher amounts of discharge due to precipitation. Most studies, e.g. Hendry et al. (2019), tested a variety of ranges like $\pm$ five days, while Ganguli et al. (2020) calculated the delay based on the catchment size of the river.

There is a valid argument made by Ward et al. (2018) that the delay can put high stress on the flood protection systems if the initial flood water cannot retreat fast enough before the discharge occurs. Due to the large area of our study, it is impossible to quantify the potential consequences of ongoing floods on the coastal protection system for each river. Hence, we decided to focus on joint occurrences of extreme events without any additional lag. Despite that, we tested our results in Chapter 2.4.2 for a lag of 3 days to investigate potential influences on our results. In our case, we used the lag as a temporal search radius around the discharge extreme event rather than a shift of the time series itself.

To identify rivers that show a higher number of compound flood events than expected by pure chance, we utilised a Monte Carlo approach. Other studies in the past also utilised data permutation; see, for example, Svensson & Jones (2002), Zheng et al. (2013), and Nasr et al. (2021). Rivers with this behaviour might indicate a common large-scale driver that causes extreme discharge and sea level at the same time. For example, Hendry et al. (2019) found that the compound events on the west coast of Great Britain have a different meteorological background than those on the east coast. A randomisation method was used to disrupt possible correlations between the data sets and see how the number of compound flood events changes in the case of independent data. First, we limited the time frame

of the data sets to the late fall and entire winter season, as storm surges mostly occur in the winter season in northern Europe; see, for example, (Liu et al., 2022b). For the winter season, we used a time frame from December to February, such as also done by Robins et al. (2021). At the same time, most discharge events are also limited to the winter and early spring seasons. Neglecting this seasonality would naturally lead to false-positive dependencies since seasonal events would be spread throughout the entire year instead of being mostly limited to their own season. As a result, we would see a much lower number of compound flood events in the non-randomised data, therefore suggesting a false dependence (Couasnon et al., 2020).

Afterwards, we determined the number of compound flood events by counting the joint occurrence of extreme events in the discharge and sea level data. To deal with the differing duration of discharge events, we counted the occurrence of multiple separate sea level extreme events during the same discharge event as separate compound flood events.

After determining the number of compound flood events in the original data sets, we prepared the randomisation of the sea level data. For this, we made sure that events were not split up by grouping data points of the same event together before the shuffling process. This was done to not artificially increase the number of extreme events by separating events that consist of more than a single data point. Every data point that was not an extreme event was put into its own group as the only member. The shuffling process of the groups with NumPy (Harris et al., 2020) assigned every group a weight based on the number of data points inside each group. After the shuffling process, the groups were disbanded and formed a randomised data set based on the new order. Afterwards, we performed the declustering process again to ensure that extreme event data points in close proximity were counted as a single event. Then we calculated the number of compound flood events for the combination of discharge data and randomised sea level data. This bootstrap process was repeated 10,000 times for each river, giving a probability distribution for each of them. The resulting probability distribution was used to determine if the initially observed number of compound flood events is within the 95.4% confidence interval of two standard deviations (2σ).

To test the robustness of our results in Chapter 2.4.2, we also created an additional randomisation approach by randomly shuffling the order of the winter months throughout the sea level data. This method was easier to implement than the one used for the main analysis. For further testing, we utilised different combinations of data sets to investigate their influence on our results. Finally, we used two different time frames to see if climate change or the choice of time period have an influence on possible spatial patterns.

The domains of all catchments, regions, and seas that we mention by name for various reasons in this study can be seen in Fig. 2.1.

2.3 DATA

In order to study compound flood events, spatial and temporal consistent long time series of daily river runoff (discharge) and sea level near the coast are required.

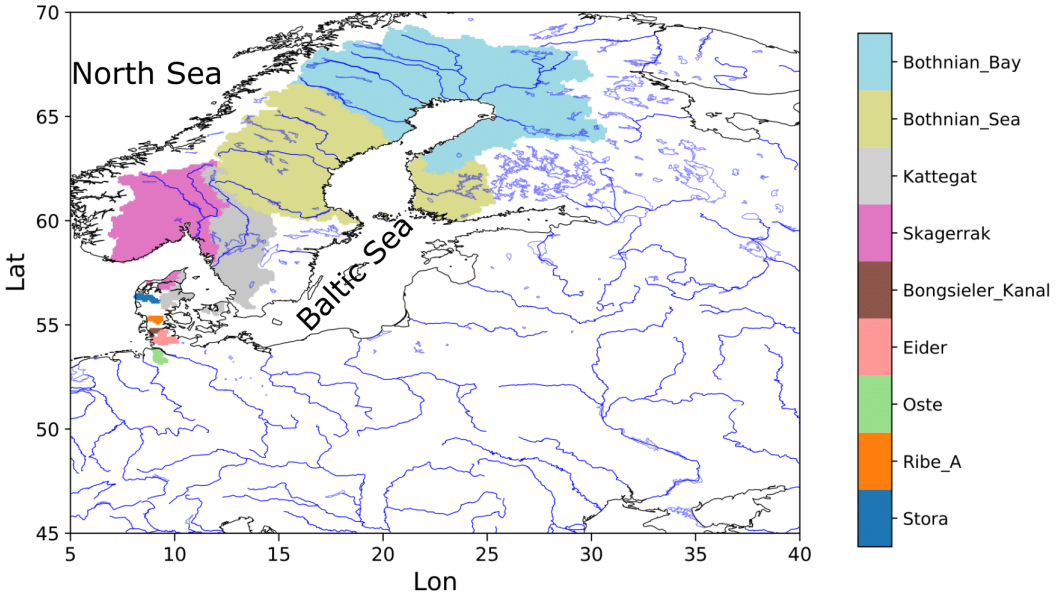

Figure 2.1: This figure contains the catchments, regions, and seas that are mentioned by name throughout the study. The first five entries in the colourbar contain maritime zones with highlighted catchment areas of rivers that discharge into them. The last five entries show the catchment area of five rivers on the German-Danish western coast.

On the one hand, observed discharges are usually not available at the respective river mouths, but they are often measured at stations further inland. In addition, periods of available daily data vary considerably between the rivers, even over the considered region that has a rather good data coverage.

Consequently, we chose several model-generated data sets that provide daily data also for sea level over a time period of at least 20 years and cover northern Europe. For our analysis, we utilised several model-based data sets which varied in forcing, regions and time frames. This was done to enable robustness tests of our analysis under a diverse set of conditions. The simulated discharges are solely caused by the atmospheric forcing and the hydrological processes over land. The influence of the sea level on discharge in the estuaries of the rivers is not considered so that this influence (e.g., Moftakhari et al. (2019)) does not cause problems in the determination of river floods. These data sets were generated by using observations and reanalysis data as forcing and they are described below. A short overview of their usage in this paper is given in Table 2.1.

2.3.1 *River Runoff*

We utilised two daily river runoff data sets that are based on consistent long-term reconstructions by the global hydrology model HydroPy (Stacke & Hagemann, 2021) and the hydrological discharge (HD) model (Hagemann et al., 2020). The river runoff was simulated at 5′ spatial resolution covering the entire European catchment region. The HD model v. 5.0 (Hagemann & Ho-Hagemann, 2021) was set up over the European domain covering the land areas between -11° W to 69° E

Data set name	Usage	Variable	Period of available data
HD5-ERA5	Main analysis Robustness against different parameter settings Robustness against different model-based data sets	discharge	1979-2018
HD5-EOBS	Time robustness Robustness against different model-based data sets	discharge	1950-2019
TRIM-REA6	Main analysis Robustness against different parameter settings Robustness against different model-based data sets	sea level	1995-2018
ECOSMO-coastDat3	Time robustness Robustness against different model-based data sets	sea level	1948-2019
ECOSMO-REA6	Robustness against different model-based data sets	sea level	1995-2015

Table 2.1: Data set names and their usage in this publication.

and 27° N to 72° N at a spatial resolution of 5′ (ca. 8-9 km). Both data sets were published as Hagemann & Stacke (2021) and utilised in Hagemann & Stacke (2023).

2.3.1.1 *HD5-ERA5*

ERA5 is the fifth generation of atmospheric reanalysis (Hersbach et al., 2020) produced by the European Centre for Medium-Range Weather Forecasts (ECMWF). It provides hourly data on many atmospheric, land-surface, and sea-state parameters at about 31 km resolution. HydroPy was driven by daily ERA5 forcing data from 1979-2018 to generate daily fields of surface and subsurface runoff at the ERA5 resolution. Here, the Penman-Monteith equation was applied to calculate a reference evapotranspiration following Allen et al. (1998). Then, surface and sub-surface runoff were interpolated to the HD model grid and used by the HD model to simulate daily discharges.

2.3.1.2 *HD5-EOBS*

The E-OBS data set (Cornes et al., 2018) comprises several daily gridded surface variables at 0.1° and 0.25° resolution over Europe covering the area 25° N-71.5° N × 25° W-45° E. The data set has been derived from station data collated by the ECA&D (European Climate Assessment & Dataset) initiative (Klein Tank et al., 2002; Klok & Klein Tank, 2009). Using E-OBS v. 22, HydroPy was driven by daily temperature and precipitation at 0.1° resolution from 1950-2019. The potential evapotranspiration (PET) was calculated following the approach proposed by Thornthwaite (1948), including an average day length at a given location. As for HD5-ERA5, the forcing data of surface and sub-surface runoff simulated by HydroPy were first interpolated to the HD model grid and then used to simulate daily discharges.

Investigations by Rivoire et al. (2021) found precipitation data from ERA5 to be of higher quality than from E-OBS. As a result, we primarily focused on HD5-ERA5 due to its higher quality compared to HD5-EOBS, as analysed in Hagemann & Stacke (2023).

2.3.2 *Sea level*

2.3.2.1 *TRIM-REA6*

COSMO-REA6 is the high-resolution regional re-analysis of the German Weather Service (DWD; Bollmeyer et al. (2015)). COSMO-REA6 data were used to force the ocean model TRIM (Tidal, Residual, and Intertidal Mudflat Model) for the period 1995-2018. The 2D version of TRIM-NP (Kapitza, 2008) is a nested hydrostatic shelf sea model with spatial resolutions increasing from 12.8 km $\times$ 12.8 km in the North Atlantic to 1.6 km $\times$ 1.6 km in the German Bight. Ten-metre-height wind components and sea level pressure were used as atmospheric forcing fields. At the lateral boundaries, the astronomical tides from the FES2004 atlas (Lyard et al., 2006) were used. We chose this data set for the main analysis of our work due to the larger region it covers.

2.3.2.2 *ECOSMO-coastDat3*

The coastDat3 data set is a regional climate reconstruction for the entire European continent, including the Baltic Sea, the North Sea, and parts of the Atlantic (Petrik & Geyer, 2021). The simulation was conducted with the regional climate model COSMO-CLM (CCLM; Rockel et al. (2008)). CoastDat3 covers the period 1948-2019 with a horizontal grid size of 0.11° in rotated coordinates, and the National Centers for Environmental Prediction-National Center for Atmospheric Research (NCEP-NCAR) global reanalysis (Kalnay et al., 1996) was used as forcing and for the application of spectral nudging (von Storch et al., 2000). CoastDat3 data were used to force the physical part of the marine ECOSystem MOdel (ECOSMO) (Daewel & Schrum, 2013; Schrum & Backhaus, 1999) for the period 1948-2019 (BSH, 2022). ECOSMO was applied at a spatial resolution of 0.033° longitude and 0.02° latitude, and its domain covers an area from 48.20333° N to 65.90333° N and 4.034667° W to 30.120333° E. The riverine freshwater inflow was taken from a Mesoscale Hydrologic Model streamflow simulation over Europe at 1/16° resolution (Rakovec & Kumar, 2022).

2.3.2.3 *ECOSMO-REA6*

For this data set, the ECOSMO model was forced with COSMO-REA6 data and covers the period from 1995-2015. The initial state was based on a simulation using coastDat2 (Geyer, 2014) forcing from 1990 to 1995. The configuration was otherwise identical to ECOSMO-coastDat3 (Chapter 2.3.2.2). While the HD model domain covers the entirety of Europe, the ocean model domains of TRIM and ECOSMO cover only parts of northern Europe. Therefore, our analysis includes a different number of rivers depending on which ocean model was used to generate the sea level data, i.e. either 181 for TRIM-based data or 126 for ECOSMO-based data.

2.3.3 *Großwetterlagen*

Großwetterlagen (GWL) are large-scale weather patterns that form over Europe. Hess & Brezowsky (1969) classified them into 29 different regimes and six circulation types. These weather regimes can persist from a few days up to several weeks in extreme cases. We used a catalogue with this classification system, which started back in 1881 and is managed by the DWD. James (2007) stated that there is a strong correlation between the Großwetterlagen and the resulting weather in various regions.

2.4 RESULTS

2.4.1 *Regional distribution of compound flood events*

Fig. 2.2 shows the distribution of compound flood events for the TRIM-REA6 and HD5-ERA5 data over northern Europe. A total of 26% of the rivers along the coasts

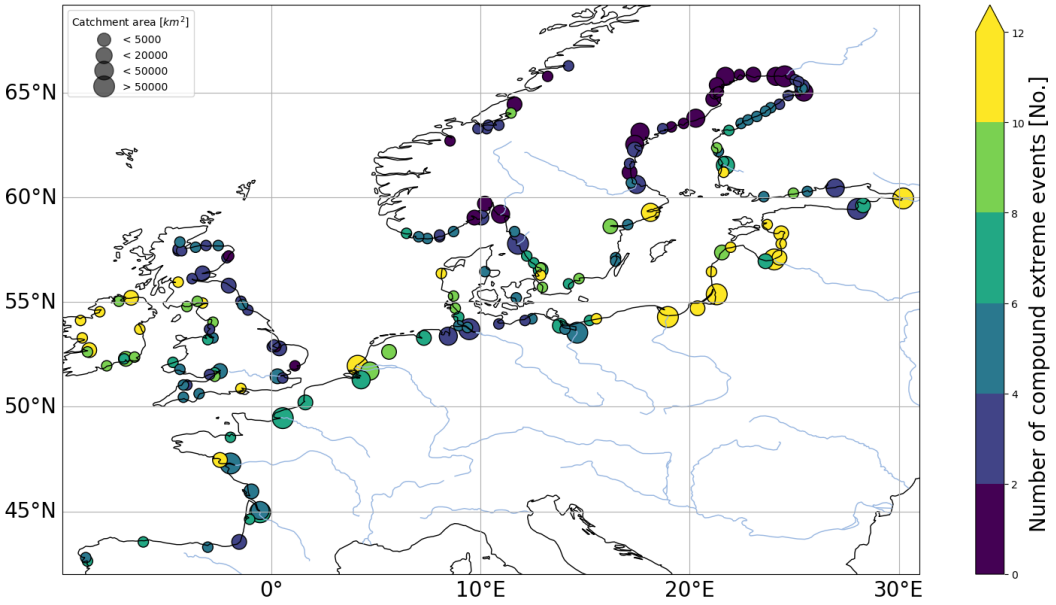

Figure 2.2: Number of compound flood events over a period of 24 years for northern Europe based on HD5-ERA5 and TRIM-REA6 data. Circle size indicates the catchment size of the corresponding river. The number of discharge and sea level extreme events was limited to two events per year on average.

had eight or more compound flood events during the time period 1995-2018. The regions with the highest number of compound flood events are Ireland and the southeastern Baltic Sea. Furthermore, the west coast of the Baltic states also shows a large amount of compound flood events. The east- and south-facing coasts of the Bothnian Bay and Bothnian Sea in the Baltic Sea, as well as Skagerrak, show the lowest frequencies of compound flood events. Similarly, the east coast of Great Britain exhibits a low number of compound flood events, in contrast to the west

coast. In general, it can be seen that west-facing coasts have a larger number of compound flood events.

Utilising our randomisation method (see Chapter 2.2) yielded Fig. 2.3, which shows if the amount of observed compound flood events for each river is within the 2σ interval produced by the randomised data sets. We see that the number of compound flood events is outside of the 2σ interval for the majority of rivers along the westward-facing coasts, while the opposite is true for the French west coast.

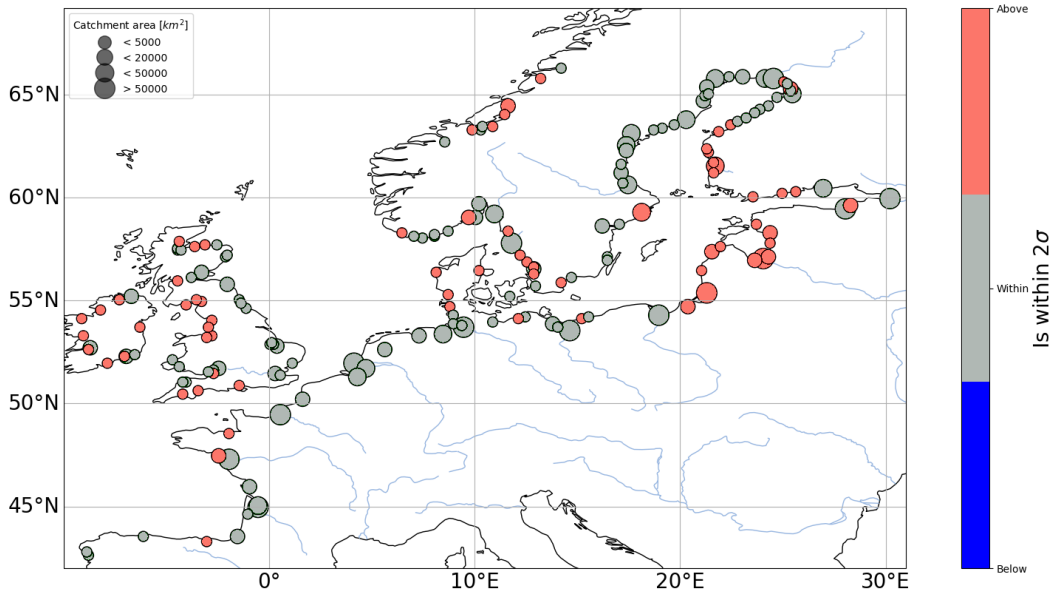

Figure 2.3: Evaluation of compound flood events for rivers in northern Europe using HD5-ERA5 and TRIM-REA6 data from 1995-2018. The colour indicates if the amount of compound flood events is within (grey), above (red) or below (blue) the expected 2σ interval. Results are obtained for the winter season with a lag of zero days (see Chapter 2.2).

2.4.2 *Robustness of the east-west pattern*

To ensure that the pattern seen in Fig. 2.3 is not the result of sampling effect, parameter, or data choice, we tested different data sets, time periods, and parameters to see whether or not the pattern remains robust. Some images for these tests are in Chapter 2.A for the sake of readability, and they are discussed in the following subsections.

2.4.2.1 *Utilisation of various data sets*

For the first robustness tests we analysed the combination of ECOSMO-REA6 with HD5-ERA5 (Fig. 2.8), ECOSMO-coastDat3 with HD5-ERA5 (Fig. 2.4a), and ECOSMO-coastDat3 with HD5-EOBS (Fig. 2.9). The overall pattern indicating that western coasts have the tendency of showing more events than expected by pure chance remains stable throughout these different data set combinations.

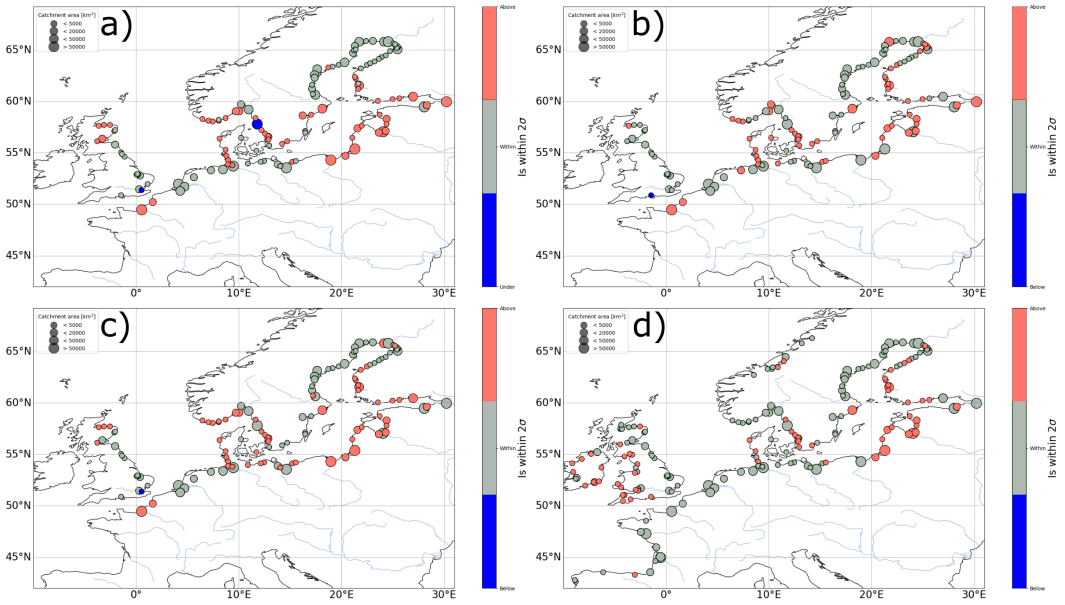

Figure 2.4: Robustness testing. As in Fig. 2.3 but with different setups. a) Utilised ECOSMO-coastDat3 and HD5-ERA5 data b) ECOSMO-coastDat3 and HD5-EOBS from 1960 to 1989 c) ECOSMO-coastDat3 and HD5-EOBS data from 1990 to 2019 d) TRIM-REA6 and HD5-ERA5 with increased lag from zero to three days.

2.4.2.2 *Validation for different time periods*

Next, we split the ECOSMO-coastDat3 and HD5-EOBS data into two 30-year periods, from 1960 to 1989 (Fig. 2.4b) and from 1990 to 2019 (Fig. 2.4c). The pattern of west-facing coasts having a higher number of compound flood events than expected by random sampling is persistent throughout different time periods, even though it is somewhat more pronounced in the more recent one.

Lastly, we added more months to the analysis by adding the month of November (Fig. 2.11) and finally expanding the time period to last from October to March of the following year (Fig. 2.12). This resulted in a slightly higher number of rivers being outside of the 2σ interval.

2.4.2.3 *Changes to parameters and randomisation*

As a first test, we changed the lag from zero to three days which is shown in Fig. 2.4d. This resulted in a slightly higher number of river catchments within the expected interval. Furthermore, we also tested the second randomisation method described in Chapter 2.2 in order to interrupt possible dependencies. For this, we randomised the order in which the years appear in our sea level data sets. The biggest difference with this simpler randomisation approach was that two additional rivers on the British east coast are below the 2σ deviation.

Additionally, we compared the influence of two different thresholding methods on the results, namely self-tuning thresholds (Fig. 2.3) and plain percentiles (Fig. 2.10), both described in Chapter 2.2. Both methods lead to nearly identical results.

2.4.3 *A common meteorological driver for compound flood events*

To see if the regions with a higher-than-expected number of compound flood events have a common large-scale meteorological driver we analysed the meteorological situation during these events. The coordinates of those regions are available in Table 2.2.

Region	Coordinates
West coast of the Baltic states	54.52–59.00° N × 20.00–24.80° E
West coast of Great Britain	50.79–55.99° N × 04.85–02.50° W
German-Danish west coast	53.81–56.46° N × 08.02–09.12° E
West-facing coast in the Bothnian Sea	61.12–62.46° N × 21.18–21.80° E
West coast of Ireland	52.48–54.72° N × 09.30–07.90° W
West-facing coast of Sweden	55.37–59.37° N × 10.90–13.20° E

Table 2.2: Regions and their corresponding coordinates sorted in alphabetical order. They are used for the analysis in Chapter 2.4.3. These regions are also utilised in the visualisation of the results in Fig. 2.6.

For our analysis, we focused first on the German-Danish west coast. This coast contains the five rivers Storå, Ribe Å, Bongsieler Kanal, Eider, and Oste. Our goal was to scrutinise whether large-scale compound flood events in these rivers have a specific Großwetterlage as their common meteorological driver. For this, we decided to examine which Großwetterlage is present when at least four of the five rivers have a compound flood event simultaneously. This requirement resulted in 16 separate compound flood events based on ECOSMO-coastDat3 + HD5-ERA5 and ECOSMO-coastDat3 + HD5-EOBS data. 15 of these events appeared during the Großwetterlage Cyclonic Westerly (Fig. 2.5), with only one appearing during Cyclonic North-Westerly (Fig. 2.6a).

The Großwetterlage Cyclonic Westerly is associated with strong westerly winds and higher-than-normal precipitation (Gerstengarbe et al., 1999) that can cause storm surges and river floods, respectively, which in combination can lead to compound flood events. Also, our analysis showed that at least 75% of the compound flood events for each river along the German-Danish west coast happened during this specific Großwetterlage. This made it the predominant Großwetterlage during compound flood events in this area. Similar results were found for the Swedish west coast in Kattegat and Skagerrak. There, all seven events that involved at least four rivers appeared during the Großwetterlage Cyclonic Westerly, based on ECOSMO-coastDat3 and HD5-ERA5 data (Fig. 2.6b).

In the west-facing coast of the Bothnian Sea, Cyclonic Westerly remained the predominant Großwetterlage. About two-thirds of the events occurred during Cyclonic Westerly and one-third during Anticyclonic Westerly (Fig. 2.6c). In the coastal area of the Baltic states, we observed again a distribution of roughly two-thirds of the events appearing during Cyclonic Westerly and one-third during Anticyclonic Westerly (Fig. 2.6d). Anticyclonic Westerly is known to lead to precipitation in the area of the Baltic countries (Jaagus et al., 2010), which in combination with the

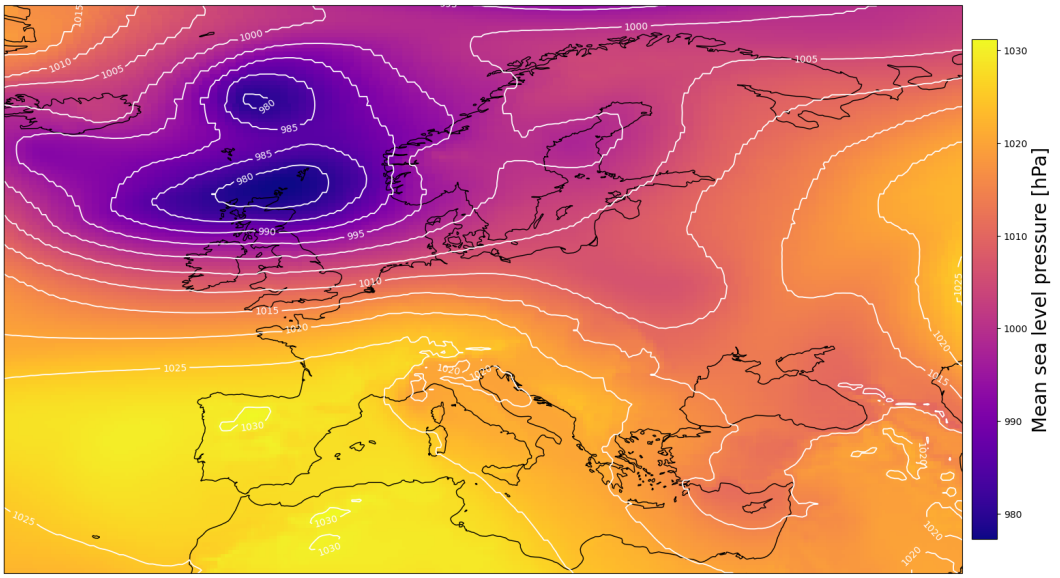

Figure 2.5: Map of the daily mean atmospheric pressure over Europe on 8th of December 2011. The characteristic low-pressure centre of the Großwetterlage Cyclonic Westerly is located north of Scotland (Hersbach et al., 2020).

southeastern wind direction are responsible for around a third of the compound flood events in the Baltic and west-facing Finnish area, due to the orientation of their coastline. For the west-facing coast of Great Britain, we found that half of the compound flood events happen during Cyclonic Westerly, a quarter of the events during Cyclonic South-Westerly and the remaining during other Großwetterlagen (Fig. 2.6e). Unlike the other cases, we did not observe any predominant Großwetterlage for compound events in Ireland, with Cyclonic Westerly accounting for less than half of the observed Großwetterlagen during compound flood events (Fig. 2.6f).

Furthermore, we investigated possible correlations between the duration of a Großwetterlage and the occurrence of compound flood events. We found that compound flood events can occur during short Großwetterlagen that only last 3 days, which is by definition the minimum duration, as well as Großwetterlagen that remain over several weeks. Therefore, we did not find any direct correlation. Additionally, we did not observe any specific sequence of Großwetterlagen that leads to an increased risk of compound flood events. Finally, the kind of Großwetterlage, which follows or precedes the Großwetterlage that causes a compound flood event, seems to be random.

2.4.4 *Correlation between the number of compound flood events and catchment size*

We analysed if there is any connection between the catchment size and the frequency of compound flood events. For this, we plotted the number of compound flood events against the size of the catchment area of each river (Fig. 2.7). The catchment size of each river was obtained from the HD model grid. The analysis was done separately for rivers based on their orientation along the coasts. Furthermore, the

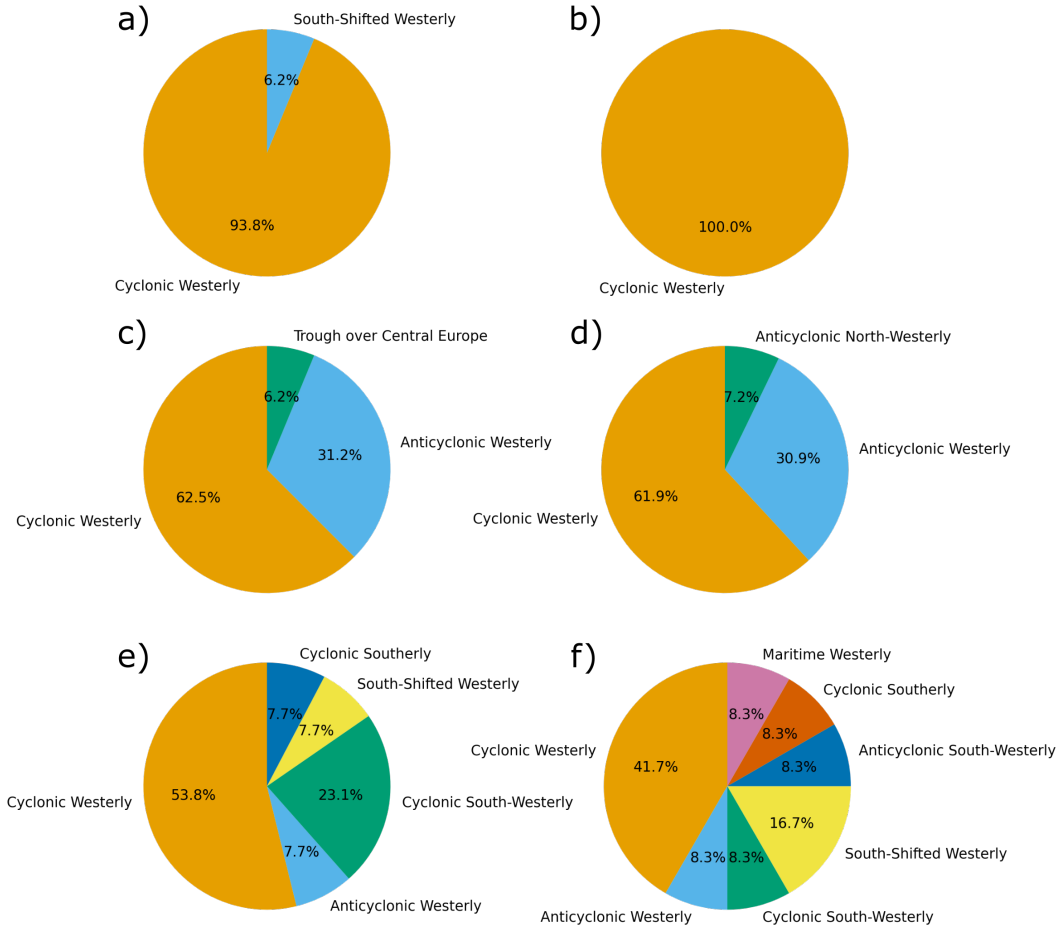

Figure 2.6: Distribution of Großwetterlagen that occurred during compound flood events in Europe. The following regions were analysed: a) German-Danish west coast, b) West-facing coast of Sweden, c) West-facing coast in the Bothnian Sea, d) West coast of the Baltic states, e) West coast of Great Britain, and f) West coast of Ireland. Coordinates of those regions are given in Table 2.2.

rivers were coloured red if the number of compound flood events is above the 2σ interval of randomised sea level data, blue if below the interval, and grey otherwise, as in Fig. 2.3. It can be seen that there is a clear correlation between the cardinal direction of the estuary and the number of compound flood events either being inside or outside of the 2σ interval. The west-facing coasts (Fig. 2.7a) were mostly above the 2σ interval and showed generally a higher number of compound flood events. Contrarily, the east-facing coasts (Fig. 2.7b) exhibited a lower amount of compound flood events and are mostly within the expected margin. Additionally, it can be seen that the number of compound flood events declined with increasing catchment area, regardless of cardinal direction.

2.5 DISCUSSION & CONCLUSIONS

In the present study, we conducted a coherent spatial analysis on the dependence of storm surges and discharge extreme events as drivers of compound flood

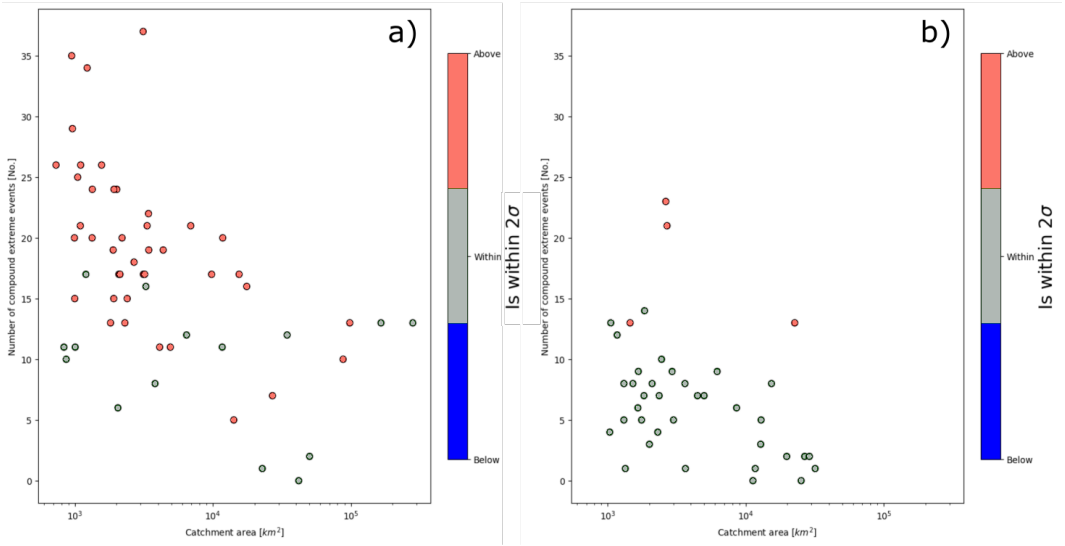

Figure 2.7: Number of extreme events for northern and central Europe over a period of 24 years plotted over the river's corresponding catchment area for HD5-ERA5 and TRIM-REA6 data using percentiles. The colour displays if the amount of observed compound flood events is within the expected 2σ deviation. Contains only rivers that are either on the a) western or b) east-facing coasts.

events over northern Europe. For this analysis, we introduced a method to analyse compound events by randomising one of the data sets to generate independent data. To our knowledge, this is the first study on compound flood events over all of Europe that does not utilise copulas. As mentioned in the introduction, copulas add unknown amounts of uncertainty to the analysis. Our method on the other hand, is easy to implement and the uncertainty is given by the standard deviation. One limitation of this method is that it cannot quantify the dependence between discharge and sea level.

Using different data sets of daily discharge and sea level, we detected a distinct pattern of westward-facing coasts having a higher number of compound flood events than expected by chance (Fig. 2.3, Fig. 2.7). These coasts were located in the European storm-track corridor comprising the British Isles, northern Germany, Denmark, and southern Sweden (Feser et al., 2015). Due to the mostly prevailing western winds, the rivers on the eastern coasts showed a lower number of compound flood events, which are usually within the expected range of two standard deviations. This finding is consistent with the results of Paprotny et al. (2018a), who noted a strong dependency in their rank correlation for west-facing coasts in northern Europe. Khanal et al. (2019b) and Kew et al. (2013) likewise reported that the most extreme events in the Rhine delta are connected to westerly winds. Similarly, Svensson & Jones (2004) reported a strong dependence between discharge and storm surge events for western Great Britain. We identified the Großwetterlage Cyclonic Westerly as the common meteorological driver for the occurrence of large-scale compound flood events in North and Baltic Sea regions.

In parts of the Baltic and west-facing Finnish coasts, the Großwetterlage Anticyclonic Westerly additionally contributed to the generation of compound flood events (about one-third). For Ireland, a distinct Großwetterlage could not be identified

as a driver of compound flood events. We speculate that this might be because it offers a wide angle of attack for storm surges.

Additionally, we were able to demonstrate that the detected spatial distribution remains stable for various sources of uncertainty. Our results proved to be robust against the utilisation of different forcing data for the simulation of discharge and sea level data, parameter settings, and randomisation approaches. Furthermore, the pattern remained relatively stable despite the ongoing climate change since the 1960s. There was a certain amount of variation in the pattern, which can be attributed to randomness and the different setups. Due to the limited number of compound flood events, even small variations to their definition, like changes in the allowed lag, have a minor influence on the results. In all cases, the pattern was present, even though it was sometimes more or less pronounced.

In addition, we demonstrated that regardless of the estuary orientation, the number of compound flood events declined on average with increasing catchment size. The reason for this might be that rivers with smaller catchment areas are capable of reacting faster to precipitation that appears during the storm events, which also causes the storm surges. There is some variation in the distribution, as expected by the design of the test, which resulted in around 4.6% of the data points being labelled incorrectly.

Our analysis here is associated with some caveats that have to be considered. We note that the utilisation of the 2σ interval in our analysis comprises some amount of uncertainty. As a result, it can be expected that five to nine rivers will be incorrectly labelled, based on the size of the data set. Another problem for our analysis was the very short time frame that was accessible with the TRIM-REA6 and ECOSMO-REA6 data of 24 and 21 years respectively. Furthermore, it is possible that the model-based data sets contain systematic errors. Despite the detected pattern being robust, it is possible that the absolute number of compound flood events may deviate from the actual number. Furthermore, the de-clustering time of 4 days might be too short for some of the longest rivers that may contain very long extreme events. The lack of a parametric model impedes the possibility of deriving engineering quantities such as design events used to assess the level of protection afforded by flood defence structures.

Future work can further examine these findings by using ensembles from climate models that cover longer time frames, e.g. 50 years or more. This could enable generating a distribution for the number of compound flood events, based on the compound flood events detected in the individual ensemble members. As a result, it would become possible to calculate how many compound flood events to expect on average in each river. This reduces the influence of randomness by not having to rely on the compound flood event number detected in a single data set. One potential drawback is the reliance on the capabilities of numerical models to adequately generate those compound extreme events correctly. Additionally, future studies could focus on locations in close spatial proximity along the west-facing coasts for which long time series of daily sea level and discharge data are available. They could also attempt to quantify the lag for each catchment individually, which is currently troubling for large rivers since their lag depends on the location of the precipitation. Another interesting question, which needs further investigation,

is why the vast majority of compound flood events on the west coasts happen during Cyclonic Westerly, while not every one of these Großwetterlagen results in compound flood events. Understanding what makes them different might offer opportunities to identify them early and set contingency plans into motion. While this study has shown the dependence between catchment size and the overall number of compound flood events, there are more characteristics that can be considered. These include, for example, the total elevation change in the catchment area and the baseflow index, which describes the ratio of baseflow to the total streamflow volume (Longobardi & Villani, 2023).

In order to support future risk assessments, it will be important to analyse how compound events will change under different climate scenarios and sea level rises (Zscheischler et al., 2018). First, the frequency change of general flood events with respect to the current standards for extreme events might change especially with increasing sea levels. Second, it will be interesting to analyse if our observed pattern caused by the Großwetterlage remains similar or if we will see changes to it due to, for example, changes in the occurrence rate of this specific Großwetterlage. This is important since it is well known that there have been frequency changes in the past as reported by Grabau (1987) and Dietz (2019). Hoy et al. (2013) found that the frequency of Cyclonic Westerly was declining during the first half of the last century, before strongly rising between 1970 and 2000. This leads to the question of how the frequency of compound flood events might change for all of Europe, which is vital for regional coastal adaptation. Third, the vast majority of compound flood events are currently centred around the winter season. It is important for our general understanding to investigate if the seasonal distribution itself will change, maybe with more events in summer, or if the distribution stays the same with different numbers.

2.6 STATEMENTS AND DECLARATIONS

Data availability: The HD discharge data were published as Hagemann & Stacke (2021) and can be obtained at the World Data Centre for Climate (WDCC) of the German Climate Computing Centre (DKRZ). TRIM and ECOSMO sea level data will be made available by the authors, without undue reservation, to any qualified researcher upon request. ERA5 reanalysis data are available at the Climate Data Store: https://cds.climate.copernicus.eu/. DWD Großwetterlagen are available at https://www.dwd.de/DE/leistungen/grosswetterlage/grosswetterlage.html.

Author contribution: Philipp Heinrich developed the analysis methods, performed the data analysis and wrote the manuscript. Stefan Hagemann initiated the study and contributed the HD discharge data while Lidia Gaslikova and Ute Daewel generated the TRIM and ECOSMO sea level data, respectively. Corinna Schrum revised the manuscript. Ralf Weisse and Stefan Hagemann revised the manuscript and contributed to the interpretation of the results. Ralf Weisse acquired the funding and Stefan Hagemann, Ralf Weisse, and Corinna Schrum supervised the research activities.

Competing interests: The authors declare that they have no known competing financial interests or personal relationships that could have appeared to influence the work reported in this paper.

Acknowledgements: This research was financed with funding provided by the German Federal Ministry of Education and Research (BMBF; Förderkennzeichen 01LR2003A). Furthermore, this research is a contribution to the PoFIV programme of the Helmholtz Association.

2.A APPENDIX: IMAGES FOR PARAMETER CHANGES

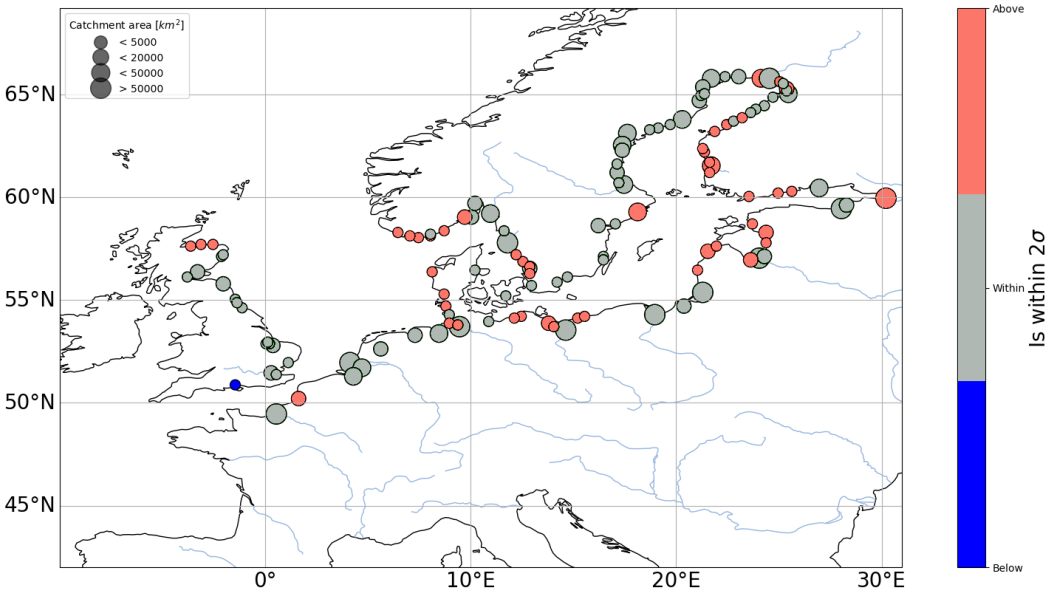

Figure 2.8: HD5-ERA5 as in Fig. 2.3 but with ECOSMO-REA6 for the sea level data.

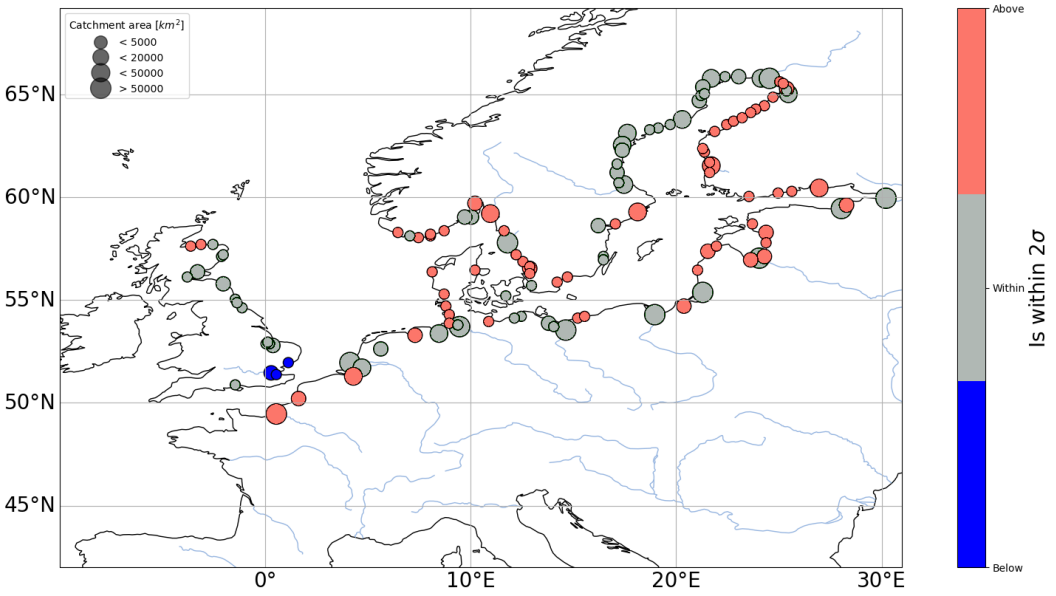

Figure 2.9: As in Fig. 2.3 but with ECOSMO-coastDat3 and HD5-EOBS data.

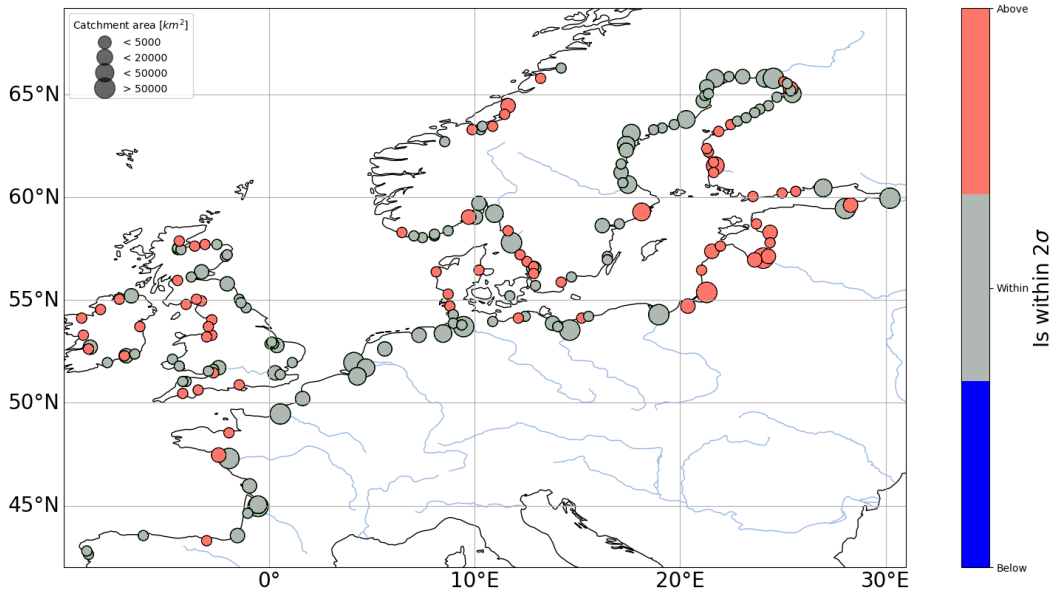

Figure 2.10: TRIM-REA6 and HD5-ERA5 as in Fig. 2.3 but utilising normal percentile instead of the adaptive thresholds.

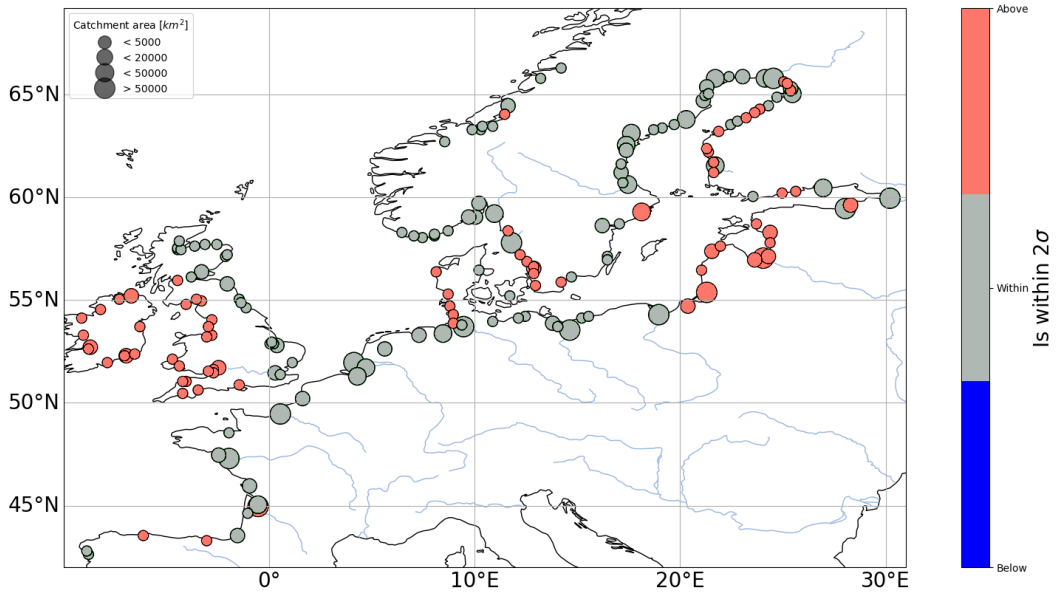

Figure 2.11: TRIM-REA6 and HD5-ERA5 as in Fig. 2.3 but for the months of November to February.

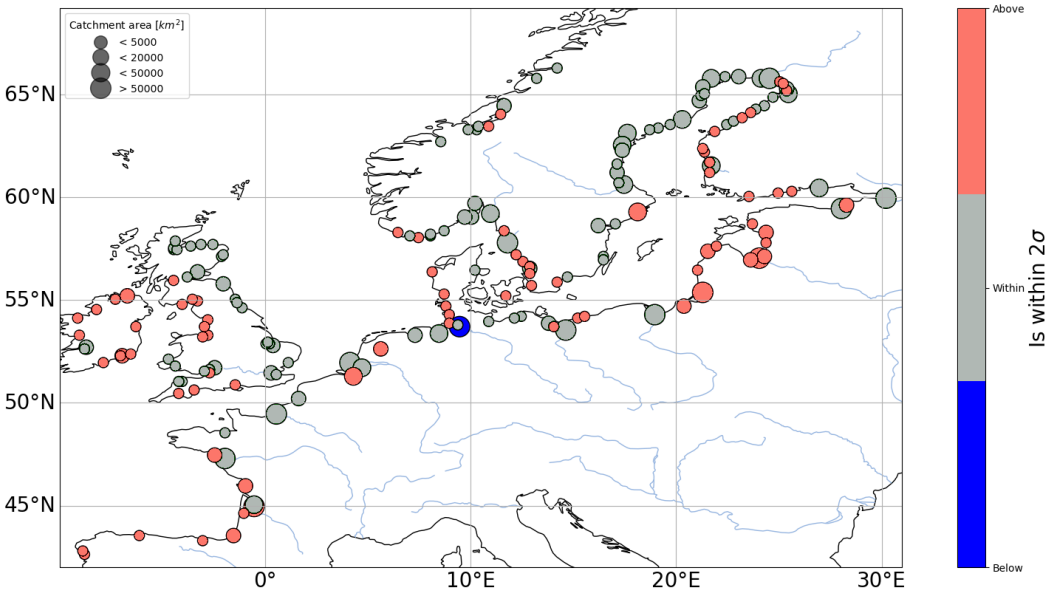

Figure 2.12: TRIM-REA6 and HD5-ERA5 as in Fig. 2.3 but for the months of October to March.

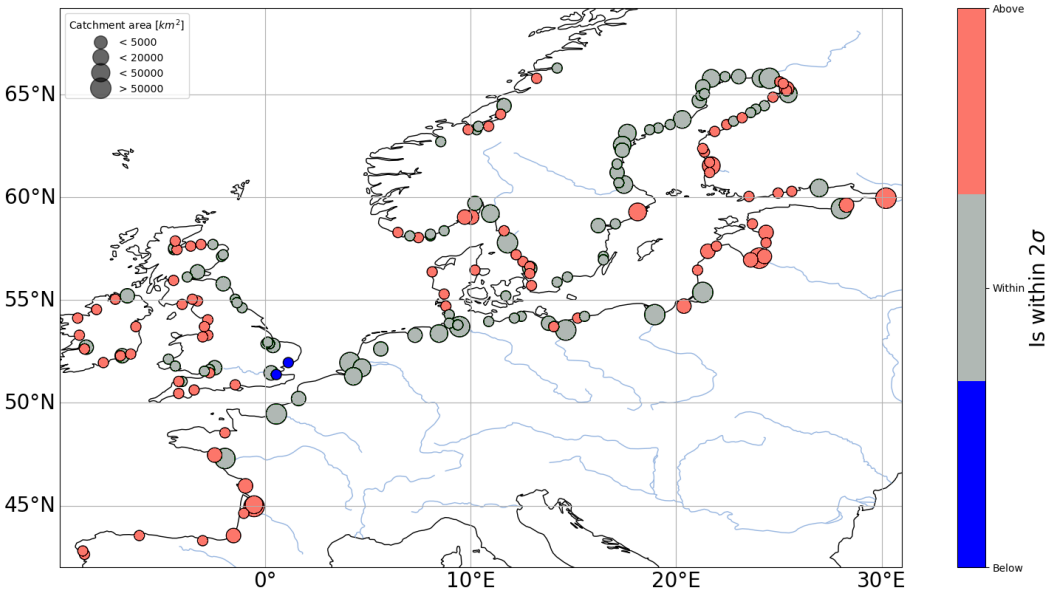

Figure 2.13: TRIM-REA6 and HD5-ERA5 as in Fig. 2.3 but swapping the years for randomisation instead of the method described in Chapter 2.2.

3

AUTOMATED CLASSIFICATION OF ATMOSPHERIC CIRCULATION TYPES FOR COMPOUND FLOOD RISK ASSESSMENT: CMIP6 MODEL ANALYSIS UTILISING A DEEP LEARNING ENSEMBLE

CHAPTER SUMMARY

The simultaneous occurrence of high river discharges and storm surges represent a substantial hazard for many low-lying coastal areas. Potential future changes in the frequency or intensity of such compound flood events is therefore of utmost importance. To assess such changes large and consistent ensembles with storm surge and hydrological models are needed that are hardly available. Often the occurrence of compound flood events is linked to the presence of certain atmospheric circulation types. Future changes in the frequency of such patterns can be directly inferred from available climate simulations. A frequently used classification of atmospheric circulation types are the so-called 'Großwetterlagen' by Hess and Brezowsky. Here possible future changes in the occurrence of these 'Großwetterlagen' were analysed using data from 31 realisations of CMIP6 climate simulations for the emission scenarios SSP1-2.6, SSP3-7.0, and SSP5-8.5. As the classification is subjective, a deep learning ensemble for the automatic classification was developed and applied. In winter, a higher frequency of the atmospheric pattern Cyclonic Westerly towards 2100 could be inferred as a robust result among all models and scenarios. As this circulation type is potentially associated with compound flooding in some parts of the European coasts, this points towards potentially increasing risks from compound flooding in the future.

3.1 INTRODUCTION

With floods being globally among the most common, expensive, and lethal natural disasters (Hu et al., 2018; Jonkman, 2005), they pose a great threat to the people living in coastal areas (Santiago-Collazo et al., 2019). Coastal flooding can be caused by various factors, including tides, storm surges, waves, precipitation, and river discharge (Wolf, 2009). The simultaneous or successive occurrence of two or more extreme flood drivers, like extreme river discharge and extreme storm surges (Bennett et al., 2023), can potentially be much more devastating than their individual effects would be under normal circumstances (Clarke et al., 2021). They pose an even bigger threat to people living in coastal areas (Santiago-Collazo et al., 2019), which also contain many big economic centres (Wahl et al., 2015). Notable examples of such events are the flash flood 1967 in Lisbon, Portugal (Trigo et al., 2016) and the 1999 flood in Lymington, United Kingdom (Ruocco et al., 2011). These so called 'compound flood events' have attracted increased attention from the scientific community in recent years, due to their destructive nature. Sadegh

et al. (2018) concluded that neglecting the interaction of flood drivers could result in a severe underestimation of the flood risk, which can severely affect critical infrastructures (Khanam et al., 2021).

The North Sea is one of the world's most industrialised seas with a population of approximately 61.5 million inhabitants living along the coast (Interreg North Sea Programme, 2021). Compound flood events, therefore, pose a big threat to the low-lying coastal areas. Research on compound flood events in northern and central Europe has been carried out on various scales. Khanal et al. (2019a) investigated the co-occurrence of storm surge and fluvial floods for the Rhine catchment and the Dutch coastal area, while Camus et al. (2022) linked specific weather types to compound flooding in estuaries along the North Atlantic coastlines. Studies conducted on the influence of anthropogenic climate change project a significant increase in the number of compound flood events in Europe (Heinrich et al. (2023b); Chapter 4). Bevacqua et al. (2019) attributed this increase to the warmer atmosphere carrying more moisture, in addition to sea level rise. The ensemble size for the analysis of those future changes is usually limited by the time required for the simulations of the necessary data.

Several studies established connections between weather patterns and the occurrence of compound flood events. Hendry et al. (2019) found a higher frequency of compound events on the western coast of the United Kingdom compared to the eastern coast. They concluded that this phenomenon is due to the fact that storms that generate high skew surges and high river discharge share common features on the western coastline, but not on the opposite shore. Likewise, I demonstrated in Chapter 2 that the west-facing coasts in northern and central Europe show a higher probability for compound flood events than expected by pure chance. By utilising the Großwetterlagen classification, which consist of 29 circulation types, they identified *Cyclonic Westerly* as the common driver for the vast majority of these events. This weather pattern is characterised by strong westerly winds and rainfall. The Großwetterlagen classification has been utilised by many studies and is likely the most widely used set of circulation patterns over Europe. Bouwer et al. (2006) found a strong correlation between the frequency of Cyclonic Westerly and river discharge in winter for many stations north of the Alps. Similarly, Hoy et al. (2014) found precipitation increase during the winter half-year in northern Europe for 1981-2010 to be correlated to increased wet westerly air mass inflow. Future changes of such weather patterns may be derived directly from global climate projections and therefore do not require an additional downsampling step that is often required for climate change impact studies. Our study aims to assess whether there is a systematic change in the frequency of patterns driving such compound flood events.

The classification system of Großwetterlagen was first introduced by Hess & Brezowsky (1969) to describe large-scale weather systems over Europe. There are a total of 29 different circulation types listed in Table 3.1. One potential downside of this classification system is its subjective nature, which introduces an element of human error and makes it challenging to apply to large amounts of simulated data. Moreover, it is worth noting that each circulation pattern must persist for a minimum of three days, which has to be taken into account for the classification.

Index	Acronym	Original German definition	Translated English definition
1	WA	Westlage, antizyklonal	Anticyclonic Westerly
2	WZ	Westlage, zyklonal	Cyclonic Westerly
3	WS	Südliche Westlage	South-Shifted Westerly
4	WW	Winkelförmige Westlage	Maritime Westerly (Block E. Europe)
5	SWA	Südwestlage, antizyklonal	Anticyclonic South-Westerly
6	SWZ	Südwestlage, zyklonal	Cyclonic South-Westerly
7	NWA	Nordwestlage, antizyklonal	Anticyclonic North-Westerly
8	NWZ	Nordwestlage, zyklonal	Cyclonic North-Westerly
9	HM	Hoch Mitteleuropa	High over Central Europe
10	BM	Hochdruckbrücke (Rücken) Mitteleuropa	Zonal Ridge across Central Europe
11	TM	Tief Mitteleuropa	Low (Cut-Off) over Central Europe
12	NA	Nordlage, antizyklonal	Anticyclonic Northerly
13	NZ	Nordlage, zyklonal	Cyclonic Northerly
14	HNA	Hoch Nordmeer-Island, antizyklonal	Icelandic High, Ridge C. Europe
15	HNZ	Hoch Nordmeer-Island, zyklonal	Icelandic High, Trough C. Europe
16	HB	Hoch Britische Inseln	High over the British Isles
17	TRM	Trog Mitteleuropa	Trough over Central Europe
18	NEA	Nordostlage, antizyklonal	Anticyclonic North-Easterly
19	NEZ	Nordostlage, zyklonal	Cyclonic North-Easterly
20	HFA	Hoch Fennoskandien, antizyklonal	Scandinavian High, Ridge C. Europe
21	HFZ	Hoch Fennoskandien, zyklonal	Scandinavian High, Trough C. Europe
22	HNFA	Hoch Nordmeer-Fennoskandien, antizykl.	High Scandinavia-Iceland, Ridge C. Europe
23	HNFZ	Hoch Nordmeer-Fennoskandien, zyklonal	High Scandinavia-Iceland, Trough C. Europe
24	SEA	Südostlage, antizyklonal	Anticyclonic South-Easterly
25	SEZ	Südostlage, zyklonal	Cyclonic South-Easterly
26	SA	Südlage, antizyklonal	Anticyclonic Southerly
27	SZ	Südlage, zyklonal	Cyclonic Southerly
28	TB	Tief Britische Inseln	Low over the British Isles
29	TRW	Trog Westeuropa	Trough over Western Europe

Table 3.1: Table with acronyms, original, and translated names of the 29 Großwetterlagen according to James (2007). The acronyms are based on the German names.

The advantages of the classification system are (i) a very long classification catalogue that begins in 1881 and is continuously updated, as well as (ii) the fact that those circulation types can be associated with consistent and typical local weather conditions (Wapler & James, 2015). The length of the classification catalogue is particularly useful when focusing on data-driven classification methods as it provides a large amount of labelled data points.

Two studies have previously focused on the automatic classification of Großwetterlagen, namely James (2007) and Mittermeier et al. (2022). James (2007) proposed an objective classification based on composite plots, whereby a circulation type was assigned to each day based on the composite with the highest correlation after temporal smoothing. In James (2006), they used this method to analyse ensemble runs of the global climate model HadGeM1 (Martin et al., 2006), but found no significant changes to the circulation pattern under climate change. In recent years, convolutional neural networks have made significant improvements in image classification (Liu et al., 2022a), with potential for weather pattern classification. Luferov & Fedotova (2020) employed convolutional neural networks to categorise 5 circulation patterns in the northern hemisphere, Chattopadhyay et al. (2020) re-identified clustered weather patterns, and Ham et al. (2019) highlighted their effectiveness for multi-year ENSO forecasting. Liu et al. (2016) utilised a deep convolutional neural network to detect extreme weathers, such as tropical cyclones, in climate datasets. Mittermeier et al. (2022) subsequently modified this neural network architecture and used it for the classification of Großwetterlagen, achieving higher accuracy than the composite method by James (2007). They used their trained neural networks ensemble to analyse future changes in a single-model initial-condition large ensemble of the global climate model EC-Earth3 under the Shared Socio-Economic Pathways (Riahi et al., 2017) 3-7.0 scenario.

Mittermeier et al. (2022) demonstrated the enhanced capabilities of neural networks in classifying Großwetterlagen. However, the occurrence rate of Cyclonic Westerly was strongly underestimated by their networks. Our goal is to improve upon their work by training neural networks with better capabilities for detecting Cyclonic Westerly. To achieve this, we introduce a new neural network architecture. This will enable us to assess future changes to this weather pattern caused by climate change. The training data and procedures were selected to be as similar as possible to those used by Mittermeier et al. (2022) to ensure the best possible comparability.

In this study we focus on the detection of Cyclonic Westerly, which is associated with compound flood events in northern and central Europe, and its future changes due to anthropogenic climate change. First, we present a novel convolutional neural network structure for the classification of Großwetterlagen and evaluate the classification results on a reference period. Moreover, we examine the influence of additional parameters on the precision of the network. We then assess the impact of internal variability on the findings using the Max Planck Institute Grand Ensemble (MPI-GE). To analyse possible future changes in the frequency of Cyclonic Westerly, we utilise 31 global climate models from the Coupled Model Intercomparison Project Phase 6 (CMIP6). For each model, we consider the three scenarios: SSP1-2.6 (low emission), SSP3-7.0 (medium emission), and SSP5-8.5 (high emission). We

use a range of different global climate models to minimise bias and uncertainty resulting from the use of a single model. A comparison of model quality during the reference period is included.

3.2 DATA

In this section, we first discuss the data used to train our neural network for the classification of Cyclonic Westerly. This is followed by an overview of the CMIP6 data used for the analysis of future changes under climate change.

3.2.1 *Training data*

The training data for our neural network, was chosen to be as close as possible to the one used in Mittermeier et al. (2022) to allow a direct comparison of the results. To train our convolutional neural network, we utilised the daily geopotential height of the 500 hPa surface and daily mean sea level pressure provided by the ERA-20C reanalysis of the European Centre for Medium-Range Weather Forecasts (ECMWF, 2014). The data set contains an atmospheric reanalysis of the 20th century for 1900-2010. As input data domain we selected the area 30° N to 75° N and -65° W to 45° E, which encompasses large parts of the North Atlantic and Europe (Fig. 3.1) and is also utilised for the subjective classification (Hess & Brezowsky, 1969).

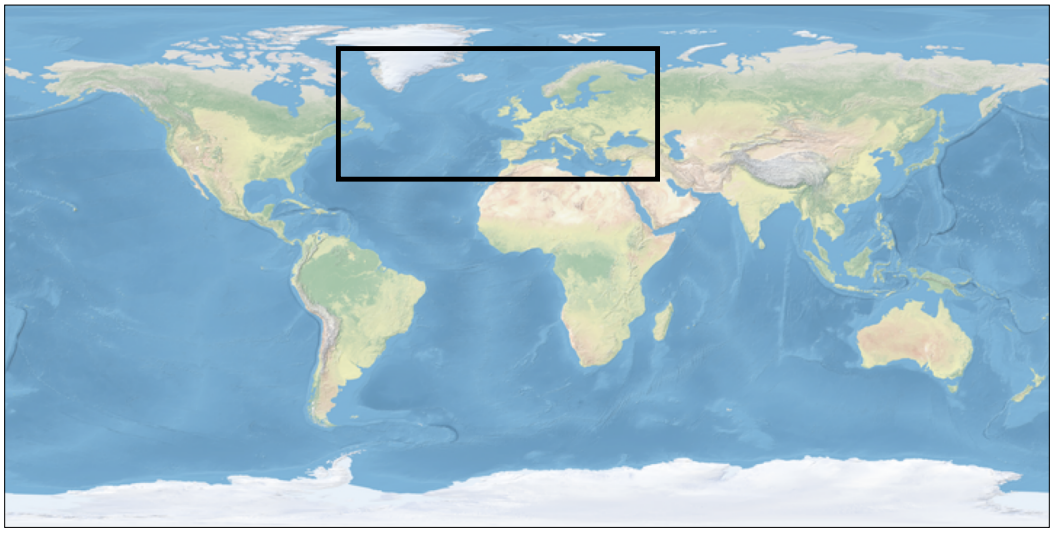

Figure 3.1: The black rectangle contains the domain used in this study for the analysis of Großwetterlagen. The area covered is 30° N to 75° N and -65° W to 45° E.

The input data were then interpolated to a spatial grid of about[1] 2.8° × 2.8°. Next, each data variable was standardised using Z-Scores. In this standardisation method, each data point is scaled by

$$x' = \frac{(x - \mu)}{\sigma} \tag{3.1}$$

1 The spatial resolution of 5° given in Mittermeier et al. (2022) is an error in the text, according to personal communication with the authors (2023).

where μ denotes the mean and σ the standard deviation of the variable. The purpose of this standardisation was to adjust the values of geopotential height and mean sea level pressure to a common scale, which enhances network performance and training stability (Huang et al., 2023). The labels used for the classification of the 29 circulation types are based on the Großwetterlagen catalogue by Hess & Brezowsky (1969) which is continuously updated to this day by the German Weather Service (DWD). This catalogue contains daily subjective classifications, dating back to 1881, derived from observational data of geopotential height and mean sea level pressure. Days marked as 'undefined' in the catalogue were discarded for training purposes since the neural network cannot learn from them. To ensure maximum comparability, we limited the training of the network to 1900-1980, as done in Mittermeier et al. (2022) because of 'implausible sudden discontinuity of the labels of the catalogue' afterwards (Mittermeier et al., 2022).

3.2.2 *CMIP6 Global Climate Model data*

Data from a set of 31 global climate models from the Coupled Model Intercomparison Project Phase 6 (CMIP6) were used to analyse changes in the frequency of the Großwetterlage Cyclonic Westerly. An overview over those models is given in Table 3.2.

For the selected models, daily data of geopotential height and sea level pressure had to be available. Furthermore, it was required that the data for the historical run, as well as the future scenarios SSP1-2.6, SSP3-7.0, and SSP5-8.5, originate from the same ensemble member. We utilised all models for which data were available via the CMIP6 data search portal of the Earth System Grid Federation (ESGF) at the end of September 2023 and that fulfilled the aforementioned requirements. Additionally, we used the AWI-CM-1-1-MR data files that were stored on the servers of the German Climate Computing Centre (DKRZ). We chose 1961 to 1990 as the historical reference period because it has been retained as a standard reference period for long-term climate change assessments by the World Meteorological Organization (WMO)[2]. For assessing future changes, we utilised the 30-year period 2071-2100 when available, otherwise the closest period was used that was available for all three future scenarios of a model (see Table 3.2 for further details). We conducted a check on all data sets to ensure that they do not contain missing values or any unreasonably large or small numbers. Afterwards, the data sets were interpolated onto the same grid as the training data to create a consistent input for the neural network. Finally, we standardised the ensemble data using Z-Scores, similar to the training data (see Chapter 3.2.1).

Furthermore, we utilised daily data from the CMIP6 version of the Max Planck Institute Grand Ensemble (Olonscheck et al., 2023) to examine the contribution of internal variability to the results. MPI-GE CMIP6 is a single-model initial-condition large ensemble of MPI-ESM1.2-LR that consists of 30 realisations for the historical period and five emission scenarios each.

2 https://community.wmo.int/en/wmo-climatological-normals

Index	Model name	Variant	Years	Institution ID	Reference
G0	ACCESS-CM2	r1i1p1f1	2071-2100	CSIRO-ARCCSS	Bi et al. (2020)
G1	ACCESS-ESM1-5	r10i1p1f1	2071-2100	CSIRO	Ziehn et al. (2020)
G2	AWI-CM-1-1-MR	r1i1p1f1	2071-2100	AWI	Tebaldi et al. (2021)
G3	BCC-CSM2-MR	r1i1p1f1	2071-2100	BCC	Wu et al. (2019)
G4	CanESM5	r10i1p1f1	2071-2100	CCCma	Swart et al. (2019)
G5	CESM2	r1i1p1f1	2071-2100	NCAR	Danabasoglu et al. (2020)
G6	CESM2-WACCM	r1i1p1f1	2071-2100	NCAR	Gettelman et al. (2019)
G7	CMCC-CM2-SR5	r1i1p1f1	2071-2100	CMCC	Cherchi et al. (2019)
G8	CMCC-ESM2	r1i1p1f1	2071-2100	CMCC	Cherchi et al. (2019)
G9	CNRM-CM6-1	r1i1p1f2	2071-2100	CNRM-CERFACS	Voldoire et al. (2019)
G10	CNRM-CM6-1-HR	r1i1p1f2	2071-2100	CNRM-CERFACS	Voldoire et al. (2019)
G11	CNRM-ESM2-1	r1i1p1ff	2071-2100	CNRM-CERFACS	Séférian et al. (2019)
G12	EC-Earth3	r1i1p1f1	2071-2100	EC-Earth-Consortium	Döscher et al. (2022)
G13	EC-Earth3-Veg	r4i1p1f1	2071-2100	EC-Earth-Consortium	Döscher et al. (2022)
G14	EC-Earth3-Veg-LR	r1i1p1f1	2071-2100	EC-Earth-Consortium	Döscher et al. (2022)
G15	FGOALS-g3	r1i1p1f1	2071-2100	CAS	Li et al. (2020)
G16	IITM-ESM	r1i1p1f1	2069-2098	CCCR-IITM	Swapna et al. (2015)
G17	INM-CM4-8	r1i1p1f1	2071-2100	INM	Volodin et al. (2018)
G18	INM-CM5-0	r1i1p1f1	2071-2100	INM	Volodin et al. (2018)
G19	IPSL-CM6A-LR	r1i1p1f1	2071-2100	IPSL	Boucher et al. (2020)
G20	KACE-1-0-G	r1i1p1f1	2071-2100	NIMS-KMA	Lee et al. (2020a)
G21	MIROC-ES2H	r1i1p4f2	2071-2100	MIROC	Kawamiya et al. (2020)
G22	MIROC-ES2L	r1i1p1f2	2071-2100	MIROC	Hajima et al. (2020)
G23	MIROC6	r3i1p1f1	2071-2100	MIROC	Tatebe et al. (2019)
G24	MPI-ESM1-2-HR	r1i1p1f1	2071-2100	MPI-M	Müller et al. (2018)
G25	MPI-ESM1-2-LR	r4i1p1f1	2071-2100	MPI-M	Mauritsen et al. (2019)
G26	MRI-ESM2-0	r4i1p1f1	2071-2100	MRI	Yukimoto et al. (2019)
G27	NorESM2-LM	r1i1p1f1	2071-2100	NCC	Seland et al. (2020)
G28	NorESM2-MM	r1i1p1f1	2071-2100	NCC	Seland et al. (2020)
G29	TaiESM1	r1i1p1f1	2071-2100	AS-RCEC	Lee et al. (2020b)
G30	UKESM1-0-LL	r8i1p1f2	2071-2100	MOHC	Tang et al. (2019)

Table 3.2: Overview over the 31 CMIP6 global climate models that were used in this study. References were based on those given in the data files, or if unavailable, the reference most commonly used by other articles was included.

3.3 METHODS: NETWORK STRUCTURE AND TRAINING PROCESS

The training of the networks was conducted on an NVIDIA Tesla V100-PCIE-16GB GPU. The architecture of our Convolutional Neural Meteorology Network (CNMN) is following the structure of well-known networks like Alexnet (Krizhevsky et al., 2017) and VGG16 (Simonyan & Zisserman, 2014). CNMN utilises two input channels for the geopotential height and sea level pressure data. Our network consists of 4 blocks, each with a single convolution layer with a ReLU activation, followed by max pooling, with the last one additionally containing a global average pooling layer (Islam et al., 2021; Lin et al., 2013) (see Fig. 3.2). One additional detail

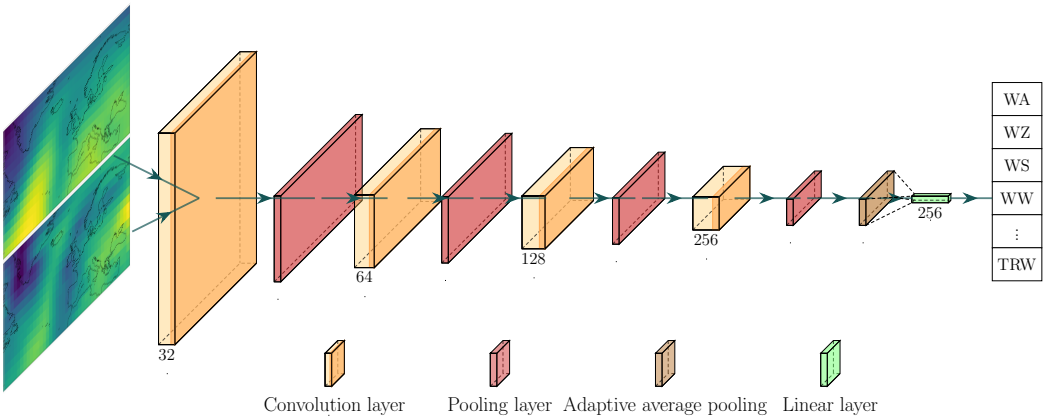

Figure 3.2: Visualisation of the neural network architecture employed in this study. The number underneath the convolution layers indicates the number of channels. The acronyms on the right hand side are those belonging to the 29 Großwetterlagen (see Table 3.1).

is that the convolutional layers use an asymmetrical kernel of size 3×7 instead of a square kernel to take the larger latitude dimension of the input data into account. The global average pooling layer collapses the input signal to size $1 \times 1 \times C$ (C=number of channels) which greatly reduces the size of the following connected layer. This reduced network size helps to mitigate overfitting (Li et al., 2022). The connected layer then ends in 29 output nodes, one for each Großwetterlage.

Our training process used the Adam optimiser introduced in Kingma & Ba (2014) and cross entropy as the loss function. We set up training for a maximum of 1000 epochs, with an early stop after 100 epochs without improvement and a batch size of 2048. Additionally, we used Gaussian noise for data augmentation to artificially increase the amount of available training data and reduce overfitting. To better assess the performance of CNMN we used k-fold cross-validation, as in Mittermeier et al. (2022). In this method the data sets are split into an inner fold containing 70 years and the outer fold containing 10 years. The inner fold is utilised for training and tuning the learning rate of our neural network, while the evaluation of the neural network is performed on the outer fold. This procedure is then repeated several times for different splits of the data (see Fig. 3.3) to obtain reliable metrics for our neural network CNMN.

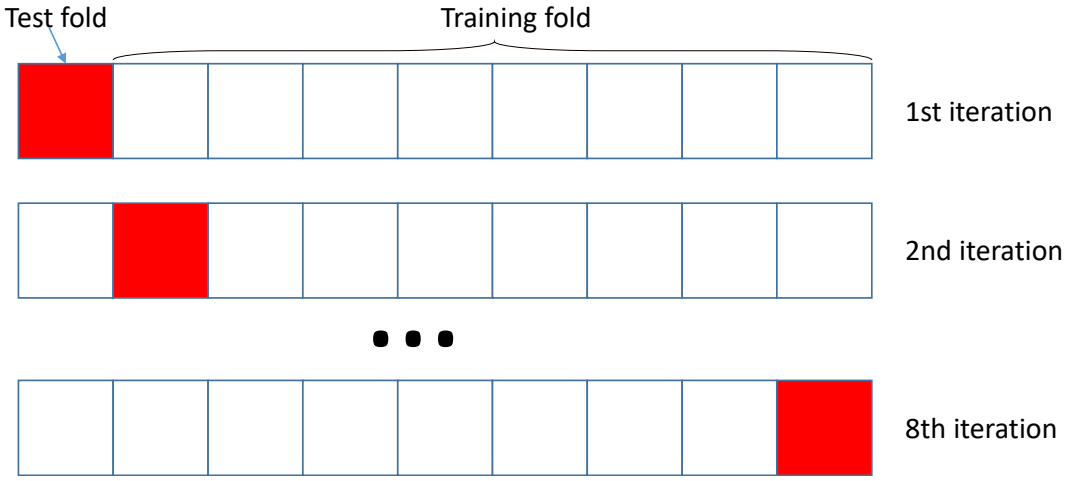

Figure 3.3: Visual representation of the nested cross-validation training process. The data set is split into eight chunks. One of them is the 'test fold' which is not used for training but for the evaluation of the network's performance. In each iteration, a different chunk is used as the test fold. This method results in eight evaluations on independent data.

The Großwetterlagen classification scheme requires all constellations to last for at least three days, which we have to take into account in a post processing step after CNMN predicted all labels. To start, we look at the first/last three elements (Fig. 3.4a). The third element of the trio will be assigned a new label, if the other two share the same label. Subsequently, the algorithm looks for elements in the predicted label classification that share the same neighbours, with the element in the middle getting changed (Fig. 3.4b). Lastly, elements with two different surrounding labels will be assigned the label of whichever neighbouring label has the highest probability as determined by CNMN (Fig. 3.4c). This procedure is repeated one more time to ensure the consistency with the 3-day rule.

To evaluate the performance of our neural network, we assess both the macro F1 score (Equation 3.5) and overall accuracy. The macro F1 score comprises precision (Equation 3.2) and recall (Equation 3.3) and is chosen to take the imbalance of the data classes into account (Jiang et al., 2020). Precision measures the ratio of correct positive identifications. For class i, precision is defined as

$$P_i = \frac{TP_i}{TP_i + FP_i} \tag{3.2}$$

where TP are true positives and FP false positives. The recall metric determines the proportion of actual positives that have been accurately identified and is calculated via

$$R_i = \frac{TP_i}{TP_i + FN_i} \tag{3.3}$$

where FN denotes false negatives. Finally, the F1 score of class i is

$$F_i = 2\frac{P_i R_i}{P_i + R_i} \tag{3.4}$$

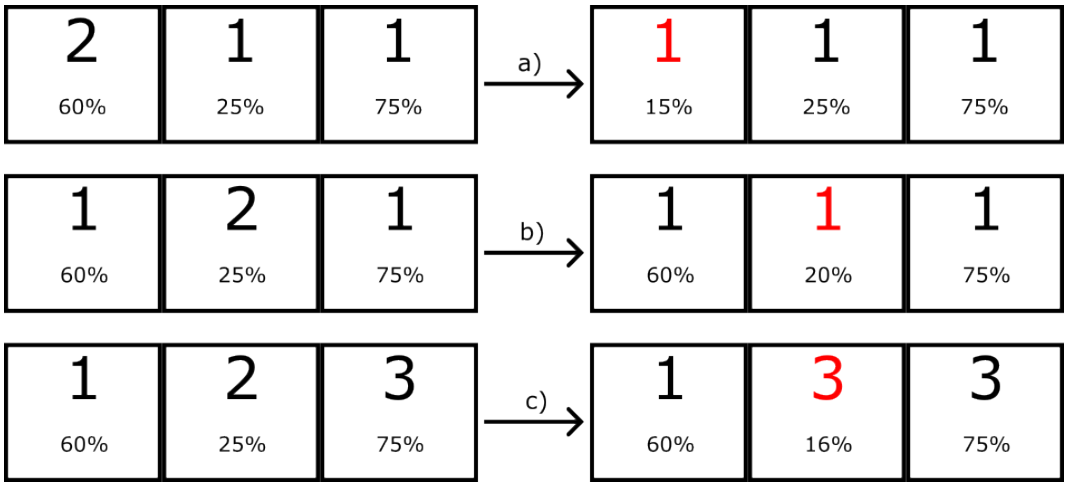

Figure 3.4: Visualisation of the algorithm used to apply the 3-day consistency rule of the Großwetterlagen classification to the data. The large numbers in each box is the index of the Großwetterlage predicted by CNMN for that day. The percentage is the probability for the classification. All values in this figure are exemplary. a) Treatment of the first/last elements of the data in case two labels are identical, b) for the same labels around the current element, and c) for different neighbouring labels.

which then results in the macro F1 score as the arithmetic mean of all classes.

$$\mathbb{F}_1 = \frac{2}{n} \sum_{i=1}^{n} \frac{P_i R_i}{P_i + R_i} \tag{3.5}$$

We trained an ensemble of 50 networks in order to minimise the variability of the network performance caused by the random initialisation of the network weights at the beginning of the training process.

3.4 RESULTS

3.4.1 *Network evaluation*

The performance of our neural network ensemble is evaluated by comparing their predictions to the actual daily Großwetterlagen in the catalogue, which is based on observational data. This evaluation is conducted on the eight outer test folds, which are independent of the training process. To increase the robustness of our evaluation, we use five different networks for each outer fold to account for the variance caused by random initialisation. Table 3.3 presents the performance comparison of our neural network CNMN with those of Mittermeier et al. (2022) and James (2007).

Our results show an increase in the macro F1 score by almost 2.2% and an accuracy increase of over 7% compared to the previous best results. Our deep ensemble of convolutional neural networks outperforms the deep ensemble of Mittermeier et al. (2022) in 22 out of the 29 Großwetterlagen and the composite method of James (2007) in 20 out of 29 Großwetterlagen. When compared to both methods, they offer the best performance metrics for more than half of the

Index	Acronym	CNMN F1 score [%]	Mittermeier F1 score [%]	James F1 score [%]
1	WA	39.58	44.60	40.32
2	WZ	63.12	47.08	52.69
3	WS	46.72	45.39	35.10
4	WW	40.82	37.70	30.11
5	SWA	29.78	35.36	36.90
6	SWZ	33.50	30.86	39.78
7	NWA	37.42	38.88	33.76
8	NWZ	40.33	37.07	43.57
9	HM	59.07	51.24	43.24
10	BM	51.73	47.29	38.05
11	TM	39.12	37.23	37.08
12	NA	17.00	24.85	15.96
13	NZ	46.22	44.32	41.55
14	HNA	54.63	45.57	45.82
15	HNZ	28.98	27.11	37.02
16	HB	52.72	50.99	44.94
17	TRM	29.96	27.86	39.58
18	NEA	43.19	41.44	30.02
19	NEZ	36.31	33.12	27.27
20	HFA	51.50	45.32	41.13
21	HFZ	24.13	24.81	32.89
22	HNFA	33.44	33.35	43.48
23	HNFZ	36.13	34.02	33.06
24	SEA	34.72	38.09	27.24
25	SEZ	36.20	37.93	31.10
26	SA	42.81	39.84	34.04
27	SZ	43.49	38.19	26.67
28	TB	47.30	42.11	38.00
29	TRW	33.96	29.34	37.85
Mean macro F1 score [%]		40.48	38.30	36.49
Accuracy [%]		48.33	41.10	39.51

Table 3.3: Table with the results of our neural network ensemble, the ones of Mittermeier et al. (2022) and James (2007). The F1 score for James (2007) is based on their results (Table 2 in the corresponding publication) for classification of ERA40 data from September 1957 to August 2002. The calculations were done without days that were labelled 'undefined'.

weather constellations. In particular Cyclonic Westerly, which is the focus of this study, exhibits significant improvements compared to the classification in previous studies, with increases of +16.04% and +10.4%, respectively. Interestingly, the composite method of James (2007) shows a clear advantage for HNFA and TRM when compared to both neural network approaches, even though it is outclassed in many other Großwetterlagen.

3.4.2 *Additional trials with modified inputs*

In addition to the inputs used to evaluate our neural networks, we attempted various modifications to improve their performance. These attempts are summarised in Table 3.4. The original Großwetterlagen classification by Hess & Brezowsky is based

Method	Mean macro F1 score [%]	Accuracy [%]
Original CNMN network	40.48	48.33
Increased resolution	38.55	47.59
Time	40.59	48.18
Wind u- and v-component	39.63	47.36
Divergence	40.25	48.06
Vorticity (relative)	40.29	48.30
Total column rain water	40.00	47.92
ResNet-18	31.84	42.10

Table 3.4: Additional metrics for modified spatial resolution, additional variables and different architecture in ResNet-18.

on mean sea level pressure and the geopotential height of 500 hPa. We investigated whether additional input variables could potentially enhance the classification of CNMN by providing more information. For this, we added an extra input channel to CNMN, resulting in three input channels. The additional variables we tested, divergence and vorticity, originate from the same ERA20C reanalysis data set and were interpolated and normalised like the data used for evaluation. However, the evaluation of the networks with additional variables did not result in improved performance metrics, but rather faster overfitting. Similarly, we provided the neural networks with additional information in the form of *time*. The time was encoded using trigonometric functions, as described by Deng et al. (2019),

$$t_d = \left\{ \cos\left(\frac{2\pi d}{y}\right), \sin\left(\frac{2\pi d}{y}\right) \right\} \tag{3.6}$$

where d represents the current day of the year and y is the total number of days in the given year. This information is encoded into two parameters, as using only one trigonometric function would result in the same representation for two days each year. The encoded time was inserted into the linear layer at the end of the network (see Fig. 3.2 for the architecture). In another attempt, we used the original spatial resolution of $1.125^\circ \times 1.1214^\circ$ from the ERA20C dataset. CNMN can handle

data from data sets with higher resolution because the global average pooling layer reshapes them to size 1×1 before they enter the linear layer.

Finally, we tested the ResNet-18 architecture (He et al., 2016) for the classification of Großwetterlagen. The ResNet (Residual Neural Network) architectures are widely used convolutional neural networks, having gained popularity after winning the ImageNet 2015 competition. We utilised it because image classification and classification of weather patterns are basically the same on a fundamental level. Despite training the smallest standard network, ResNet-18 performed poorly compared to our CNMN architecture due to very fast overfitting.

3.4.3 *MPI-GE*

First, we compare the number of days classified as Cyclonic Westerly in the historical period for the MPI-GE ensemble members to those found in the ERA20C data set for 1961-1990 (Fig. 3.5). The analysis indicates that all MPI-GE ensemble

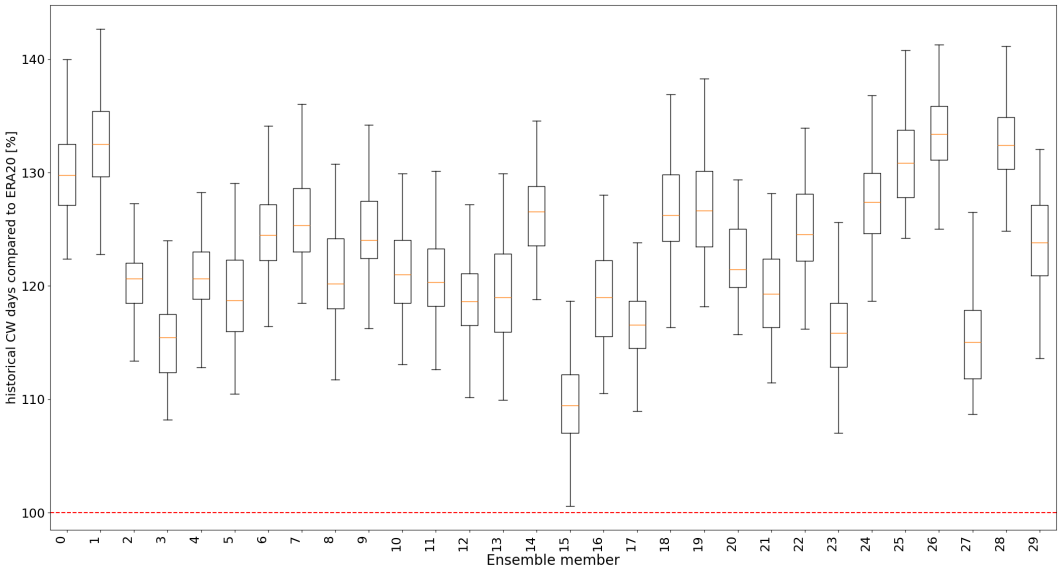

Figure 3.5: Number of days classified as Cyclonic Westerly over the 30 year historical period (1961-1990) for the 30 ensemble members of MPI-GE in percentage of the number classified in ERA20C for the same time period. The percentages were calculated for each of the 50 neural networks separately. Outliers that fall outside the whiskers of the boxplots are excluded from the visualisation.

members differ in the number of Cyclonic Westerly days by approximately +23% on average over the 30-year period. The uncertainty introduced by the random initialisation of the 50 neural networks accounts for only 16% of the total uncertainty, while the internal climate variability of 30 MPI-GE ensemble members has a much greater impact. These calculations are based on the differences in variability for one network and all MPI-GE ensemble members, as well as the variability observed for 50 neural networks and the same MPI-GE ensemble member.

For analysis of changes in the future (2071-2100), we divided the year into two seasons: summer and winter. The summer season runs from 16th April to 15th October, while the winter season runs from 16th October to 15th April. Fig. 3.6

reveals that both seasons show different trends under climate change. During

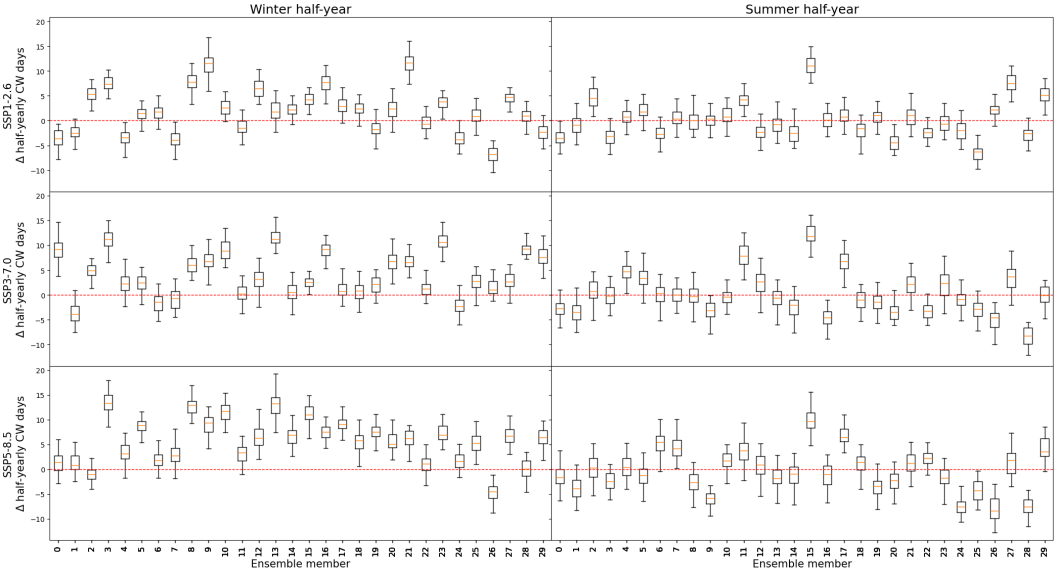

Figure 3.6: Changes to the number of annual CW days in MPI-GE for the three future climate change scenarios SSP1-2.6, SSP3-7.0, and SSP5-8.5 for the far future (2071-2100) when compared to their historical reference period (1961-1990). The left hand side is the winter half-year (16th October to 15th April) while the right side is the summer half-year (16th April to 15th October). Outliers that fall outside the whiskers of the boxplots are excluded from the visualisation.

winter seasons, there is a growing number of ensemble members projecting an increase in semi-annual Cyclonic Westerly days for stronger emission scenarios. For SSP1-2.6, 20 out of 30 members project an increase in Cyclonic Westerly days, which rises to 28 members for SSP5-8.5. On average, the number of CW days increases by 2.01 days (SSP1-2.6), to 4.07 days (SSP3-7.0), and lastly, up to 5.70 days (SSP5-8.5) per winter season.

The summer half-year shows no clear trend, with a slight majority of the members favouring a minor decrease of CW days. For SSP1-2.6, half of the members project an increase of days with Cyclonic Westerly in the summer season, while the other half shows a decrease, resulting in an average change of +0.2 days throughout the ensemble. For both SSP3-7.0 and SSP5-8.5, the ensemble members are similarly split, with roughly half the members in favour of each type of change. This results in an average close to zero, with a difference of -0.5 days under the strongest climate change scenario, SSP5-8.5. There is noticeable variability between the members, even within the same model, for both future changes and the historical time period. The standard deviation for the historical reference period over all 1500 data points (30 ensemble members and 50 neural networks) for each of the three scenarios is around 4.5 days.

3.4.4 *CMIP6 models*

When comparing the number of days classified as Cyclonic Westerly in the 31 CMIP6 models to ERA20C reanalysis data for the historical reference period, a

significant variation is evident among the models (Fig. 3.7). Most models show

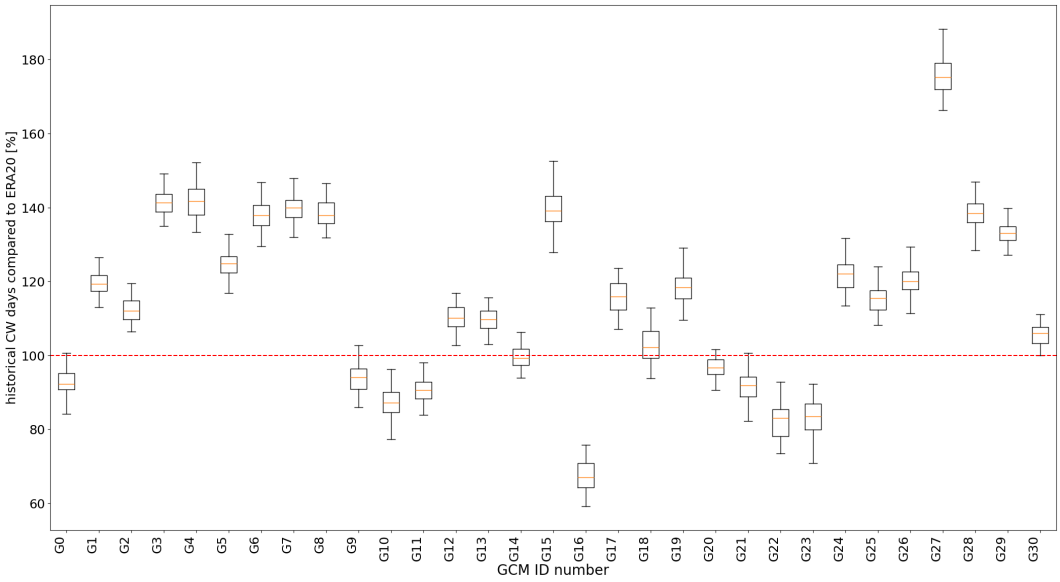

Figure 3.7: Number of days classified as Cyclonic Westerly over the 30 year historical period (1961-1990) for the 31 CMIP6 models (see Table 3.2 for the corresponding names) in percentage of the number classified in ERA20C for the same time period. The percentages were calculated for each of the 50 neural networks separately. Outliers that fall outside the whiskers of the boxplots are excluded from the visualisation.

a higher number of Cyclonic Westerly days, with NorESM2-LM (G27) showing the largest divergence of approximately 70%. Many other models overestimate the number of Cyclonic Westerly days by around 20-40%. Nearly a third of the models underestimate the number of Cyclonic Westerly days, but usually within a 20% difference of the historical numbers from ERA20C data. EC-Earth3-Veg-LR (G14), INM-CM5-0 (G17), and KACE-1-0-G (G20) are the three models that closely match the historical values for ERA20C.

The 31 CMIP6 models show clear trends under climate change in the future (2071-2100, Fig. 3.8). Like in Chapter 3.4.3, the year is divided into two halves: the winter half-year (16th October to 15th April) and the summer half-year (16th April to 15th October). The 31 CMIP6 models project an increase in the number of semi-annual Cyclonic Westerly days during the winter half-year. Two-thirds of the CMIP6 members project an increase under scenario SSP1-2.6, with an overall average change of 1.93 additional days of Cyclonic Westerly per year for the winter seasons. This trend increases under SSP3-7.0 and culminates in SSP5-8.5, where all but one model project an increase. The mean over all models increases to 8.31 additional Cyclonic Westerly days during the winter season in SSP5-8.5. Most models, such as EC-Earth3-Veg, show a steady increase for stronger emission scenarios. However, there are some exceptions, such as ACCESS-CM2, which shows a decline in Cyclonic Westerly days for SSP3-7.0 before rising again in SSP5-8.5. Similarly to MPI-GE, an increasing number of models project the same trend with a stronger climate change signal, but the numbers projected by the individual models do not necessarily increase significantly. Some models project changes roughly

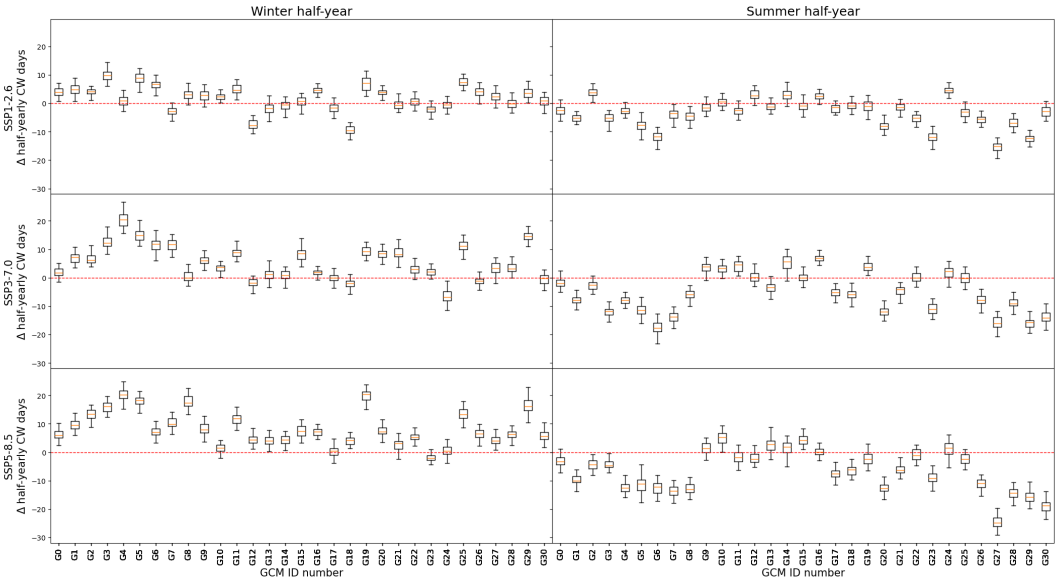

Figure 3.8: Changes to the number of annual CW days in the 31 CMIP6 models (see Table 3.2 for the corresponding names) for the three future climate change scenarios SSP1-2.6, SSP3-7.0, and SSP5-8.5 for the far future (2071-2100) when compared to the historical reference period (1961-1990). The left hand side is the winter half-year (16th October to 15th April) while the right side is the summer half-year (16th April to 15th October). Outliers that fall outside the whiskers of the boxplots are excluded from the visualisation.

within the same range throughout all three scenarios, while others increase with higher scenarios.

In the summer half year the models overall tend to project a decrease in Cyclonic Westerly days, but not all models point in the same direction. For the summer half year the mean over all model projections is -3.5 days for SSP1-2.6 and decreases further in the following scenarios to -5.02 days under SSP3-7.0 and -6.60 days under SSP5-8.5. For all three scenarios more than 60% of the models project a decrease. There are some models like EC-Earth3-Veg-LR that continuously project a slight increase, while most others don't.

3.5 DISCUSSION

Comparing the performance of our CNMN network architecture with the results of James (2007) and Mittermeier et al. (2022) showed an improvement in the classification for the majority of weather systems. While the performance is only slightly better for some Großwetterlagen, it was especially enhanced for Cyclonic Westerly. The improved classification skills by CNMN can be mostly attributed to the new network architecture, because we aimed to closely replicate the training conditions described in (Mittermeier et al., 2022) to enable a direct comparison.

Our convolutional neural network is deeper and features 912K trainable parameter, which is larger than the networks in the previous study, which had 144K. State-of-the-art networks have significantly improved in classification skill over the last decade, partly due to the increased depth and size of the networks. However,

it is important to note that simply increasing the size of the architecture does not lead to better results in our case. As demonstrated, the larger Resnet-18 with 11.2M trainable parameter performs worse than our smaller CNMN network due to faster overfitting. Despite the extreme similarities between image classification and the classification of weather pattern, it is worth noting that the amount of available training data and the size of the utilised architecture in this study are significantly smaller than those used in state of the art image classification. For comparison: CoCa (Yu et al., 2022), a network with 2100M trainable parameters, achieved the third best performance (as of February 2024) on the ImageNet data set (Russakovsky et al., 2015), which consists of 14,197,122 annotated images; a much larger amount when compared to our 29,585 days of Großwetterlagen. We currently lack the necessary training data to prevent overfitting on deeper and wider networks (Liu et al., 2016), even when utilising techniques like data augmentation to increase the amount of available training data. Many common data augmentation techniques, such as mirroring or rotating the input data cannot be applied in our study as the location of, e.g. pressure systems, matters for the correct classification. This makes it important to strike a balance between larger networks and faster overfitting.

Our attempts to overcome the size limitation of the neural network by utilising additional variables from the ERA20C data set did not lead to better results. The neural networks seem to be unable to acquire additional information that would assist in the classification of weather patterns. Instead, overfitting occurs at a faster rate due to the additional parameters introduced with the additional input channels. Even if the additional variables had improved accuracy, fewer CMIP6 models would have been available for this study due to the absence of the required variables in some of the CMIP6 model data provided on the ESGF portal. Similarly, it was found that the networks perform well when trained on the coarse resolution data (about $2.8° \times 2.8°$, see Chapter 3.2.1) but training on the higher resolution data did not lead to an improved performance. This is caused by the large-scale character of the Großwetterlagen do not require fine details for their classification. Another advantage of coarse resolution is that it requires less training time, and the output resolution of the CMIP6 models is less of a concern. The reason for the worse performance of higher resolution data is that the network architecture settings, such as kernel size, were selected based on the coarse resolution. Although the inclusion of time improved the F1-score of the network, it resulted in a lower overall accuracy due to Cyclonic Westerly being classified less accurately. Similarly, using time as an input variable for the channels instead of adding it in the linear layer did not improve the overall classification of Cyclonic Westerly. For this study, we chose not to include time as an input due to its unknown impact on the classification in future scenarios.

The analysis of the MPI Grand Ensemble revealed noticeable variability even among members of the same ensemble. It is therefore important to point out that our comparison between the frequency of Cyclonic Westerly in the ERA20C reanalysis data and the historical CMIP6 runs (Fig. 3.7) should not be seen as a direct measure of the models' ability to represent weather systems accurately. This is because we may have randomly selected an ensemble member that performs

better or worse than the average ensemble member of a certain model, in case there was more than one run available. However, it is evident that some models more closely match the reanalysis data than others. Due to the data augmentation used during the training it is unlikely that potential biases in the global climate model data for the mean sea level pressure and geopotential height significantly influence the detection of Cyclonic Westerly by CNMN. Similarly, we did not sort the models based on how closely they match the reanalysis data, because a good representation of the past does not necessarily mean a good representation of the future.

Although there are variations in the accuracy of the historical representation, the CMIP6 models and the ensemble members of MPI-GE exhibit clear trends for the winter season. We found that the models project an increase in the number of annual Cyclonic Westerly days. This trend becomes more pronounced for the scenarios with a stronger climate change. If it is assumed that the internal variability of MPI-GE is similar to the other CMIP6 members, it can be concluded that the overall change signal is larger than the internal variability. These results are based on a wide range of the most recent global climate models, increasing the robustness of this signal.

A higher frequency of Cyclonic Westerly, known for strong winds and precipitation, suggests a higher chance for compound flood events in the future. Winter is already the primary season for those events in northern Europe, since this is where storm surges mostly occur (Liu et al., 2022b). Compound events can also occur on a small scale and may pose problems for inland drainage, potentially leading to inland flooding behind the dykes in severe cases. One example of this issue can be seen at the Leysiel tidal gate in northern Germany. A tidal gate is a closeable water passage in a dyke. Depending on the tide, it is normally closed when the water level is higher on the sea side, whereas it is opened when the water level is lower on the sea side. Strong winds that generate high waves and sea level may hinder the opening of the tidal gates for multiple tide cycles and cause an increase in the inland water level due to precipitation. The majority of the ten highest inland water levels over the past 22 years occurred during the Großwetterlage Cyclonic Westerly (Table 3.5). An increase in Cyclonic Westerly, in addition to sea level rise, would therefore pose an even bigger challenge for inland drainage. The two previous studies on future changes to Großwetterlagen found no such changes. James (2006), using their composite method, attributed this to the internal variability of the HadGEM1 which they had used for their analysis. However, we have overcome this limitation with 31 global climate models. Another important factor are the significant advancements that global climate models have made since their work was published. Mittermeier et al. (2022) reported no median change in the number of Cyclonic Westerly days during winter under SSP3-7.0 for a single-model initial-condition large ensemble, whereas our work assessed a larger variety of models.

Other studies utilised different weather pattern classification methods to investigate changes to atmospheric circulation. Huguenin et al. (2020) used a classification that is based on Großwetterlagen, which created 10 circulation types. Analysing 19 CMIP5 models they found no frequency changes in winter for their circulation types. Hansen et al. (2023), utilising Simulated Annealing and Diversified Random-

Date	T-3	T-2	T-1	T
2002-02-23	NWZ	NWZ	NWZ	NWZ
2002-10-28	CW	CW	CW	CW
2003-12-15	CW	CW	CW	CW
2004-02-01	TRM	TRM	CW	CW
2007-01-12	CW	CW	CW	CW
2007-01-19	WA	CW	CW	CW
2007-12-08	CW	CW	CW	TRM
2011-12-09	CW	CW	CW	CW
2012-01-04	CW	CW	CW	CW
2015-11-19	CW	CW	CW	CW

Table 3.5: Dates of the ten highest observed inland water levels in Leysiel, Germany during the past 22 years and observed Großwetterlagen at the same day (T) and the x days before (T-x). See Table 3.1 for the acronyms.

ization to group sea level pressure fields into 10 circulation types, also did not find any significant increase in westerly flow circulation types for the winter. On the other hand, several studies have reported an increase in westerly circulation types, which is consistent with our findings. For example, Hoy et al. (2014) found that westerly inflow has increased in the recent past, leading to higher precipitation in northern Europe. Similarly, Cahynová & Huth (2016) categorised daily sea-level pressure fields over Europe for 1961-2000 into 24 circulation types and reported an increasing frequency of westerly types. Rohrer et al. (2017) analysed climate projections for the Alpine region and found a decrease in winter easterlies and an increase in westerlies until the end of the current century. Demuzere et al. (2009) also reported similar changes in Europe under climate change, using the Lamb weather types for the ECHAM5-MPI/OM climate model. Stryhal & Huth (2019) conducted a study on 25 CMIP5 global climate models over the British Isles and central Europe. They found an increase in westerlies, but noted that the strength depends on the classification used.

For the summer season, a contrary trend has been noted with the majority of models projecting a decrease in Cyclonic Westerly days. This signal is even stronger for scenarios with higher greenhouse gas emission. While the overall mean of the CMIP6 models shifts, some models project little to no change or even an increase under SSP5-8.5. This is in contrast to the winter season where almost all global climate models project a shift in the same direction. These results are consistent with the findings of Otero et al. (2018). They employed Jenkinson-Collison classification, which is based on mean sea level pressure to analyse ten CMIP5 global climate models. They discovered a decrease in westerlies during the summer months under SSP8-5.8 for 2081-2100. Herrera-Lormendez et al. (2023) followed up on this research with an analysis of 21 CMIP6 models and found a decrease in the frequency of westerlies in the summer months.

Several studies, e.g. Osman et al. (2021), suggest that climate change may cause a poleward shift of the North Atlantic jet in the future. It is uncertain how the neural network classification would respond to large-scale changes in weather systems, as model data from future scenarios may become too dissimilar to the reanalysis data on which the neural networks were trained. We therefore investigated whether the days identified by the networks as Cyclonic Westerly had the same synoptic patterns in both historical and future data. To do this, we created composites of the days classified as Cyclonic Westerly by the networks for each CMIP6 model and their corresponding historical and future scenarios (Fig. 3.9). We then calculated

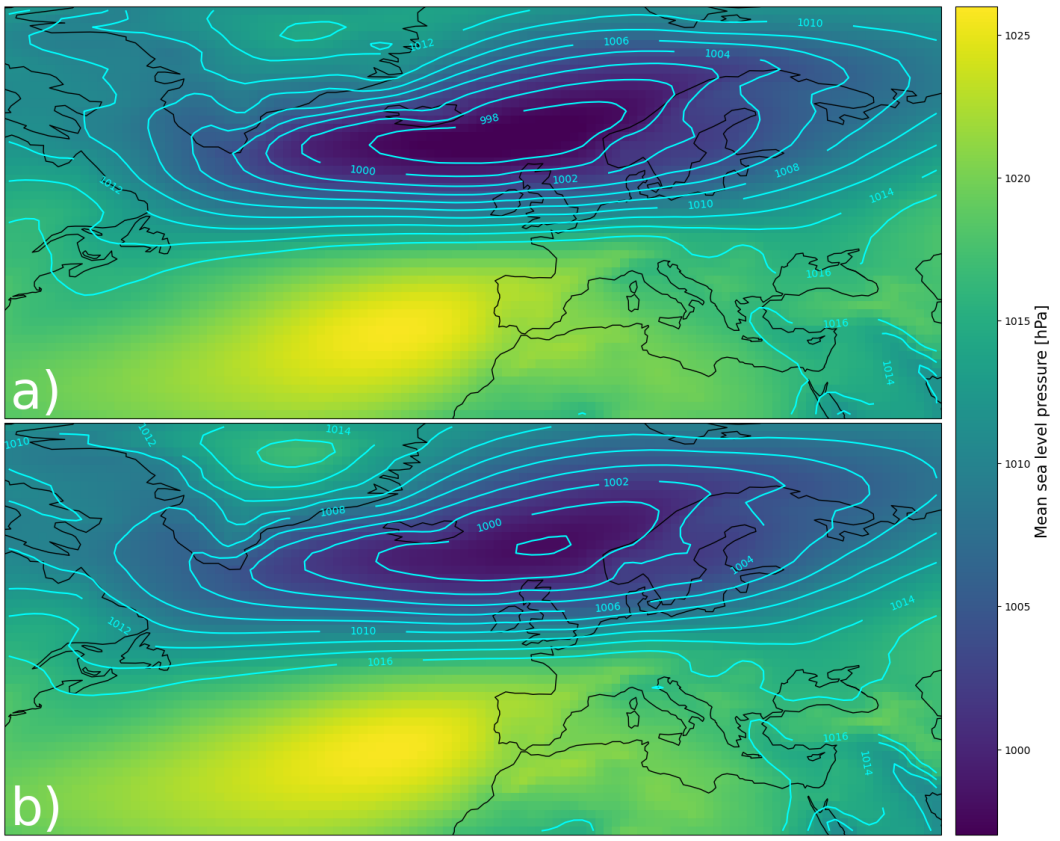

Figure 3.9: The figure displays composites of mean sea level pressure for days with Cyclonic Westerly in a) the historical data and b) the SSP5-8.5 scenario in EC-Earth3-Veg-LR as an example.

the Pearson correlation coefficient between the historical composites and those of the future scenarios. A Pearson correlation coefficient of 0.999 was obtained for all CMIP6 model-scenario combinations, showing that the networks still detect the same weather patterns under climate change. Although there are no spatial shifts, there is an increase in the geopotential height values in the composites of days with Cyclonic Westerlies. Those findings are in line with the increase under climate change in 500 hPa geopotential height reported by Ozturk et al. (2022).

The results of this study naturally come with some caveats. Although our network's accuracy and F1-score have improved compared to previous work, they are not flawless. Additionally, the CNN's overall accuracy is inherently limited

by the subjective human influence on the classification in the Großwetterlagen catalogue and the 3-day rule. When comparing the historical reference period of the global climate models to the ERA20C reanalysis data, it became apparent that some models have difficulties with correctly representing the frequency of Cyclonic Westerly. As demonstrated, there is a certain amount of variation among the ensemble members of MPI-GE. Unfortunately, many global climate models provide only one or a limited number of ensemble members with the required three scenarios and variables, making it impossible to assess the variation among them.

There are several interesting directions that future research can take to improve on the results presented in this study. One possibility to improve the classification is the construction of deeper architectures, that are at the same time less prone to overfitting. In addition to data augmentation, there are other techniques such as gradient penalties, semi-supervised pre-training, channel shuffle, and many others that are used to reduce overfitting during training, but were beyond the scope of the current study. Another option is to consider the temporal aspect of the data which has so far not been utilised. Currently, classification is based on the daily mean of a single day, but with ERA20C's 3-hourly data, it could be classified similar to a video, which is simply a sequence of images. While there are networks available for classifying video clips, they may be too large and prone to overfitting. It is important to note that, for a study similar to ours, collecting the necessary CMIP6 data on a sub-daily scale may be difficult as they are not readily available for most global climate models. One alternative approach could involve taking into account the surrounding days during the classification process for the 3-day rule.

3.6 CONCLUSION

Previous studies have demonstrated that Großwetterlagen can serve as a proxy for extreme or compound events (see Chapter 2). In this study, we utilised a convolutional architecture that improved the automatic classification of Großwetterlagen over Europe. This trained network was then utilised to analyse future changes under three climate change scenarios in 31 CMIP6 models and the Max Planck Institute Grand Ensemble. This is one of the first studies to conduct weather pattern classification for Europe for a large CMIP6 ensemble. Our analysis showed that there is a certain internal variability among the ensemble members of MPI-GE caused by the different initialisations, with some members deviating from the general trend of more Cyclonic Westerly days in winter. Although the CMIP6 models are the latest generation of global climate models, only a few match closely the frequency of Cyclonic Westerly for the historical reanalysis data of ERA20C. Despite this, the models clearly showed a rise in Cyclonic Westerly days during the winter season, but a decline in the summer.

Projected changes in Cyclonic Westerly days are in line with the general consensus of hotter and dryer summers, while the winter will become wetter. The strength of the change increases under stronger climate change scenarios; from almost no signal under SSP1-2.6 to a very strong signal under RCP5-8.5. As winter is already the primary season for compound flood events, an increase in Cyclonic Westerlies

in the future suggests a potentially higher number of such events. These changes, combined with sea level rise, will pose significant challenges for coastal protection in the future.

3.7 STATEMENTS AND DECLARATIONS

Acknowledgements: We would like to thank Tobias Schanz and Ha Ho-Hagemann for their support.

Data availability: AWI-CM-1-1-MR files are stored on the servers of the German Climate Computing Centre (DKRZ) and were accessed after personal correspondence with Dr. Tido Semmler (Alfred-Wegener-Institut). All other CMIP6 data sets were downloaded via https://esgf-data.dkrz.de/search/cmip6-dkrz/ (last access 29. November 2023). ERA-20C data is available at https://rda.ucar.edu/datasets/ds626.0/ (last access: 27. August 2023). Großwetterlagen classification provided by the DWD can be accessed at https://www.dwd.de/DE/leistungen/grosswetterlage/grosswetterlage (last access: 15. June 2023). The neural networks and scripts for running them are available on Zenodo: https://zenodo.org/doi/10.5281/zenodo.10959808 (Heinrich, 2024).

Authors' contributions: Philipp Heinrich developed the analysis methods, performed the data analysis and wrote the manuscript. Ralf Weisse and Stefan Hagemann supervised the research activities, discussed the outline of the study and its results, revised the manuscript, and contributed to the interpretation of the results.

Competing interests: The authors declare that they have no known competing financial interests or personal relationships that could have appeared to influence the work reported in this paper.

Funding: This research was financed with funding provided by the German Federal Ministry of Education and Research (BMBF; Förderkennzeichen 01LR2003A). Furthermore, this research is a contribution to the PoFIV program of the Helmholtz Association.

4

CHANGES IN COMPOUND FLOOD EVENT FREQUENCY IN NORTHERN AND CENTRAL EUROPE UNDER CLIMATE CHANGE

CHAPTER SUMMARY

The simultaneous occurrence of increased river discharge and high coastal water levels may cause compound flooding. Compound flood events can potentially cause greater damage than the separate occurrence of the underlying extreme events, making them essential for risk assessment. Even though a general increase in the frequency and/or severity of compound flood events is assumed due to climate change, there have been very few studies conducted for larger regions of Europe. Our work, therefore, focuses on the high-resolution analysis of changes in extreme events of coastal water levels, river discharge, and their concurrent appearance at the end of this century in northern and central Europe (2070-2099). For this, we analyse downscaled data sets from two global climate models (GCMs) for the two emissions scenarios RCP2.6 and RCP8.5. First, we compare the historical runs of the downscaled GCMs to historical reconstruction data to investigate if they deliver comparable results for northern and central Europe. Then we study changes in the intensity of extreme events, their number, and the duration of extreme event seasons under climate change. Our analysis shows increases in compound flood events over the whole European domain, mostly due to the rising mean sea level. In some areas, the number of compound flood event days increases by a factor of eight at the end of the current century. This increase is concomitant with an increase in the annual compound flood event season duration. Furthermore, the sea level rise associated with a global warming of 2 K will result in double the amounts of compound flood event days for nearly every European river estuary considered.

4.1 INTRODUCTION

Floods are worldwide the most common natural disaster (Douben, 2006). Drivers for coastal floods are usually a combination of tides, waves, precipitation, storm surges, and strong river discharge (Zscheischler et al., 2020). They pose a big threat to some of the most important economic centres in Europe and the 50 million people living in the low-elevation coastal zone (Neumann et al., 2015). The damage caused by floods is potentially even higher when two driver of floods, like strong river discharge and high coastal water levels, occur at the same time or in close succession (Seneviratne et al., 2012). Leonard et al. (2014) defined compound flood events as an 'extreme impact that depends on multiple statistically dependent variables or events'. There has been a number of studies conducted for compound flood events in the past, like Hendry et al. (2019) or Zscheischler & Seneviratne

(2017), which found that neglecting the dependence of drivers results in a large underestimation of coastal flood risks. Due to their severe nature, compound flood events are becoming more and more relevant for risk assessment and scientific research.

Due to the large damage that can be caused, it is essential to understand how compound floods will change in the future because of anthropogenic climate change (Zscheischler et al., 2018). To better analyse different climate futures, the fifth Assessment Report (Pachauri et al., 2014) of the Intergovernmental Panel on Climate Change (IPCC) introduced four Representative Concentration Pathways (RCP) scenarios. These pathways represent different possible climate futures based on different developments of factors such as greenhouse gas and aerosol concentrations, or land use (Moss et al., 2010). Recently, the RCP scenarios have been extended by the Shared Socioeconomic Pathways scenarios, which have been used for the climate simulations in the AR6 report (IPCC, 2023). However, due to the availability of required data at high spatial resolution, the present study utilises data from RCP2.6 and RCP8.5 scenarios for assessing future climate change. RCP2.6 assumes a reduction in carbon dioxide emission starting from 2020 and negative emission at the end of the century and is therefore often referred to as the 'peak' scenario (Van Dingenen et al., 2018). This scenario is in line with the goal of the Paris Agreement, which aims to limit the global mean temperature rise to 'well below 2 °C' (United Nations, 2015). It requires a massive reduction in the emission of other greenhouse gases like methane (Van Vuuren et al., 2011a). RCP8.5 on the other hand projects a rise in greenhouse emissions throughout the century and is generally seen as a worst-case scenario (Hausfather & Peters, 2020). Both scenarios are accompanied by a rise in mean sea level which will pose a major threat along the coastlines (Vousdoukas et al., 2018b).

The potential changes in coastal flood damage due to sea level rise were investigated by various studies. Vousdoukas et al. (2020a) estimate up to € 239 billion annual costs from damage caused by coastal flooding towards the end of the century in Europe for RCP8.5 if no countermeasures are taken. The damages caused by coastal floods will therefore represent a noticeable share of some countries' national gross domestic product (GDP) at the end of the century in case of a high-emissions scenario like RCP8.5 (Feyen et al., 2020). Despite those findings, a recent study by McEvoy et al. (2021) revealed that still not all European countries plan for sea level rise and therefore do not improve their flood protection accordingly.

There are several studies that investigated future changes to compound flood events in Europe. Most of them were local, while a few addressed the problem from a global perspective. These comprise, for example, the studies by Bermúdez et al. (2021) for the rivers Mandeo and Mendo in Spain, Harrison et al. (2022) for the estuaries Humber and Dyfi in the United Kingdom, Kew et al. (2013) for the Rhine delta, Klerk et al. (2015) for the Rhine-Meuse delta, Pasquier et al. (2019) for the Broadland River in England, and Poschlod et al. (2020) for Norway. While a European perspective is to some extent inherent in global studies, like in Bevacqua et al. (2020), Ridder et al. (2022), and Couasnon et al. (2020), they lack regional details due to coarse resolution. To the authors' knowledge, the studies of Bevacqua et al. (2019) and Ganguli et al. (2020) are the only ones that analyse future changes

to compound flood events in Europe on a continental scale. Bevacqua et al. (2019) carried out their analysis for the period of 2070-2099 and considered precipitation and sea level under emission scenario RCP8.5. They projected a strong increase of compound flood events, due to the warmer atmosphere allowing storms to carry more moisture, in addition to sea level rise. Ganguli et al. (2020) studied changes under RCP8.5 using high-resolution dynamically downscaled regional climate model simulations available at a EURO-CORDEX domain for the time period 2040-2069. Their analysis focused on discharge and sea level extremes in northwestern Europe. For the majority of locations, they reported a lower risk of compound flood events in the projected scenario due to a lower dependence between storm surges and river discharge extremes, which they attributed to a potential poleward shift of the North Atlantic jet. Furthermore, they noted that considering the projected SLR suggests an increase in compound flood potential across low elevated lands, i.e., ∼30% of sites. Both studies were conducted for different decades of the current century and focused on different drivers. Their results can therefore hardly be directly compared. However, those studies did not provide a detailed analysis on changes in different scenarios. Our work aims to contribute further to this scientific discussion by adding detailed analysis of the scenarios RCP2.6 and RCP8.5 to it.

For the analysis of the dependence of the factors driving compound flood events tail correlation coefficient methods or copulas are often utilised (Xu et al., 2023). They are used to evaluate the complex dependence structures and describe the bivariate joint distribution (Couasnon et al., 2020). For robust estimates, large data sets are needed (Serinaldi, 2013; Serinaldi et al., 2015) which are often unavailable. For this reason we use a Monte Carlo-based approach that is less dependent on sample size (see Chapter 2.2) to study the dependence between drivers of compound flood events.

In the present study, we focus on a detailed analysis of changes in compound flood events in Europe towards the end of the current century (2070-2099). Using high-resolution coastal water levels, discharge data, and regional sea level projections from the Sixth Assessment Report (AR6) of the IPCC, we provide an assessment of future changes in compound flooding across northern and central Europe. The assessment is made for the high-emission scenario RCP8.5 and the low-emission scenario RCP2.6 to account for different climate futures. Especially for RCP2.6 very little scientific analysis in terms of compound flood analysis has been done, with most studies focusing on the more extreme high-emission scenario RCP8.5. First, we compare the historical runs of the dynamically downscaled global climate models to reconstruction data in order to evaluate their skill in representing compound flood events. We used their output to simulate discharge and coastal water levels. Afterwards, we examine how different aspects of extreme events change for the two emission scenarios which includes sea level rise caused by global warming. This is combined with an analysis on how much future developments in coastal water levels and discharge contribute to those changes. Furthermore, we analyse changes in the extreme event seasonality, i.e., the number of months in which extreme events can occur. Additionally, we investigate if future scenarios show differences in the intensity of extreme events. Finally, we look into potential

changes in correlations between discharge and coastal water levels extremes. This enables us to examine if the underlying mechanisms that might cause compound flood events may change in the future.

4.2 DATA

Spatial and temporal consistent long time series of daily river runoff (discharge) and coastal water levels are required to study compound flood events. These were derived from existing climate change scenario simulations at a sufficiently high spatial resolution. We selected two data sets from the COordinated Regional climate Downscaling Experiment (CORDEX; Giorgi et al. (2009)), i.e. from its EURO-CORDEX initiative[1] that provides regional climate projections for Europe at 12.5 km (0.11°) resolution (Jacob et al., 2014). These two data sets comprise regional climate model (RCM) simulations (Chapter 4.2.1) that were dynamically downscaled from simulations of two different global climate models (GCMs). The simulations cover a historical period (1950-2005) and two different future climate scenarios each that range until the end of the 21st century (2006-2099) without any gaps. The RCM simulations were then used to generate the necessary data for the analysis of compound flood events. For one thing, time series of daily river runoff were simulated with the Hydrological Discharge model (Chapter 4.2.2). For another, tide-surge levels were generated with the Tidal Residual and Intertidal Mudflat model (Chapter 4.2.3). A flowchart of the modelling framework can be seen in Fig. 4.1. Note that the choice of the EURO-CORDEX simulations was largely constrained by the data requirements of the coastal water levels simulations. In addition, we utilised long-term reconstructions of river runoff and coastal water levels (Chapter 4.2.4) to evaluate the simulated compound flood events during the historical period.

In our study we consider and analyse data from central and northern Europe. Our analysis region is shown in Fig. 4.2 in which the names of all seas, regions and river catchments that are used in the study are introduced. Figures used in the remainder of this study show only the largest rivers to avoid visual clutter. All together there are 181 river mouths shown by circles, regardless of the rivers being displayed in the following figures.

4.2.1 *EURO-CORDEX data*

In order to generate high-resolution water level data, hourly data of near-surface (10 m height) wind components and sea level pressure are required (see Chapter 4.2.3). At the time of the study, only two data sets from the EURO-CORDEX archive were available to us that fulfilled this requirement. Both data sets comprise historical simulations from 1950-2005, and two scenarios following the Representative Concentration Pathways RCP 2.6 and 8.5 (Van Vuuren et al., 2011b), which span from 2005 until the end of the 21st century. The historical simulations are not based on reanalysis and can be only compared in a statistical sense.

1 https://www.euro-cordex.net/

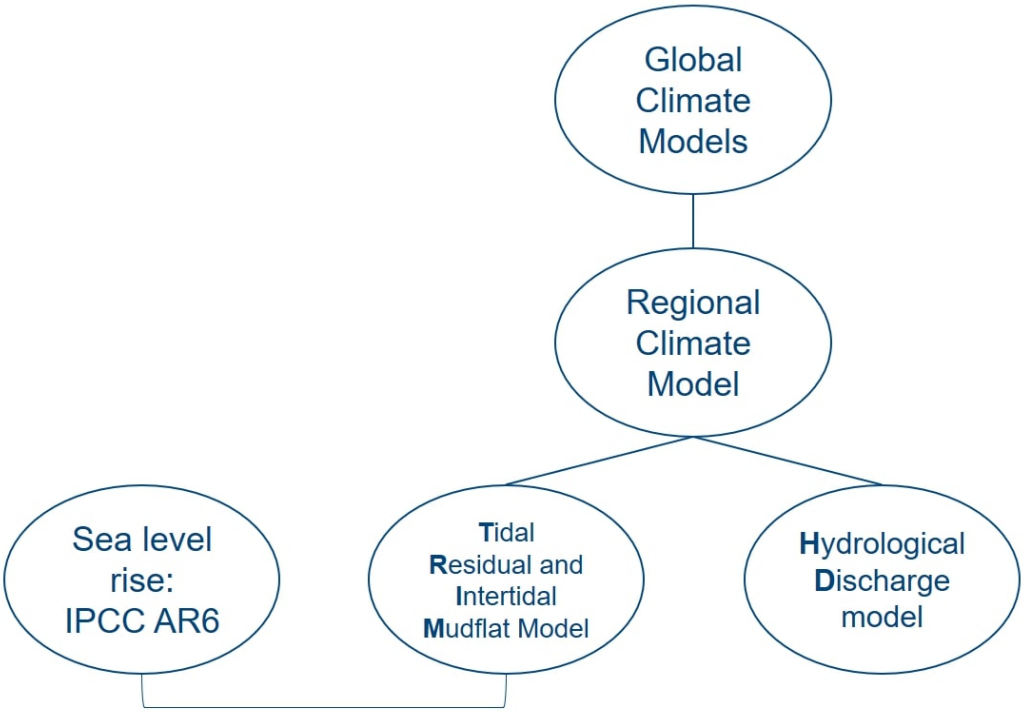

Figure 4.1: Flowchart of the modelling framework for the REMO-MPI and REMO-Had data.

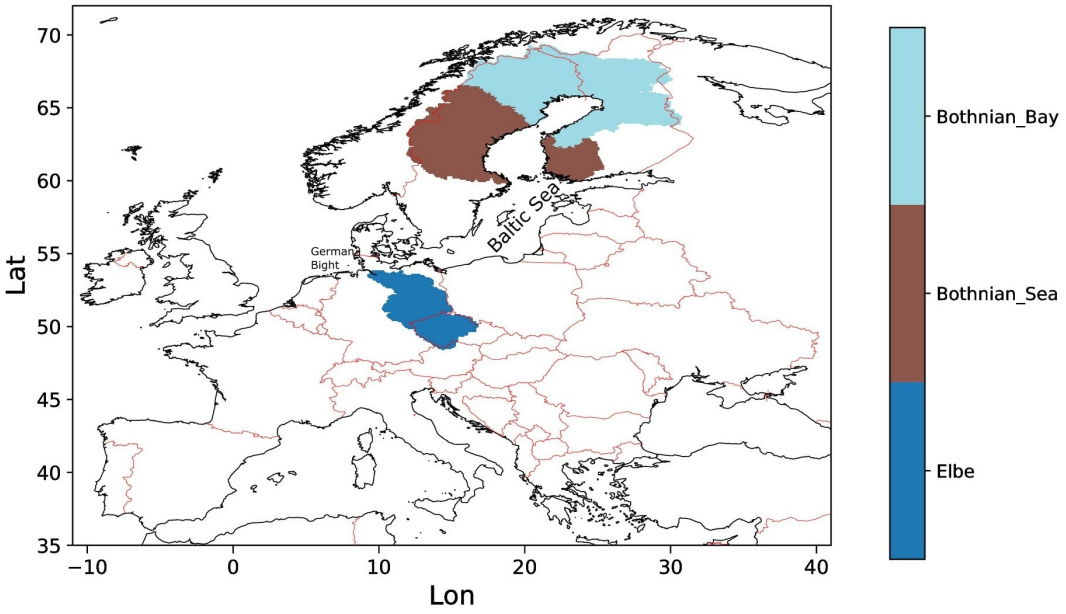

Figure 4.2: This image displays the seas, catchments, and regions that are mentioned by name in this study. The first two entries in the colourbar are catchment areas of rivers that discharge into the Bothnian Bay and Bothnian Sea. The last entry is the catchment area of the river Elbe.

We used two available atmospheric data sets, REMO-MPI and REMO-Had (see below), originating from two different GCMs that were dynamically downscaled to the EURO-CORDEX 0.11° domain with two different versions of the RCM REMO (Jacob et al., 2007). REMO is a three-dimensional, hydrostatic, atmospheric circulation model within a limited area, which is hosted at the Climate Service Center Germany (GERICS). The forcing data from the global simulations are prescribed at the lateral boundaries of the European domain with an exponential decrease towards the centre of the model domain. The main direct influence of the boundary data lies in the eight outer grid boxes using a relaxation scheme according to Davies (1976). Both REMO versions used 27 hybrid sigma-pressure levels, which follow the surface orography in the lower levels but are independent from it at higher atmospheric model levels.

4.2.1.1 *REMO - MPI*

In REMO-MPI, the global climate simulations were conducted with MPI-ESM, the Earth System Model (ESM) of the Max Planck Institute for Meteorology (Giorgetta et al., 2013). The MPI-ESM consists of coupled general circulation models for the atmosphere and the ocean, and their subsystem models for land and vegetation and for the marine biogeochemistry, respectively. For the atmosphere, the LR configuration was used with a T63 (∼1.9°) horizontal resolution and 47 hybrid sigma-pressure levels, while the ocean utilised a bipolar grid with 1.5° resolution (near the equator) and 40 z-levels. The two RCP scenario simulations cover actual years for the period 2005-2099. The MPI-ESM simulations were downscaled with REMO2009 (Jacob et al., 2012).

4.2.1.2 *REMO - Had*

REMO-Had has utilised global climate simulations that were conducted with HadGEM2-ES, the ESM of the UK Met Office Hadley Centre (Jones et al., 2011). HadGEM2-ES is a coupled atmosphere-ocean GCM that also represents interactive land and ocean carbon cycles as well as dynamic vegetation. It was setup with an atmospheric resolution of N96 (1.875° × 1.25°) and 38 vertical levels and an ocean resolution of 1° (increasing to 1/3° at the equator) and 40 vertical levels. HadGEM2-ES simulations are run with 30-day months and the two RCP scenario simulations cover the period 2005-2099. The HadGEM2-ES simulations were downscaled with REMO2015 (Remedio et al., 2019).

4.2.2 *River Runoff - HD model*

River runoff was simulated with the hydrological discharge (HD) model (Hagemann et al., 2020) covering the entire European catchment region. The HD model v. 5.0 (Hagemann & Ho-Hagemann, 2021) was set up over the European domain covering the land areas between -11° W to 69° E and 27° N to 72° N with a spatial grid resolution of 5′ (ca. 8-9 km). The HD model separates the lateral water flow into the three flow processes of overland flow, baseflow, and riverflow. Overland flow and baseflow represent the fast and slow lateral flow processes within a grid box, while

riverflow represents the lateral flow between grid boxes. The HD model requires gridded fields of surface and subsurface runoff (drainage) as input for overland flow and baseflow, respectively, with a temporal resolution of one day or higher. These input fields of surface runoff and drainage were taken from the REMO simulations and interpolated to the HD model grid to simulate daily discharges.

4.2.3 *Coastal Water Levels*

Coastal water levels are the result of an interplay of different factors that are considered in different ways. Strong onshore winds that push water masses towards the coast cause a rise of the sea surface that is commonly referred to as a storm surge. When storm surges coincide and interact with high tides the resulting water level is often referred to as storm-tide level. When mean sea level rises, this will further increase storm tide levels. In the following, we refer to storm tide levels including the effects of mean sea level rise as coastal water levels.

Daily tide-surge levels were obtained from tide-surge simulations with the Tidal Residual and Intertidal Mudflat Model (TRIM). In particular, a 2D version of TRIM-NP (Kapitza, 2008) was used which is a nested hydrostatic shelf sea model with spatial resolutions increasing from 12.8 km $\times$ 12.8 km in the North Atlantic to 1.6 km $\times$ 1.6 km in the German Bight. Zonal and meridional wind components at 10 m height and sea level pressure from the REMO-MPI and REMO-Had simulations were used as hourly atmospheric forcing fields to derive tide-surge levels in the German Bight. To include tides, data from the FES2004 atlas (Lyard et al., 2006) were used at the lateral boundaries.

4.2.4 *Long-term reconstructions*

In order to evaluate compound flood events during the historical period (see Chapter 4.4.1), we utilised two long-term reconstructions for discharge and three tide-surge data sets. The two daily discharge data sets are based on consistent long-term reconstructions by the global hydrology model HydroPy (Stacke & Hagemann, 2021) and the hydrological discharge (HD) model (Hagemann et al., 2020). To generate these data sets, both models were forced with the ERA5 reanalysis (Hersbach et al., 2020) of the European Centre for Medium-range Weather Forecasts (ECMWF) for the time period 1979–2018 and E-OBS data (Cornes et al., 2018) for 1950–2019. Both discharge data sets cover the same European domain as described in Chapter 4.2.2. The data sets were published as Hagemann & Stacke (2021), and their generation and evaluation is described in Hagemann & Stacke (2023).

The three tide-surge reconstructions were generated by two different shelf sea models. In the first two reconstructions, the TRIM model was forced with the high-resolution regional re-analysis COSMO-REA6 of the German Weather Service (DWD) for the period 1995-2018 (Bollmeyer et al., 2015). In the second and third reconstruction, COSMO-REA6 data and data from the regional climate reconstruction coastDat3 (Petrik & Geyer, 2021) were used to force the physical part of the marine ECOSystem MOdel (ECOSMO) (Daewel & Schrum, 2013; Schrum & Backhaus, 1999) for the period of 1948–2019 (BSH, 2022).

Further information on the models, reconstructions and their evaluation are available for the HD5-ERA5 and HD5-E-OBS data in Hagemann & Stacke (2023), for ECOSMO-coastDat3 in BSH (2022), as well as for TRIM in Gaslikova et al. (2013) and Weisse et al. (2015).

4.2.5 *Mean Sea Level Rise*

While changing tide-surge levels are primarily a result of changing wind climatology, changes in total coastal water levels are a result of both, changing tide-surge levels and rising mean sea levels. While changes in tide-surge levels can be obtained from the described model simulations, rising mean sea levels remain unaccounted for. In a first approximation, both effects may be added linearly (Howard et al., 2010; Sterl et al., 2009) although some errors will be introduced in shallow waters caused by the modification of tide-surges through rising mean sea level (Arns et al., 2015). Non-linear effects are typically in the order of a few centimetres for sea level rises up to 5 m (Howard et al., 2010) which can still be considered small compared to uncertainties from other neglected effects such as changing bathymetry (Benninghoff & Winter, 2019).

While for tide-surge and discharge simulations we used atmospheric forcing for the two RCP scenarios of IPCC AR5, we were unaware of regionalized sea level projections for those scenarios. We, therefore, used 50th percentiles of corresponding regionalized projections from the IPCC AR6 (Fox-Kemper et al., 2021; Garner et al., 2021; Kopp et al., 2023) for the Shared Socioeconomic Pathways (SSP) scenarios SSP1-2.6 and SSP5-8.5 (see Fig. 4.3). The SSP scenarios approximately correspond

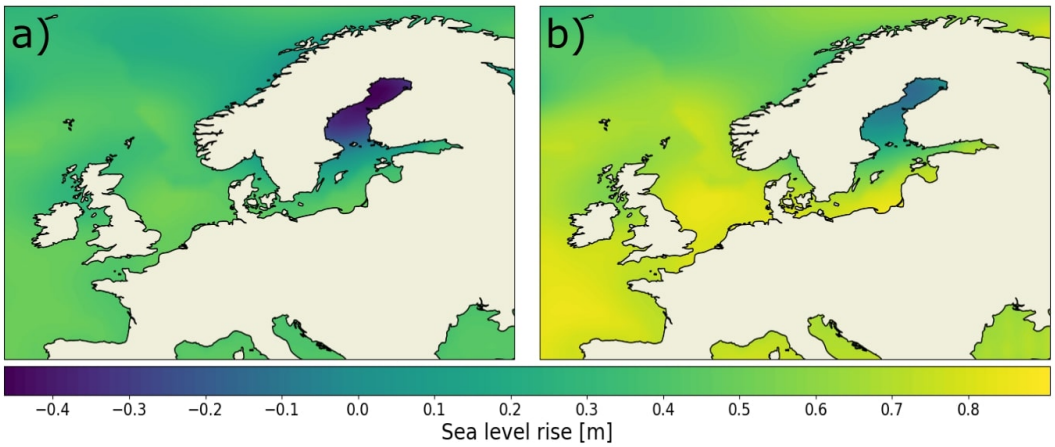

Figure 4.3: Projected relative sea level rise by 2099 in Europe for the 50th percentile a) SSP1-2.6 and b) SSP5-8.5 based on medium confidence scenario (Garner et al., 2021).

to the RCP scenarios with the same label (Meinshausen et al., 2020). Given that the ranges of projections by 2100 are in the order of several decimetres, the error introduced by this approach is probably small. Relative regional sea level was used so that vertical land movements are accounted for. The latter is particularly important in the Baltic Sea where ongoing glacial isostatic adjustment (GIA) is

large (Weisse et al., 2021). The region around the Gulf of Bothnia experiences a relative sea level fall, contrary to the rest of Europe. To obtain estimates of total coastal water levels the 50th percentiles derived from these projections were linearly added to the corresponding tide-surges obtained from the model simulations.

4.3 METHODS

4.3.1 *Compound flood events*

There are several ways to identify extreme events, with no standardised method being used in published research. The goal is always to manage the trade-off between finding a low number of extremes because they are rare per definition, while at the same time having enough data points for statistical analysis. Two commonly used methods are block maxima (for example, in Moftakhari et al. (2017)) and Peaks over Threshold (POT) (for example, in Fang et al. (2021)), both having their upsides and downsides which were discussed in studies like Jaruskova & Hanek (2006) or Ward et al. (2018). Here, we chose Peaks over Threshold and followed a percentile-based approach for each river individually since we otherwise might miss out on events if, for example, two extreme events occur in one year. For both the water level and discharge data sets, we started at the 90th percentile. We then continued to raise the percentile in small incremental steps until the resulting thresholds for each river yielded on average two extreme events per year. This was done for the historical runs, with the same thresholds being used for future scenarios unless stated otherwise. To ensure that extreme events identified that way are independent of each other we additionally applied a de-clustering algorithm that guaranteed that different extreme events are separated by at least three days. Due to the scale of the study domain it is not feasible to employ a site specific de-clustering time for each individual river. Therefore, we chose a time that was used by previous large scale studies like Ward et al. (2018) and Bevacqua et al. (2019). In other words, all events that are less than four days apart from each other are considered to belong to the same extreme event. An event was counted as a compound event when an extreme discharge and extreme coastal water level event occurred on the same day. Some studies use temporal delay (*lag*) to account for the delays between variables reacting to an event. Ganguli & Merz (2019) calculated the lag based on the catchment area, but for long rivers like the Elbe the actual delay heavily depends on the location of the occurring precipitation. We did not utilise lag so that we only detect events where the variables are extreme at the same time.

4.3.2 *Dependence between drivers*

We utilised a Monte Carlo-based approach to identify those rivers in which compound flood occurred more frequently than expected for uncorrelated drivers. Compound flood events in rivers that show a higher number of compound flood events than expected by chance might have a common driver. For this analysis, we limited the data sets to the winter seasons, since this is where storm surges mostly occur in northern Europe (Liu et al., 2022b). To remove possible correlations

between the data sets we shuffled the tide-surge data. This creates a data set where discharge and tide-surge data are independent. Afterwards, we counted the number of compound flood events for the combination of discharge and randomised coastal water level data to see how it changed compared to a data set with possible dependence between extreme events. The process was repeated 10,000 times to create a probability distribution for uncorrelated events for each river. This allowed us to assess whether or not the observed distribution is outside the 95.4% range (2σ) of the distributions for independent drivers which provides an indication for correlated drivers. A more detailed analysis, including the reasoning for our choices, is given in Chapter 2.2.

4.3.3 *Seasonality in compound flooding*

We calculated the duration of each season in order to analyse changes in the seasonality of compound flood events. The duration of a season was defined as the shortest time period that contains at least 90% of the compound flood event days, similar to the definition by Bevacqua et al. (2020). For this, we first counted the number of compound flood event days per month in the time period of the data set, e.g., the number of days that occur each March throughout the entire time period that we analysed. We accumulated the number of days instead of the number of compound flood events to take into account that the length of compound flood events might change in the future, so simply counting the number might underestimate the differences. Furthermore, this approach takes into consideration that a compound flood event might start at the end of a month and continue into the next month. Then we used the NumPy sliding window view function (Harris et al., 2020) to find the shortest combination of months that contained at least 90% of the accumulated compound flood event days. If there was a month without compound flood event days in a season, it was counted as part of it for the sake of continuity.

4.3.4 *Extreme event intensity*

The intensity of extreme discharge events was defined as the average amount of discharge during an extreme event. This means that the intensity is based on the total discharge during this event. These calculations were also done for coastal water levels, where the intensity is the total water height during the extreme event.

4.3.5 *Contributions to changes of future compound flood event frequency*

To disentangle the contributions of the different drivers to future changes in compound flood event frequency, we set up different data set combinations (Table 4.1). As shown in Chapter 4.4.4, tide-surges do not show any significant changes under RCP2.6 and RCP8.5 scenarios, as long as sea level rise is neglected. For the analysis it was important to not distort correlations between extreme events of discharge and coastal water levels because this would influence the number of compound flood event days (Chapter 2). To have a reference, we calculated the number of compound

Purpose	CFEs based on
Reference period	historical discharge and tide-surge
CFE changes caused by changes in discharge	future discharge and tide-surge, but without sea level rise
CFE changes caused by changes to coastal water level	historical discharge and tide-surge with sea level rise 2070-2099

Table 4.1: Purpose of data sets to analyse the contribution of discharge and sea level rise to future compound flood event frequency.

flood event days in both REMO data sets for the historical time period 1976-2005. To test the contribution of discharge to frequency changes in future compound flood events, we used discharge and tide-surge from the future time period 2070-2099 since the historical and future tide-surge levels are nearly identical. Afterwards, we evaluated the contribution of sea level rise by adding it to the tide-surge levels of the historical data sets. This again preserves possible correlations.

4.4 RESULTS

In the following sections we first evaluate the historical runs of our data sets, then investigate the changes of the separate drivers before proceeding to look into future changes to compound flood events.

4.4.1 *Evaluation of historical runs*

Fig. 4.4 shows a comparison between the historical runs of the REMO downscaled global climate models and the reconstruction data HD5-ERA5+TRIM-REA6 for the number of compound flood events over a time period of 24 years. Generally, the REMO data sets show a similar number of compound flood events. Only for the northern coast of Norway and occasionally rivers near the Baltic States a systematic overestimation is obtained. Using the Monte Carlo-based approach (see Chapter 4.3.2), we estimated which rivers show a larger number of compounds than could be expected from uncorrelated drivers. The reconstruction data set of HD5-ERA5+TRIM-REA6 shows a larger number of rivers along the western-facing coasts having a higher number of compound flood events than could be expected by random coincidence of uncorrelated extremes (Fig. 4.4a,b). A comparable pattern could also be identified in the REMO data sets, even though it is less pronounced (Fig. 4.4d,f). A comparison of the REMO data sets with HD5-E-OBS+ECOSMO-coastDat3 and HD5-ERA5+ECOSMO-coastDat3 over a time period of 30 years shows again a slight overestimation like the TRIM-based data sets (Fig. 4.5). No information is available on potential deviations in Norway and parts of western Europe like Ireland, because ECOSMO-coastDat3 covers a smaller domain. As in the reconstruction data sets, the compound flood events in the REMO data sets are mostly limited to the period of November to March.

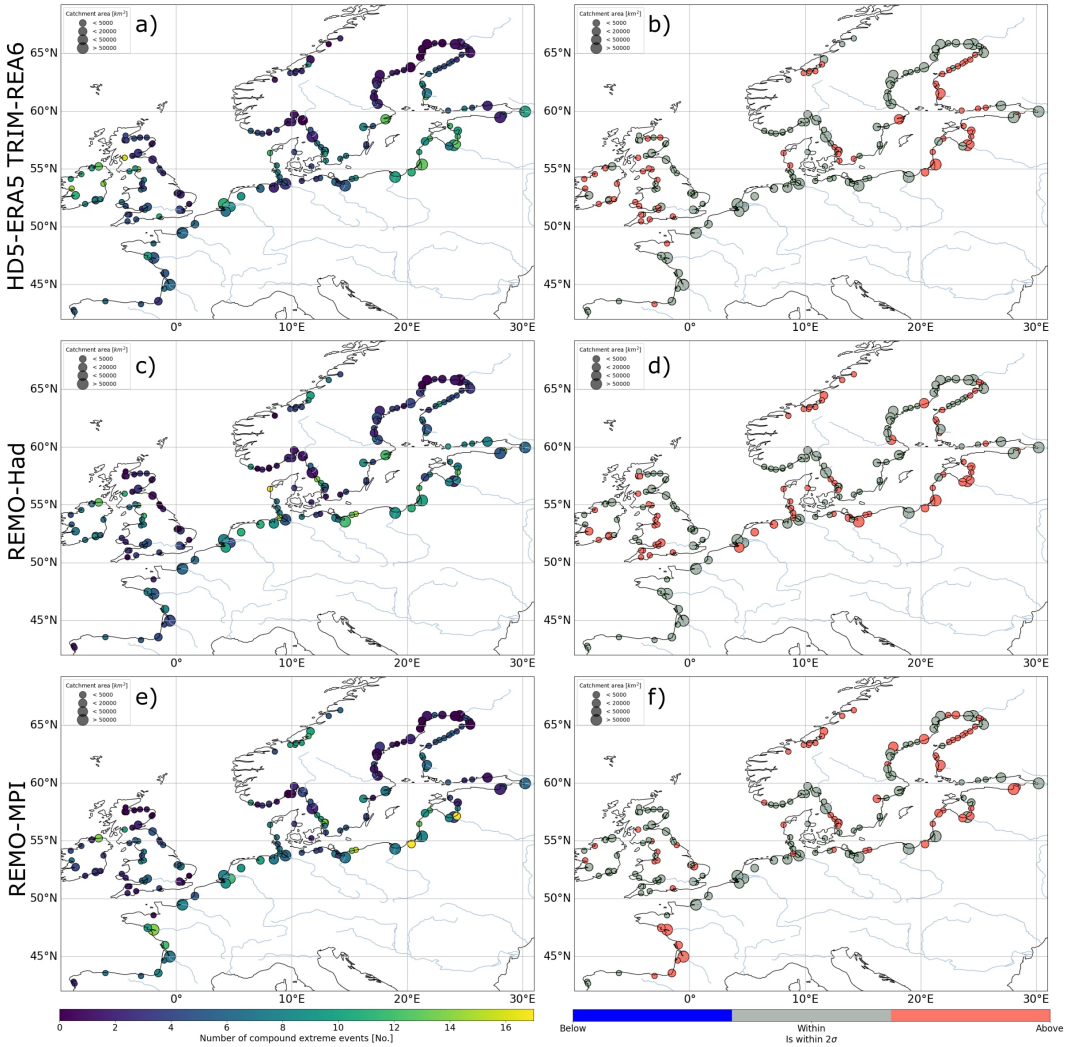

Figure 4.4: Number of compound flood events (left) and dependence/independence between drivers (right) in the HD5-ERA5+TRIM-REA6 reconstruction (top), the REMO-Had (middle) and the REMO-MPI (bottom) historical runs. Colours indicate the number of compound events over 24 years and whether or not this number is within (grey), above (red) or below (blue) the expected 2σ interval derived from randomised Monte Carlo simulations. The size of the circles indicates the catchment area.

4.4.2 *Future changes in discharge*

We investigated changes in the frequency and intensity of discharge extreme events for the two scenarios. Discharge intensity increases for most catchments in Ireland and Great Britain under the RCP 2.6 scenario while it decreases for most of the rivers discharging into the Baltic Sea (Fig. 4.6a,c). Similar changes can be observed for the number of extreme discharge days (Fig. 4.7a,c). Slight disagreements arise between the data sets for central Europe. REMO-MPI projects a decrease in intensity at the western coast of the Bothnian Bay, Great Britain, and the north-facing coasts of France, Germany, and Poland, while REMO-Had projects an increase under RCP2.6 for those regions. For the regions with disagreement, the projected changes

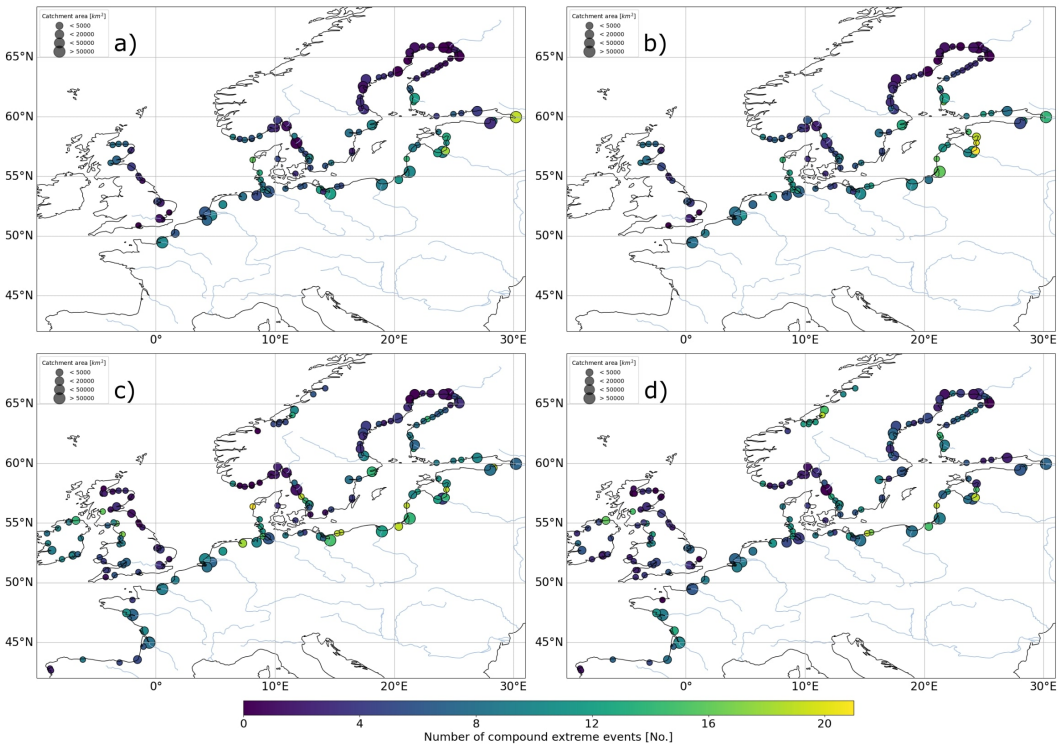

Figure 4.5: Number of compound flood event days over 30 years compared between a) HD5-EOBS20+ECOSMO-coastDat3, b) HD5-ERA5+ECOSMO-coastDat3, c) REMO-Had, and d) REMO-MPI.

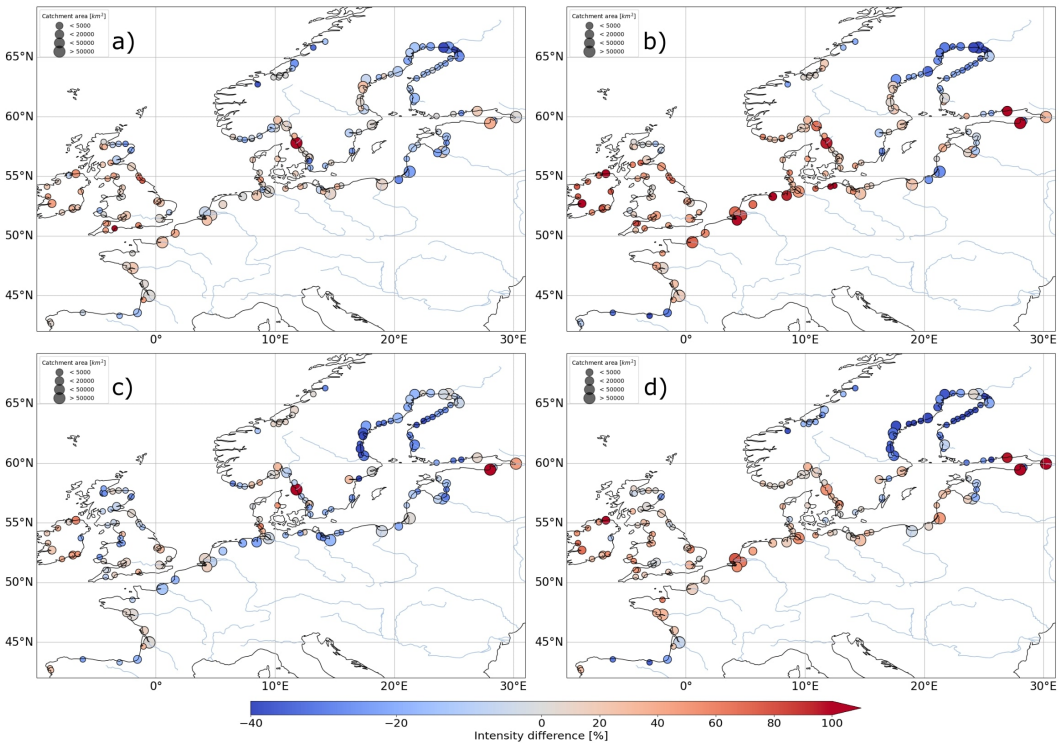

Figure 4.6: Changes in discharge intensity towards the end of the century (2070-2099) relative to the historical reference period (1976-2005). a) REMO-Had RCP2.6, b) REMO-Had RCP8.5, c) REMO-MPI RCP2.6, d) REMO-MPI RCP8.5.

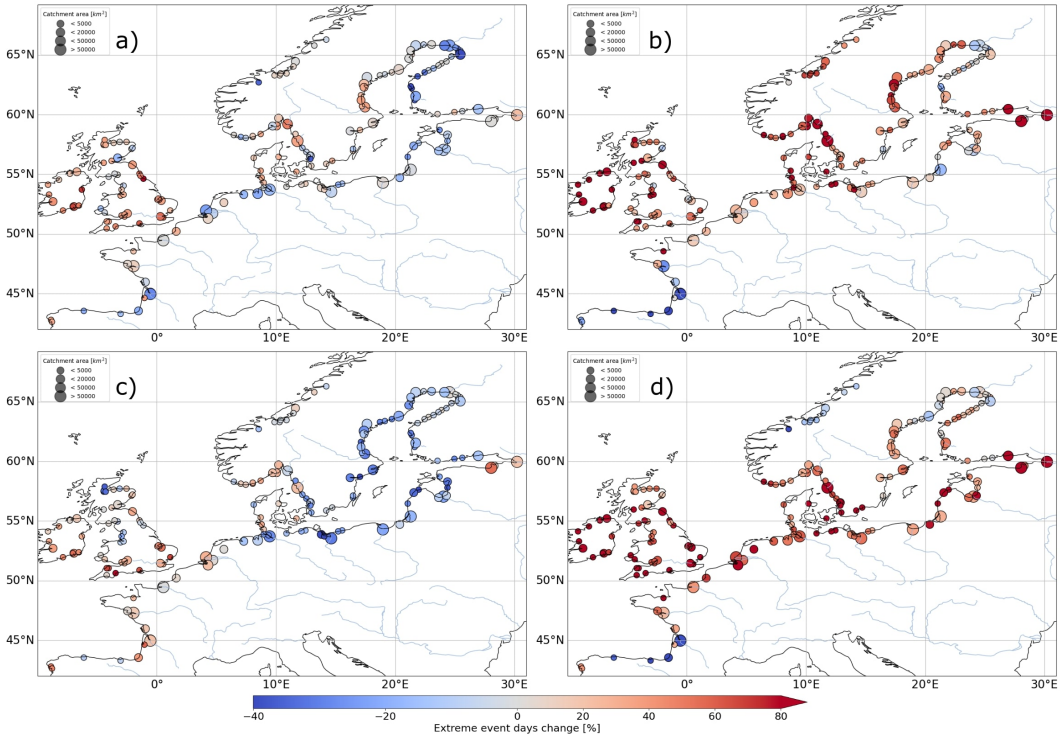

Figure 4.7: Changes in the total number of days with extreme discharge towards the end of the century (2070-2099) relative to the historical reference period (1976-2005). a) REMO-Had RCP2.6, b) REMO-Had RCP8.5, c) REMO-MPI RCP2.6, d) REMO-MPI RCP8.5. The percentages are calculated as changes to the number of days with extreme discharge in the historical period.

are rather minor. Despite that, REMO-Had and REMO-MPI mostly agree in their assessment that the northern coasts of Poland and Germany will have a lower number of extreme event days.

The REMO data sets show a stronger agreement for intensity and number of extreme days changes under RCP8.5, with most of Europe experiencing an increase for both parameters (Fig. 4.6b+d and Fig. 4.7b+d). A lower intensity is anticipated by both REMO data sets only for northern Spain and the Bothnian Bay. The number of days with extreme discharge increases throughout all of Europe, with the exception of northern Spain. As in RCP 2.6, the REMO data sets disagree for the northern Norwegian coast and the western coast in the Bothnian Sea. The increases and decreases of both variables are much stronger than under RCP2.6.

4.4.3 *Future changes in coastal water levels*

The tide-surge component of the total coastal water level shows no significant change in both RCP scenarios; that is if sea level rise is neglected. Fig. 4.8 exemplifies this for the coastal water levels at the Elbe river mouth. Both tide-surge data sets show very similar distributions in the histogram. The same behaviour can be seen for all other rivers. As a result, the intensity and number of the extreme tide-surge events does stays similar.

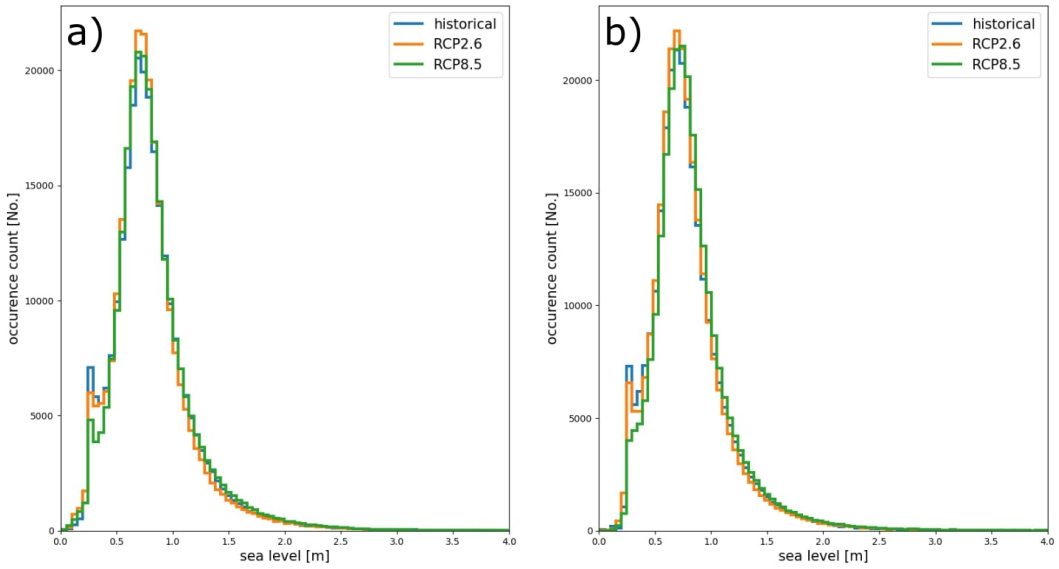

Figure 4.8: Histogram containing hourly tide-surge level values for a) REMO-Had and b) REMO-MPI as calculated by the TRIM model at the Elbe river mouth. The histogram is based on 100 bins with sea level rise being neglected. The historical time period is 1976-2005, while future scenarios RCP2.6 and RCP8.5 cover the years 2070-2099.

4.4.4 *Future changes in compound flood events*

The number of compound flood event days at the end of the century shows large local differences (Fig. 4.9). While nearly all of Europe experiences an increase in the number of compound flood events in RCP2.6 and RCP8.5, this is not the case for the Bothnian Bay and Bothnian Sea. There we see mostly similar amounts of compound flood event days under RCP2.6 at the end of the current century, with some rivers even indicating a decrease. The reason for this is that this regions already has a low number of compound flood event days in the historical reference period and in the RCP scenarios, discharge slightly increases while the sea level lowers at the same time. For RCP8.5, the increase of compound flood event days for this region is weaker compared to the rest of Europe. This is because the sea level is similar to the historical one, while there is an increase in discharge event days.

The mean duration of the compound flood event season in all rivers elongates in both REMO data sets for the future scenarios (Table 4.2). For RCP2.6, REMO-Had

	REMO-Had	REMO-MPI
historical	3.51 months	3.94 months
RCP2.6	4.38 months	4.29 months
RCP8.5	5.17 months	5.09 months

Table 4.2: Average compound flood event season duration calculated over all rivers that are considered in this study. The historical reference period is 1976-2005, while the future scenarios are for the years 2070-2099.

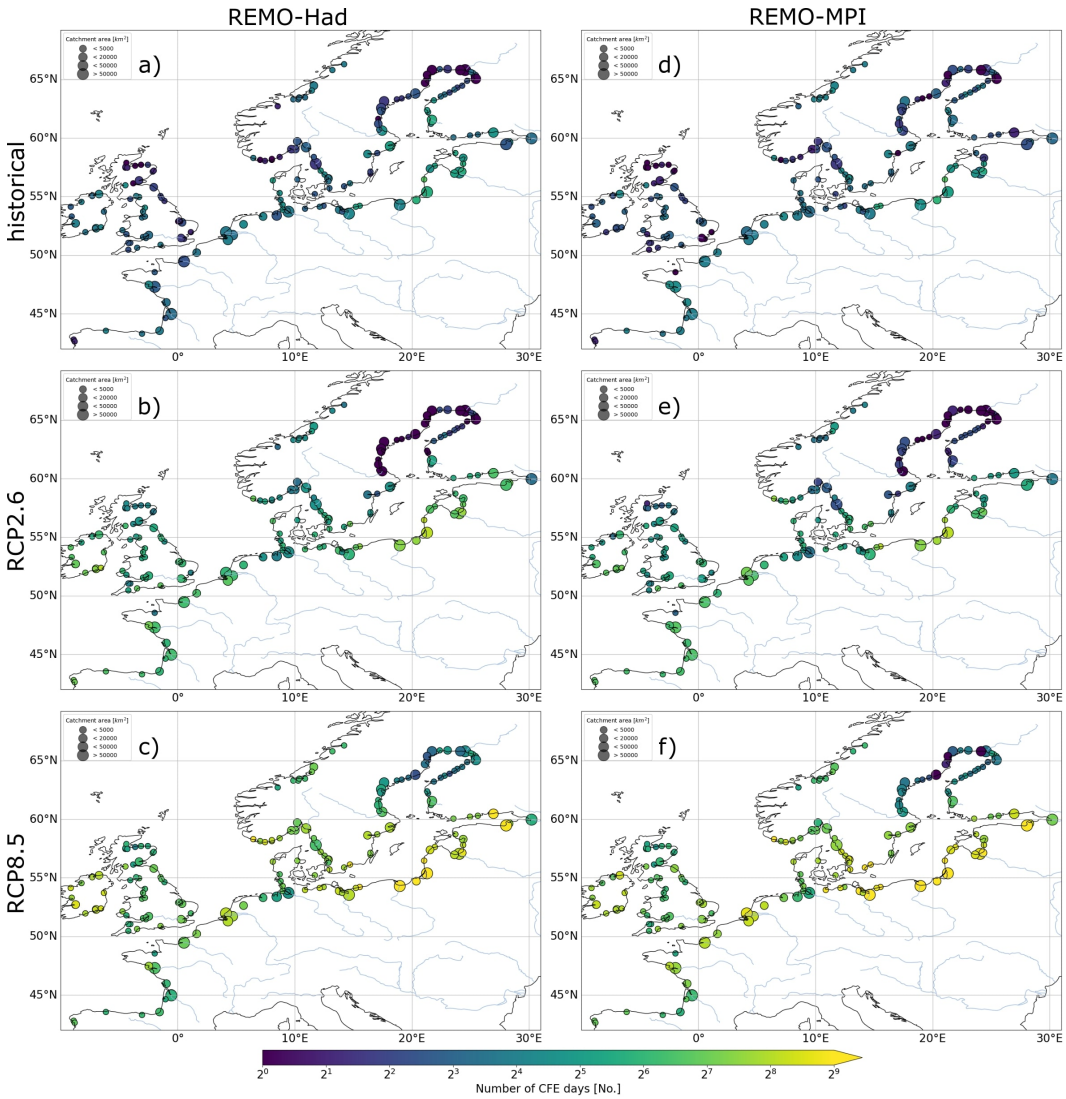

Figure 4.9: Number of compound flood event days in Europe over a period of 30 years on a logarithmic scale. The historical reference period covers 1976-2005, while the future scenarios cover 2070-2099. The left column shows the REMO-Had scenarios a) historic, b) RCP2.6, and c) RCP8.5. In the same way, the right column shows REMO-MPI for d) historical scenario, e) RCP2.6, and f) RCP8.5.

and REMO-MPI project an increase of around 0.8 and 0.3 months respectively. For RCP8.5 the compound flood event season is even longer by around 1.6 and 1.1 months in comparison to the historical reference period. This increase can be attributed to the rising sea level extending the duration of the storm surge season and therefore creating a bigger overlap with the discharge season.

In the historical period (Fig. 4.10) western-facing coasts have a higher chance of showing more compound flood events than expected by chance. If the chosen thresholds are adapted to the future scenarios (see Chapter 4.3.1), a similar pattern can be inferred. If thresholds are not adapted to future changes, however, nearly all rivers will have a number of compound flood events that is above the expected 2σ

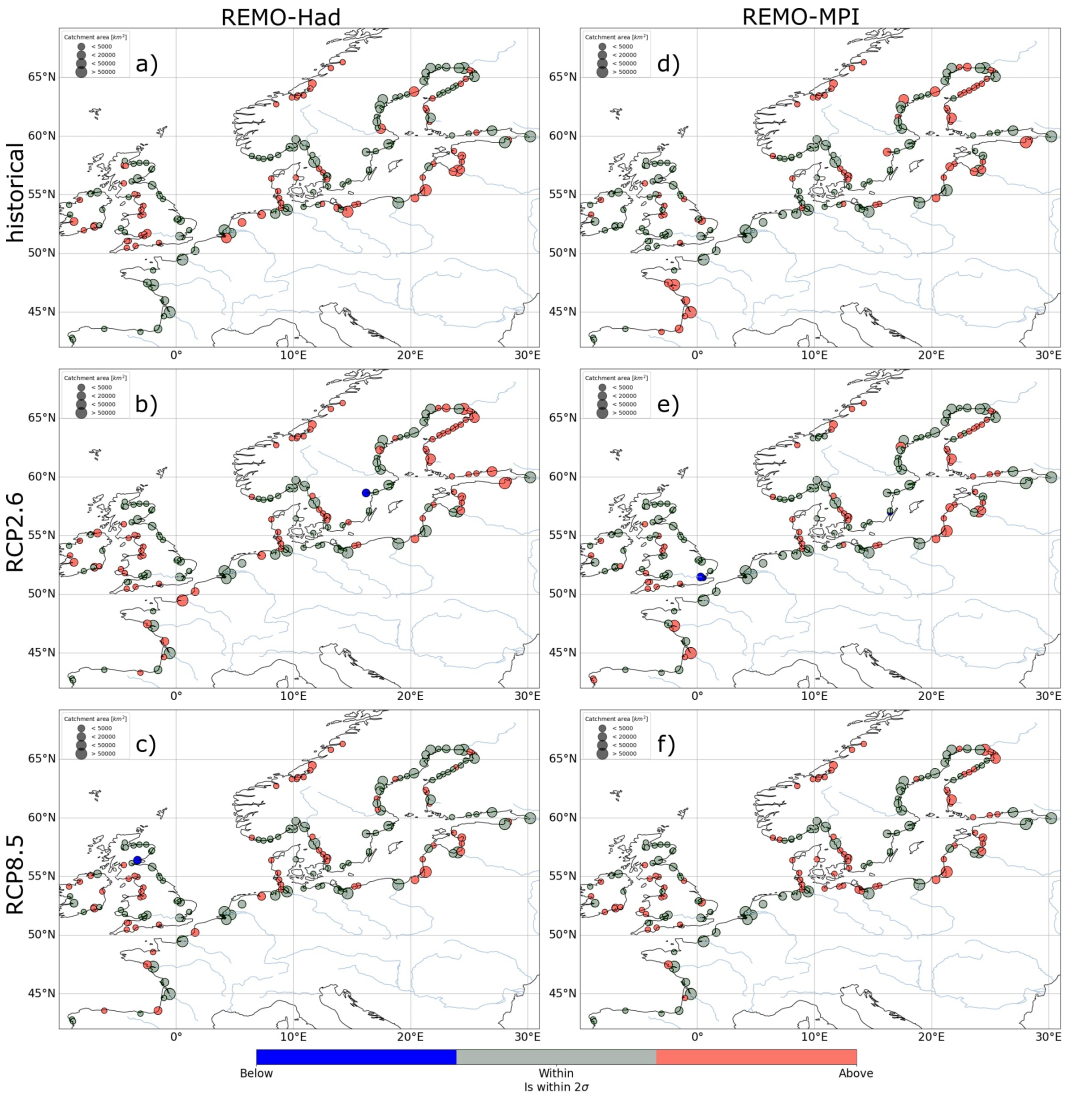

Figure 4.10: Comparison of dependence/independence between drivers for rivers in northern Europe for the historical reference period (1976-2005) and the end of the century (2070-2099), with each using thresholds that were newly calculated for the corresponding time period. The colour of the circles displays if the amount of compound flood events is within (grey), above (red) or below (blue) the expected 2σ interval derived from randomised Monte Carlo simulations. Left column contains REMO-Had data and the right one REMO-MPI. The rows contain historical reference (top), RCP2.6 scenario (middle), and RCP8.5 scenario (bottom).

value of the historical reference period. The only exception to this are the rivers in the Bothnian Bay and Bothnian Sea.

How much future changes in discharge and sea level rise contribute to changes in the number of compound flood event days, can be seen for RCP2.6 in Fig. 4.11 and for RCP8.5 in Fig. 4.12. It shows that sea level rise is the main contributor to the observed changes in compound flood events. Nevertheless, future changes in discharge will add to those changes, tide-surge share in it is negligible.

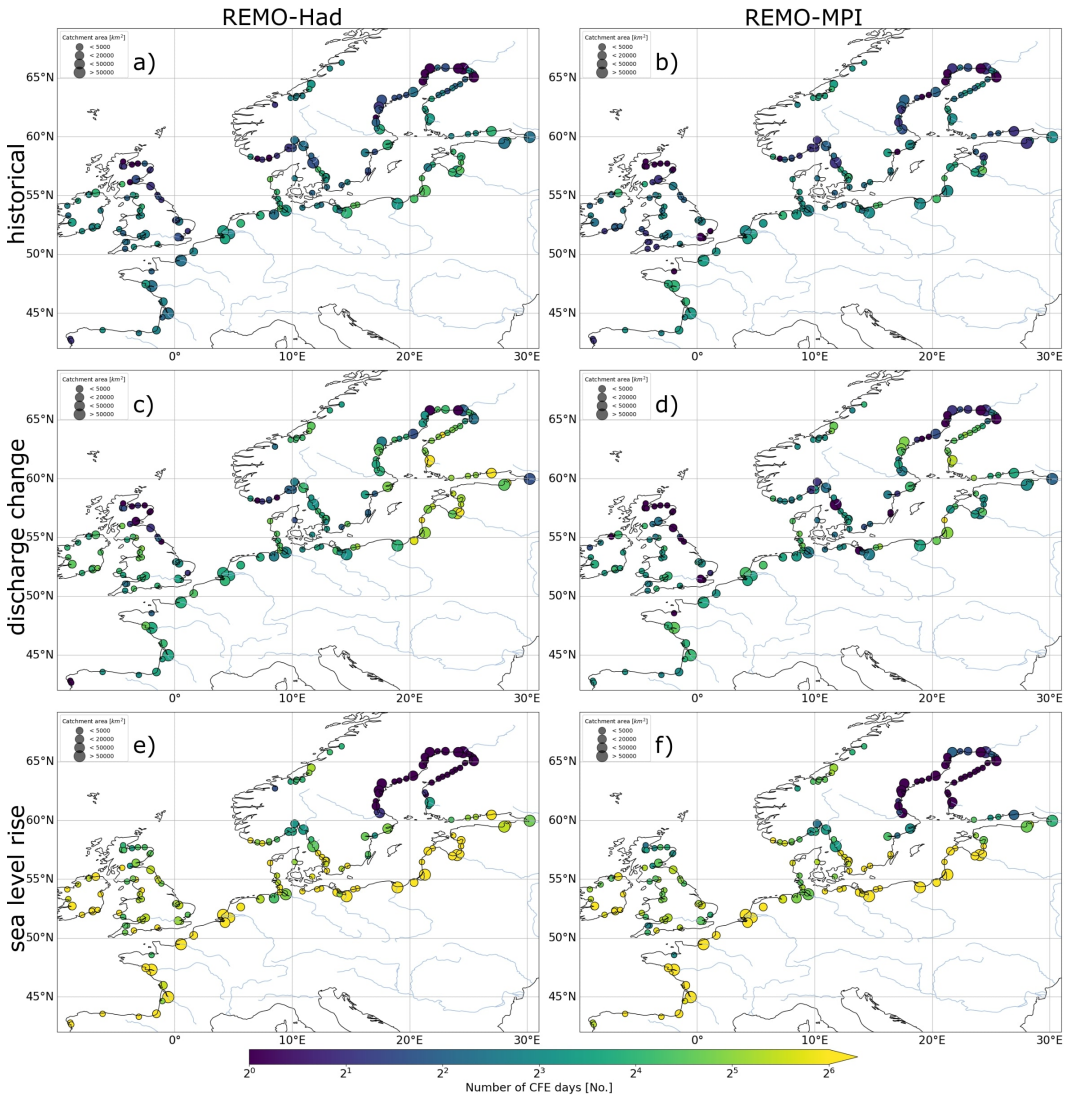

Figure 4.11: Contribution of discharge and sea level rise to changes in the total number of compound flood event days under RCP2.6. The left column contains changes for REMO-Had, right column for REMO-MPI. The top row contains the number of compound flood events of the historical runs. The middle row utilised discharge and tide-surge level (without sea level rise) of the time period 2070-2099 to calculate the compound flood events. The bottom row used the discharge and total coastal water level (tide-surge plus mean sea level) from the historical time period but added the sea level rise that corresponds to 2070-2099. An explanation for those choices is given in Chapter 4.3.5.

4.5 DISCUSSION

Comparing the historical runs of the REMO data sets with the reconstruction data (Chapter 4.4.1) showed a very similar behaviour. Both REMO data sets show a number of compound flood events that is similar to those of the reconstruction data sets, even if the compound flood events for northern Norway are overestimated. Furthermore, there is a certain amount of variability due to the events being infrequent and the analysis time period being comparably small. For both REMO

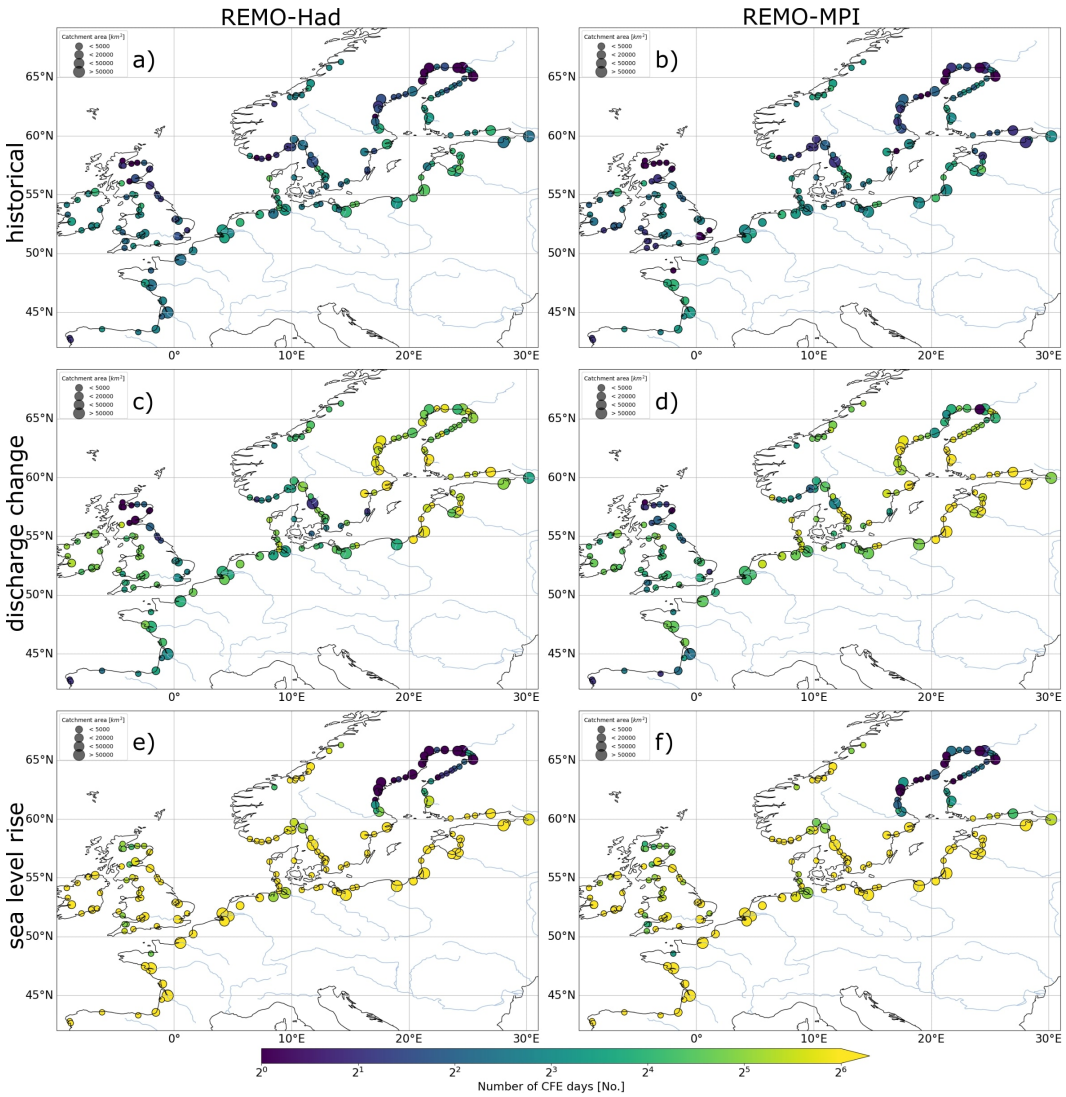

Figure 4.12: Contribution of discharge and sea level rise to changes in the total number of compound flood event days under RCP8.5. The left column contains changes for REMO-Had, right column for REMO-MPI. The top row contains the number of compound flood events of the historical runs. The middle row utilised discharge and coastal water level (without sea level rise) of the time period 2070-2099 to calculate the compound flood events. The bottom row used the discharge and total coastal water level (tide-surge plus mean sea level) from the historical time period but added the sea level rise that corresponds to 2070-2099. An explanation for those choices is given in Chapter 4.3.5.

data sets the majority of compound flood events happen in the winter months. Also, the 2σ maps (Fig. 4.4), which show if a river has more compound flood events than expected by chance, show a similar pattern, with the western-facing coasts tending to be above the 2σ range. The deviations we observe are potentially caused by slightly different storm trajectories in the REMO data sets and natural climate variability which does not allow a one to one comparison since they are not based on reanalysis.

If sea level rise is neglected, we do not see changes in the coastal water levels. There are studies that project an increase in cyclone number and mean wind speed (e.g. Zappa et al. (2013)) as well as a poleward shift of the storm tracks (e.g. Kjellström et al. (2018)). However, those results are sensitive to the chosen forcing and the choice of the global climate model (Feser et al., 2015; Ozturk et al., 2022). Gonzalez et al. (2019) concluded that those projections should be viewed with some caution. Discharge on the other hand shows a change in the number of extreme event days and intensity. These changes in discharge are caused by an increase in global temperature. Higher temperature results in the atmosphere carrying more moisture, which eventually leads to more extreme precipitation events in most parts of northern Europe in winter (Pfahl et al., 2017). Furthermore, due to warmer winters, the snow melt will start sooner (Blöschl et al., 2017), leading to a seasonality shift in many regions like Scandinavia. Hattermann et al. (2015) found that a combination of those factors would lead to an increase in winter discharge for almost all large German rivers. This makes it important to have proper discharge data available that take snow melt into account like in the current study, instead of only precipitation. The period of strong discharge events will begin earlier in winter and therefore lasts for an extended period in comparison to the historical time frame. This, combined with more precipitation events leads to changes in the number of extreme event days. The increased annual precipitation (Rajczak & Schär, 2017) will result in a generally higher discharge level in Europe (Thober et al., 2018). An exception to this is northern Spain where we see a reduction in intensity and extreme discharge days due to less precipitation. While the signals are very clear in the REMO data sets for RCP8.5, this is not the case for RCP2.6. Like in Di Sante et al. (2021), clear changes to discharge can be seen for Scandinavia and the Baltic States, but not for most of central and western Europe. The decrease in extreme discharge event days under RCP2.6 might be caused by the warmer temperature leading to less snowmelt-generated discharge. Overall, our results match the generally expected future discharge changes.

Due to sea level rise and increased discharge, we expect a strong increase in compound flood events towards the end of the century in both scenarios. The changes are significant for both RCP scenarios, but much stronger in RCP8.5. Our analysis reveals that sea level rise will be the main contributor to those changes for most of Europe (see Fig. 4.11 and Fig. 4.12). However, even if sea level rise is ignored, the changes in discharge under RCP8.5 are large enough to cause major shifts in compound flood event frequency. Despite that, it is essential to take into account, that changes in discharge event frequency and intensity will have impacts on a local scale. The developments of sea level rise and discharge will furthermore cause an increase in the compound flood event season duration which is projected to extend up to 5 months under RCP8.5 at the end of the current century. Furthermore, we see that by adapting the thresholds to future scenarios, the pattern in Fig. 4.10 remains similar, indicating that the generating mechanism for most compound flood events stays the same. If those thresholds are not adapted and stay on the historical level, nearly all rivers show more events than in the past. Our results, therefore, align with the work of Bevacqua et al. (2019) who projected a rise in compound flood events towards the end of the century. Our results do not find any indication of a

widespread lower risk of compound flood events over Central Europe as described by Ganguli et al. (2020). One reason for the difference in results might be that their study investigated the middle of the century (2040-2069), while the climate change signals increases in magnitude throughout the century. It also must be noted that our approach to classify compound flood events is different to the one used by Ganguli et al. (2020). The present study utilises a Peaks over Threshold approach, while the former uses annual maxima high coastal water levels and high river discharge within ± 7-days of occurrence of the high coastal water level.

As discussed, sea level rise is the dominant factor responsible for future changes in compound flood events. To assess how sea level rise may affect the number of compound events for different global warming levels, we added the corresponding sea level rise to the historical tide-surge data sets and left the discharge unchanged. As shown in Fig. 4.3, the Bothnian Bay and Bothnian Sea do not experience sea level rise and will therefore not be explicitly named every time in the following as an exception to the general trends. A sea level rise associated with a 1.5 K global warming already rises the number of compound flood event days strongly. Here, SSP1-2.6 (Fig. 4.13) and SSP5-8.5 (Fig. 4.14a) will double the amount of compound flood event days for southern England, eastern coast of Great Britain, Ireland, and the Western Baltic. Nearly all European rivers will experience an increase of 50%

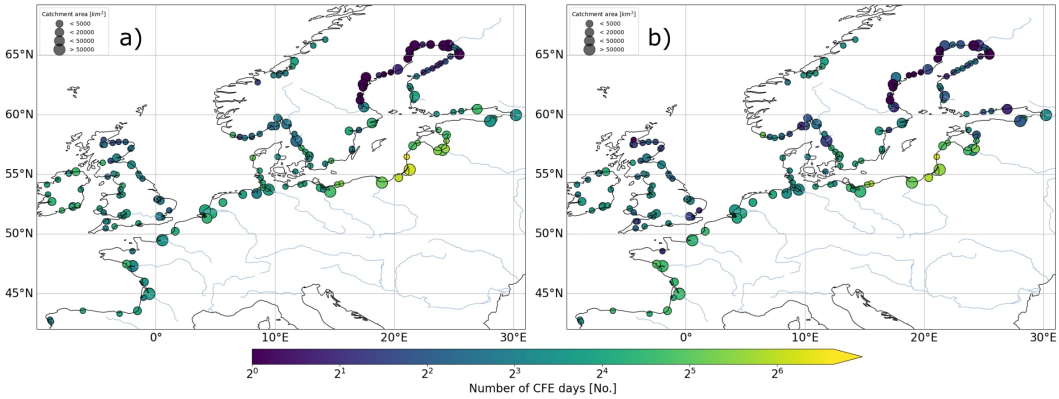

Figure 4.13: Number of compound flood event days over 30 years if the sea level rise, which is associated with a specific level of global warming in SSP1-2.6, had occurred in the historical time period (1976-2005). a) shows those changes for REMO-Had and b) for REMO-MPI. The global average temperature increase is 1.5 K. The point at which the temperature increase is reached can be seen in Table 4.3.

Scenario	1.5 K	2.0 K	3.0 K	4.0 K
SSP1-2.6	2032			
SSP5-8.5	2028	2042	2064	2084

Table 4.3: This table displays the years in which the mean of the projections for scenarios SSP1-2.6 and SSP5-8.5 will reach a certain global warming according to the Sixth Assessment Report of the IPCC (Masson-Delmotte et al., 2021).

or more, with the exception of northern Norway. With global temperature rise

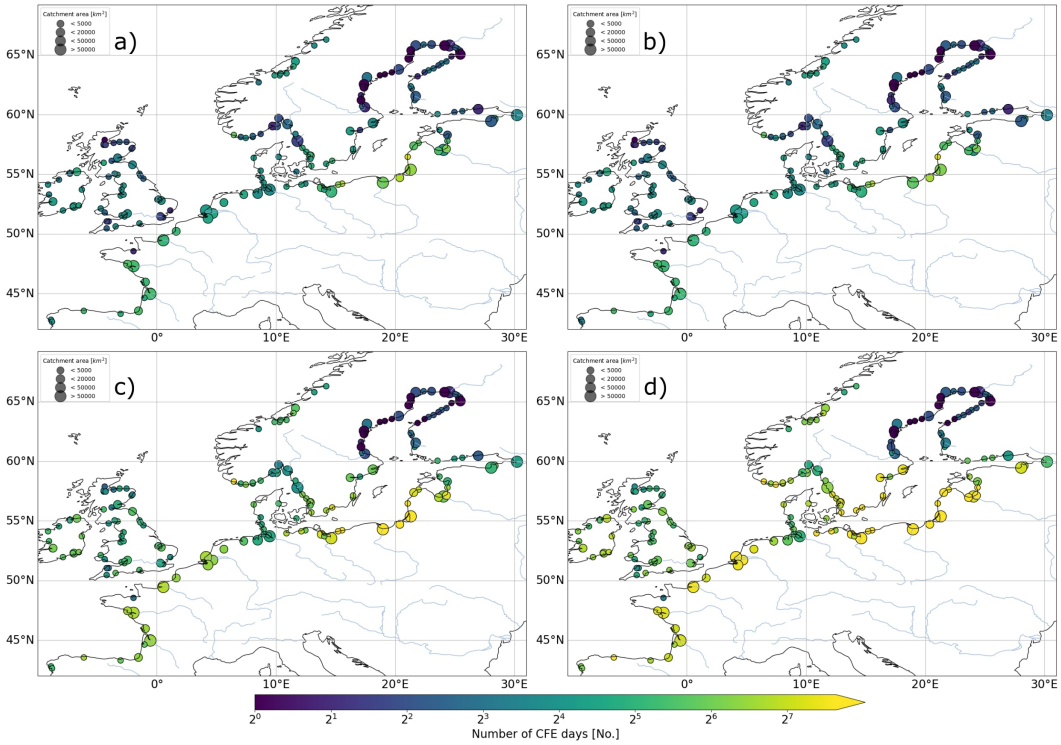

Figure 4.14: Number of compound flood event days over 30 years if the sea level rise, which is associated with a specific level of global warming in SSP5-8.5, had occurred in the historical time period (1976-2005). This image shows REMO-MPI. The similar figure for REMO-Had looks very similar (Fig. 4.15). The temperature increase is 1.5 K in a), 2 K in b), 3 K in c) and 4 K in d). The point at which the temperature increase is reached can be seen in Table 4.3.

crossing a warming of 2 K all of Europe would experience twice the number of compound flood events compared to the historical reference period (Fig. 4.14b), except for northern Norway and the northwestern German coast. In a similar fashion, a 3 K temperature increase would triple the numbers of compound flood event days (Fig. 4.14c) and 4 K would raise it by a factor of 5 (Fig. 4.14d). This demonstrates, that even if the global warming will be limited to 2 K or less, the resulting sea level rise will impose a massively increased risk on the European countries.

It should also be taken into account that the number of annual compound flood events underlies natural variability. This can be seen in the variations of the 5 year average (Fig. 4.16).

A clear separation between RCP2.6 and RCP8.5 starts to emerge around the 2060s for both REMO data sets. The climate signal strength and amount of changes depend on the forcing and the time period, with most changes happening in the second half of the century. Nevertheless, a generally rising trend can be seen for the entire time period.

A large-scale study like this comes with inevitable caveats. Only data sets from two downscaled different global models were available due to the required high temporal resolution for the TRIM simulation. Due to not having an ensemble of

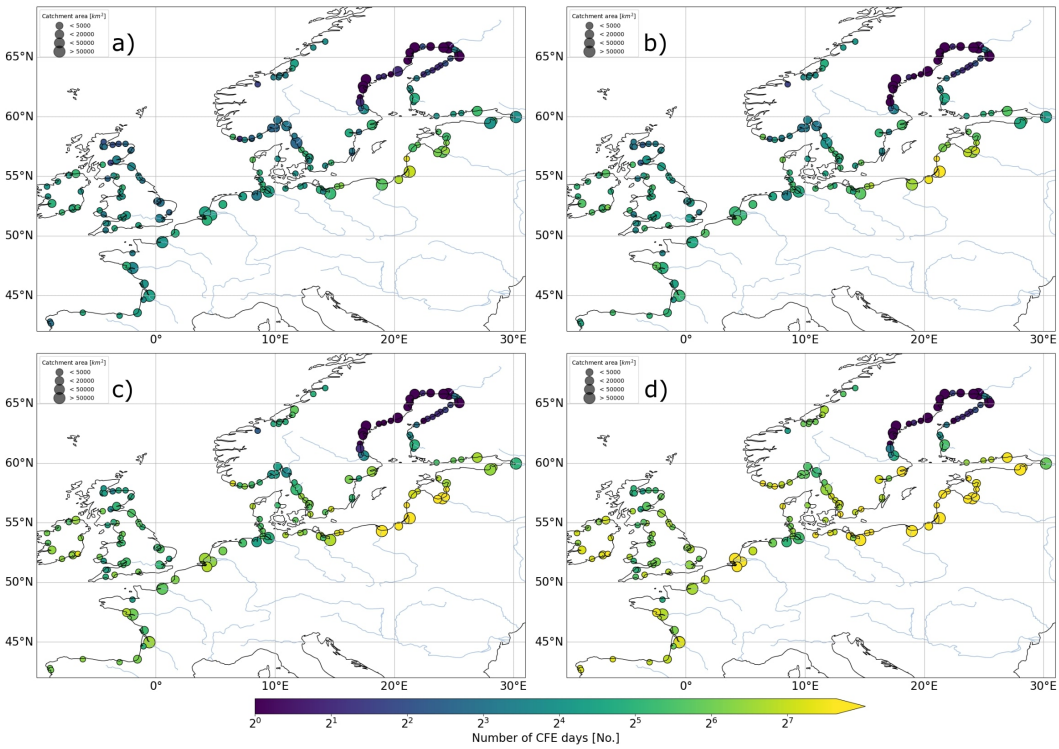

Figure 4.15: Number of compound flood event days over 30 years if the sea level rise, which is associated with a specific level of global warming in SSP5-8.5, had occurred in the historical time period (1976-2005). This image shows REMO-Had. The temperature increase is 1.5 K in a), 2 K in b), 3 K in c) and 4 K in d). The point at which the temperature increase is reached can be seen in Table 4.3.

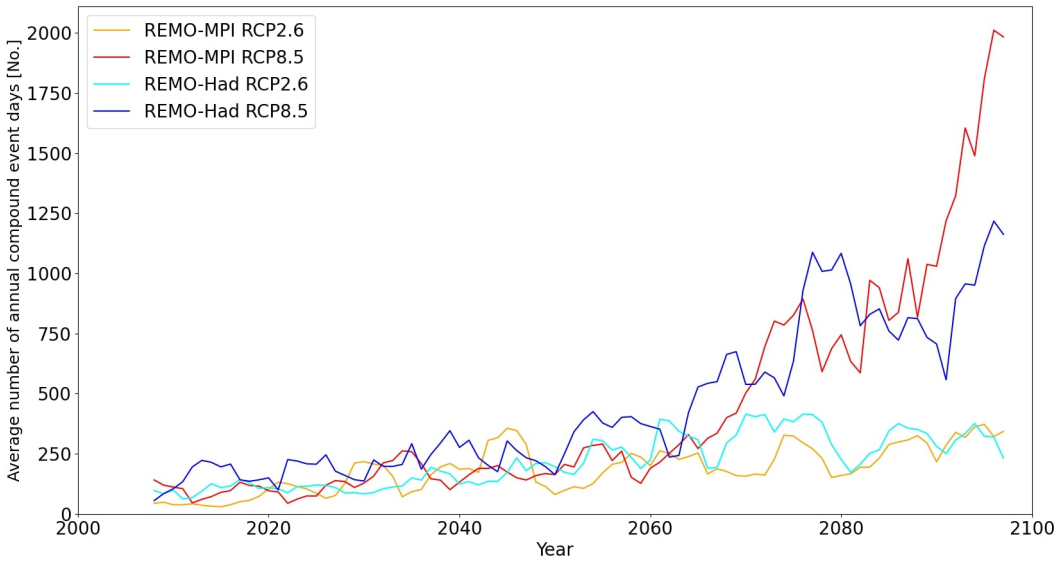

Figure 4.16: Sum of annual compound flood event days over a 5 year moving average for all rivers combined in the study area from 2006 to 2099. The calculation of compound flood events includes local changes to the coastal water levels caused by sea level rise.

available data sets we yielded uncertain changes in the discharge under RCP2.6 for parts of Europe. This goes hand in hand with compound flood events being a phenomenon that underlies large variability as seen in Fig. 4.16. Therefore, even 30-year time frames have a certain amount of variability, especially with the ongoing influence of climate change. Furthermore, the evaluation of the model performance showed that the general patterns can be represented, but differences exist nonetheless due to limitations in the modelling frameworks. Additionally, the uncertain absolute amount of sea level rise, as well as the linear superposition of tides with sea level rise, adds a noticeable uncertainty to the question of how strong the changes in future extreme events will be since it is the predominant factor. Note that due to the large scale of the domain of our study, it was not possible to take local factors like flood protection and topography into account.

4.6 CONCLUSION

In the present study, we conducted an analysis of future changes in compound flood events over northern and central Europe and the contributing factors to it without the use of copulas. We have demonstrated that the number of compound flood events will strongly increase in the future, regardless of the scenario. Furthermore, we analysed future changes in discharge and coastal water levels. To the authors' knowledge, this is the first study that investigates these changes without the use of copulas in Europe. It is important to point out that this study should be seen as a general trend analysis for future scenarios and not as an actual prediction that can be used for precise flood risk assessment. Scenario RCP2.6 shows a less extreme increase in compound flood events compared to RCP8.5. The main contributor to those changes is sea level rise, while changes in river discharge are less severe but are not negligible. The sea level rise will lead to a strong increase in compound flood events, even when the global warming is limited in line with the Paris Agreement. The magnitude of those changes increases towards the end of the current century. In general, REMO-Had and REMO-MPI show strong agreement for RCP8.5, but less for RCP2.6. Additionally, we see in a future with adjusted thresholds that west-facing coasts experiencing a higher number of flood events than expected by pure chance, just like in the historical reference period. This implies that the strongest compound flood events in future scenarios will still be caused by a common driver like a specific weather constellation. Future work can further examine climate change under RCP2.6 and RCP8.5 by utilising an ensemble of global climate models. This, paired with a better understanding of sea level rise on a local level, will be important to lower the uncertainty in changes to future compound flood events, which is essential for accurate risk assessment.

4.7 STATEMENTS AND DECLARATIONS

Conflict of Interest Statement: The authors declare that the research was conducted in the absence of any commercial or financial relationships that could be construed as a potential conflict of interest.

Author Contributions: Philipp Heinrich developed the analysis methods, performed the data analysis and wrote the manuscript. Stefan Hagemann initiated the study and contributed the HD discharge data while Lidia Gaslikova generated the TRIM data. Ralf Weisse and Stefan Hagemann supervised the research activities, revised the manuscript, and contributed to the interpretation of the results. Ralf Weisse acquired the funding.

Funding: This research was financed with funding provided by the German Federal Ministry of Education and Research (BMBF; Förderkennzeichen 01LR2003A).

Acknowledgments: This research is a contribution to the PoFIV program of the Helmholtz Association. We thank the projection authors for developing and making the sea-level rise projections available, multiple funding agencies for supporting the development of the projections, and the NASA Sea Level Change Team for developing and hosting the IPCC AR6 Sea Level Projection Tool.

Data Availability Statement: The HD5-ERA5 and HD5-E-OBS discharge data were published as Hagemann & Stacke (2021) and can be obtained at the World Data Centre for Climate (WDCC) of the German Climate Computing Centre (DKRZ). HD discharge data based on the REMO data sets and TRIM coastal water level data will be made available by the authors, without undue reservation, to any qualified researcher upon request. ERA5 reanalysis data are available at the Climate Data Store: https://cds.climate.copernicus.eu/. REMO downscaled EURO-CORDEX data were provided by the Climate Service Center Germany (GERICS).

5 SUMMARY, CONCLUDING REMARKS, AND OUTLOOK

Since I started my Ph.D. in April 2021, there have been several devastating floods in Europe. In July 2021, a flood in Germany, Belgium, and the Netherlands caused more than 180 fatalities and an estimated damage of € 32 billion (Mohr et al., 2023). In August 2023, a flash flood in Slovenia caused damage equivalent to 15% of the national GDP (Bezak et al., 2023). These events show that flooding is far from a solved problem. In addition, my hometown in Lower Saxony was threatened by high discharge of the river Hase during the Christmas flood of 2023. The flooding was caused by heavy rainfall on already saturated ground. Throughout the month of December, westerly winds prevailed, with the Großwetterlage Cyclonic Westerly occurring during the Christmas days until the end of the year. All of this felt even more personal because of the research I had done for this dissertation on Großwetterlagen and floods. Although these floods were neither coastal floods nor compound flood events, they highlight the amount of work that still needs to be done for better forecasting, protection, and general understanding of floods. I have endeavoured to answer the research questions posed in Chapter 1 in order to contribute to these goals by providing a better understanding of compound flood events in Europe and their future changes. A summary of the answers is given in the following Chapter 5.1, while Chapter 5.2 provides concluding remarks on the implications of my findings and an outlook on future research possibilities.

5.1 SUMMARY OF MY RESULTS

1. Do compound flood events in northern and central Europe occur randomly?

To address the initial research inquiry, I performed a comprehensive spatial analysis examining the dependence of storm surge and discharge extremes as drivers for compound flood events in the North and Baltic Sea catchments across northern and central Europe. This was one of the first studies to investigate compound flood events on a continental scale for Europe, and the very first to do so without the usage of copulas, which otherwise introduce large uncertainties due to the small number of data points. Using a Monte Carlo-based approach, I analysed a total of 181 rivers across northern and central Europe, using HD5-ERA5 data for the discharge and TRIM-REA6 data for sea level. My analysis was focused on the winter and early spring season, as this is the main season for compound flood events in this region. I was able to show that the west-facing coasts tend to experience a higher number of compound floods than expected randomly by chance alone, suggesting the existence of a common meteorological driver. I also demonstrated the robustness of the results by reproducing the same pattern with different data sets, changes in parameter settings, and variations in the randomisation approach. In addition, I showed that the pattern remains stable, despite the ongoing climate change since the 1960s. Finally, I showed that rivers with larger

catchment areas tend to show less compound flood events. This finding can be explained by the fact that in larger catchments it takes longer for precipitation to increase the river discharge significantly, and therefore the storm surge often ends earlier. These findings are further detailed and discussed in Chapter 2. Uncertainty in the results arises from the use of the 2σ interval and the comparatively short time period of available data. Although the results have been shown to be robust, they could certainly benefit from longer periods of available data. Furthermore, the number of reported compound flood events should be treated with some caution, as the thresholding method cannot account for local topography or flood protection measures. Furthermore, the river discharge patterns can vary strongly between rivers. A river with a single large discharge event in spring due to snowmelt may have a different number of extreme discharge events than a river with several short events due to precipitation. This type of problem can only be addressed by a local study for each river individually.

2. **Are there Großwetterlagen that favour the development of compound flood events and how is their frequency changing due to climate change?**

With previous results suggesting the existence of a common meteorological driver that causes many of the compound flood events in the North and Baltic Sea catchments, I examined the events identified in Chapter 2. I found that the majority of these events occurred during the Großwetterlage Cyclonic Westerly. This weather system is characterised by strong westerly winds and high precipitation, creating therefore optimal conditions for high storm surges and extreme discharge, which explains the high number of compound flood events on western-facing coasts. This connection enabled me to use Cyclonic Westerly as a proxy for compound flood events northern and central Europe. To better understand how this Großwetterlage changes under anthropogenic climate change and the implications for changes in the frequency of compound flood events, I analysed 31 CMIP6 global climate models and the MPI Grand Ensemble for three different climate scenarios. The Großwetterlagen classification has the advantage that, due to its large-scale nature, it can operate directly on global climate model data and does not require an additional downsampling step for higher resolution. In order to overcome the hurdle that Großwetterlagen are a subjective classification, I developed the Convolutional Neural Meteorological Network (CNMN) in Chapter 3. This neural network was able to outperform the two already existing studies on the automatic classification of Großwetterlagen. My analysis showed that, towards the end of the current century (2071-2100), the CMIP6 models project an increase in the frequency of Cyclonic Westerly during the winter half year. On the contrary, the frequency of Cyclonic Westerly decreases during the summer season in the majority of global climate models. The strength of change increases with a stronger climate change signal. This trend indicated by the global climate models implies an increase in the frequency of the weather pattern that are conducive to the occurrence of compound flood events, and thus an increased likelihood of these events under climate change. The neural network ensemble used in this study have been made available to other researchers to provide an easy way to automatically classify Großwetterlagen (Heinrich, 2024). However, uncertainty arises from the classification skills of the

neural networks. Although they have the best performance of any method currently available, there is certainly room for improvement. The problems are caused by the requirement that all Großwetterlagen must last at least three days (see Chapter 3.3), the lack of temporal awareness of the neural networks, and the transition between different Großwetterlagen where the exact classification is somewhat ambiguous. Moreover, as the entire classification catalogue is subjective, there is no guarantee that the people responsible for it are always correct in their classification. However, visual comparisons have shown that the days identified by CNMN as Cyclonic Westerly match the pattern of human classification. Therefore, it is unlikely that improved classification will change the results of this study in any meaningful way, but there is no absolute certainty. I have demonstrated several attempts to improve the classification (see Chapter 3.4.2), for example by adding additional variables, but to no avail. More sophisticated methods to avoid overfitting might allow for larger and deeper networks that could take into account the temporal aspect of the data. Additionally, there are deep learning libraries such as PyTorchVideo (Fan et al., 2021) focused on video understanding that could be used in combination with hourly rather than daily data to improve classification. An alternative approach would be to develop a bespoke objective classification that characterises the meteorological conditions that give rise to compound flood events, once they are better understood.

3. **What influence will different factors have on the frequency of compound flood events in the future?**

To answer the final research question, I examined in Chapter 4 two climate simulations from the global climate models MPI-ESM and HadGEM2-ES that had been downscaled by the regional climate model REMO. For both climate simulations I analysed the emission scenarios RCP2.6 (low emission) and RCP8.5 (high emission), looking at changes to coastal water level, discharge and sea level rise. First, I verified that the models are able to reconstruct the west coast facing pattern previously shown in Chapter 2 for the historical reference period. I then showed that storm surge levels do not change significantly under climate change and therefore do not contribute to changes in the frequency of compound flood events. In contrast, I found a strong increase in the number of days with extreme discharge and an increase in the duration as well as intensity of these events under RCP8.5 due to global warming leading to more moisture in the atmosphere. Those changes for discharge are less pronounced under RCP2.6 due to the weaker climate change signal. Furthermore, I demonstrated an increase in the number of compound flood events caused by sea level rise for almost all of Europe, even when discharge and coastal water level remain at historical level. Separate analysis has shown that the sea level rise is the dominant contributing factor, but discharge changes have to be taken into account as well. As a result of those changes, the period during which compound flood events occur throughout the year will become longer and compound flood events last longer. Overall, my analysis showed a drastic increase in the number of compound events, accelerating in the second half the current century. Finally, I found that the models project a doubling in the number of compound flood event days, even if global warming level is limited according to the Paris Agreement. The largest source of uncertainty in this study

is the projected sea level rise. For example, the Sixth Assessment Report of the Intergovernmental Panel on Climate Change (Fox-Kemper et al., 2021) projects a *likely* range of 0.63 m to 1.01 m for the global mean sea level rise until 2100 under SSP5-8.5. This uncertainty can only be lowered by improved modelling of sea level rise and a better understanding of the relevant processes. As explained in the answer to the first research question, uncertainty stems naturally from the chosen definition of extremes and the impossibility of taking local properties into account for such a large-scale study. Furthermore, our analysis on future changes to discharge under RCP2.6 could be improved by analysing a wider range of models, because the two models available to us at that time showed opposite changes in some regions. However, even this uncertainty cannot disguise the fact that the number of compound flood events will increase significantly as a result of anthropogenic climate change.

5.2 CONCLUDING REMARKS AND OUTLOOK

Much work has been done on flood risk assessment and management in Europe over the last two decades, following the so-called 'Floods Directive' (2007/60/EC, 2007) of the European Parliament and the Council of the European Union. Compound flood events are one aspect that needs to be taken into account in coastal and flood protection for proper risk assessment and adequate protection of citizens. They become even more important with the projected increase in the frequency of compound flood events due to global warming, as shown in this dissertation.

My research has shown that the Großwetterlage Cyclonic Westerly is a meteorological driver of compound flood events in northern and central Europe. This allowed me to analyse future changes in compound flood events in two different ways, namely changes in the frequency of Cyclonic Westerly as well as changes in the different components of compound flood events. The analysis of these changes showed that the number of compound flood events will increase significantly in the future due to anthropogenic climate change. This increase is the result of two different contributing factors. First, sea level rise and increases in the intensity and duration of discharge events will cause more compound flood events by the end of the century. Second, the frequency of weather patterns conducive to the occurrence of compound flood events is increasing, leading to more opportunities for them to occur. All of this emphasises the need for coastal protection that can withstand the more frequent and stronger compound flood events that are going to occur in the future.

The methods presented in this dissertation are flexible and can easily be applied to different types of compound events and other regions. The Monte Carlo approach for testing dependence was, for example, used for rain-on-snow events in Norway (Poschlod et al., 2020). Moreover, there are currently plans to apply this method for the analysis of compound flood events in Vietnam. Similarly, studies focusing on, for example, the simultaneous occurrence of heat and drought events can use this method to test for dependence and also to examine large-scale weather patterns to better understand these events. However, the neural networks that I have made available to other researchers for the automatic classification of Großwetterlagen

(Heinrich, 2024) can only be used for Europe. This is for one because the neural networks were trained on data of a specific domain (see Fig. 3.1) and for another because Großwetterlagen are only defined for Europe specifically. However, the idea of identifying synoptic circulation patterns that favour the occurrence of compound events can be applied to other parts of the world and the neural networks trained on corresponding data. Neural networks can then be used to automatically identify these weather patterns if an objective classification is not possible. Finally, the idea of analysing how different elements of compound events will change in the future due to climate change, and how these changes contribute to the overall frequency of compound events, can be carried out without being restricted to a specific region. For example, it could be analysed how the frequency and duration of droughts and heatwaves change and how each of those changes contributes to the future occurrence rate of compound heat and drought events in Australia.

The findings presented in this dissertation have implications not only for coastal protection, but also for inland water drainage. An example of this is the tidal gate Leysiel at the North Sea coast of Lower Saxony in Germany, which was briefly mentioned in Chapter 3. It is opened at low tide to drain the water stored inland, and closed at high tide to prevent the inflow of seawater. There, most of the high inland water levels, caused by high precipitation and high sea levels, occurred during Cyclonic Westerly. An increase in the frequency of Cyclonic Westerly, as projected by the CMIP6 global climate models, could therefore lead to more situations where the tidal gate is blocked for an extended period while precipitation occurs, which in worst case can lead to inland flooding. An example for this already happening in the recent past is a near-flood event in January 2012, where high water levels in the North Sea resulted in excess water that could not be discharged for several consecutive tidal periods. van den Hurk et al. (2015) provided a detailed report for the same event for Lauwersmeer in the Netherlands. Inland drainage will additionally become even more challenging in the future as sea level rise creates a higher baseline for external sea levels (Bormann et al., 2023). However, compound flood events are still often neglected in the planning stages of future coastal protection and inland drainage. For example, Weisse et al. (2024) recently reported that the local water boards in the region of Western East Frisia (Germany), which includes Leysiel, are aware of the dangers of compound flood events, but do not currently take them into account when planning coastal protection measures. As with any natural hazard, coastal protection should be proactive rather than reactive to avoid financial damage and the loss of lives. However, coastal protection is not the only aspect of proper risk assessment. Similarly, emergency plans need to take compound flood events into account. A road that is normally used for evacuation during a storm surge might be inundated if high river discharge occurs at the same time. This dissertation highlights the importance of compound flood events and will hopefully contribute to a better understanding of these events, demonstrate the urgency of adaptation, and raise awareness of future changes.

Local studies will be needed to develop bespoke protection measures, as they can take local topography and existing protection measures into account, all things that cannot be done in large-scale studies. They can aim to answer site-specific questions like ‘What is extreme for this location?’ and ‘Do these extremes cause

problems?'. These questions will be answered very differently for a city on a hill than for a city that needs to be protected from being flooded by regular sea levels; an example of the latter is more than a quarter of the Netherlands. The need for adaptation goes hand in hand with the analysis of existing protection measures like dykes, polders, and diversion canals. In addition, the decision making processes in case of emergency and the time needed to make these decisions can be analysed. Although several local studies exist to date, they all use different time frames, data sets, threshold methods, and statistics. It is therefore difficult to compare them or combine their results to see the bigger picture. Even if there were a massive project to carry out a plethora of local studies using identical time frames, data sets, and statistics for analysis, it would still suffer from the specific definition of 'extreme' for each site. However, perhaps someone will eventually develop a unifying method and definition that is universally applicable. Nevertheless, large-scale studies such as those presented in this dissertation will remain important for policies and strategies at the national level. Furthermore, they can aid in developing a better understanding for compound flood events on a large scale, as demonstrated in this dissertation.

Although compound floods have attracted a great deal of research interest over the last decade, many questions remain unanswered. In general, it would be great to see more studies investigating a wider range of scenarios instead of only RCP8.5/SSP5-8.5, which shows the strongest climate change signal. While humanity is currently doing a poor job of reducing greenhouse gas emissions, it is not a given that the worst-case scenario will happen, and it is important to have a good understanding of what might happen in other scenarios. One of the main questions arising from my dissertation is: Why do only some Cyclonic Westerly situations cause compound floods, but not all? It was shown in Chapter 2 that these events do not depend on the duration of Cyclonic Westerly or on a specific sequence of other Großwetterlagen. Therefore, further factors, like soil saturation caused by previous precipitation events or an increase of snowmelt due to rain, need to be taken into account to better understand why only some Cyclonic Westerlies are causing compound flood events. A better understanding of the exact circumstances that lead to Cyclonic Westerly causing compound flood events can be used to improve the prediction of compound flood events, which in turn can be used for early warnings in case of a strong event and provide additional preparation time for protective measures. An already existing tool that follows a similar thought process is the 'Coastal Decider' developed by Neal et al. (2018) for the Flood Forecasting Centre in the United Kingdom. Their tool utilises 30 predefined weather patterns with associated likelihoods of coastal flood in the United Kingdom. It analyses medium- to long-range forecast data to support early warnings. So far, no tool like this exists for compound flood events, but their work makes a compelling argument to further analyse weather patterns for flood forecast in order to potentially include compound flood events in the future.

Most studies, including those presented in this dissertation, analyse compound flood events where two or more drivers are extreme at the same time. However, the factors contributing to compound flood events do not have to be extreme to amplify each other and have a strong effect in combination. An example of this

is the tidal gate Leysiel. There, the majority of high inland water levels were a combination of 'above average' rainfall and sea level (Fig. 5.1). The aforementioned near-flood event in January 2012 is the only instance where one driver was at an extreme high during periods of high inland water levels. Preliminary analysis of

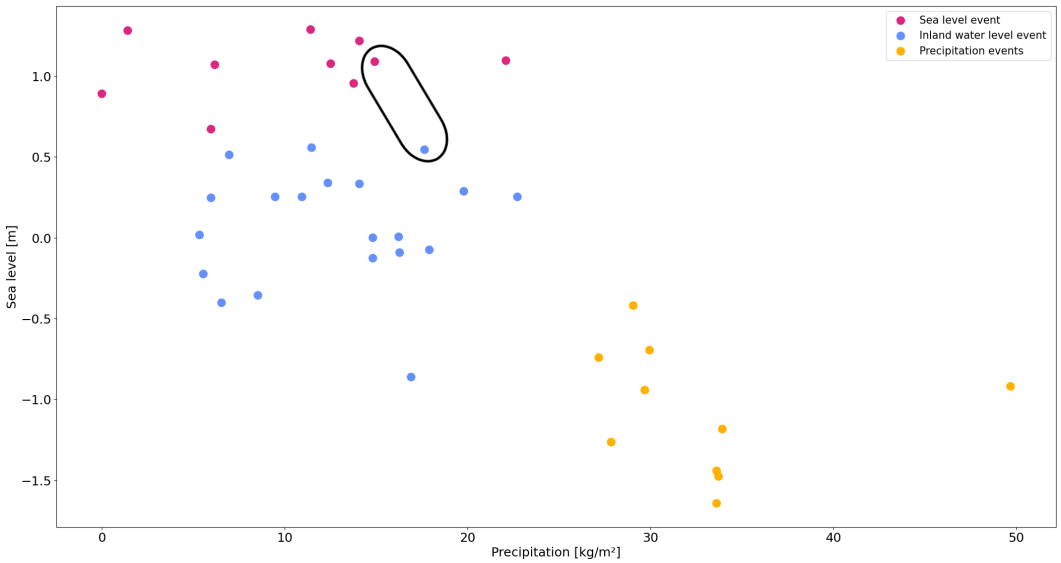

Figure 5.1: Highest measured values of sea level, precipitation and inland water level at the tidal gate Leysiel for 2002-2021. In pink are the ten highest sea level days, in blue the twenty highest inland water level days, and in blue the ten highest precipitation days. Each dot marks a separate day. The two markers highlighted belong to the near-flood event in January 2012 but are from two different days.

these events suggests that they do not occur on a single day, but are the result of precipitation on previous days, followed by high sea level in combination with even more precipitation. Further work is needed to better understand and predict these events.

As with many scientific topics, the analysis of compound flood events would benefit greatly from more data points. Insufficient observational data can lead to significant uncertainties in characterising the interactions between flood drivers. Consequently, risk assessments based on observations alone may underestimate the occurrence and interdependence of flood drivers in compound flood events. Observational data of multiple drivers are usually not available over long periods, although rapidly improving climate models could help to alleviate this problem. Nevertheless, it is often preferable to have observational data because the ramifications on the real world are a known quantity in hindsight. In particular, the calculation of additional variables such as the resulting inland water levels requires further computational and human resources.

Another very intriguing topic is the utilisation of machine learning for the analysis of compound flood events. As machine learning tools become faster and more accurate, there will be many applications for them in the future, for example rapid flood prediction to improve forecasting. An example for this is the recent network introduced by Google researchers for the prediction of extreme riverine events in ungauged watersheds (Nearing et al., 2024). While training a neural

network on events that occur infrequently in data sets is challenging, there are an increasing number of networks, such as ClimateNet (Prabhat et al., 2021), that are emerging for climate extremes research. In addition, many new techniques have been developed in recent years, such as semi-supervised pre-training, which could help to mitigate overfitting caused by the relatively small number of data points available for the classification of Großwetterlagen.

In addition to the research that needs to be done on the scientific side, there is the need to inform decision-makers and policymakers so that compound flood events are taken into account in the planning of future coastal protection. Only cooperation between scientists, politicians and local decision-makers can bring about the necessary changes. All those are aspects of the project 'Wasser an den Küsten Ostfrieslands' (WAKOS), which my studies are part of. The aim of this project is to inform local stakeholders in the region of East Frisia about the projected changes due to climate change, and at the same time to gain an understanding of the information they need, their own assessment of the situation based on their experience, and the underlying decision-making structure. I therefore hope that the insights gained in my studies will prove useful in this knowledge transfer process. Weisse et al. (2024) provided a detailed report on the findings in the first phase of this project.

Overall, my dissertation provides new insights into the emerging topic of compound flood events in northern and central Europe and their future changes under climate change.

A

PRESERVATION OF INFORMATION ON THE FLOODING OF LYMINGTON IN 1999

INFORMATION

The flooding of Lymington in 1999 is often highlighted in literature as an example of compound flood events, but a lot of information has been lost to time. While doing my research for this dissertation, I requested the final report on this particular event, titled 'Final Report of Flood event 24th December to 26th December 1999' (O'Connell, 2000), from the Environment Agency under the Freedom of Information Act 2000 and the Environmental Information Regulations 2004.

Another piece of information is the presentation 'Integrating Wetland Restoration and Flood Risk Management' by Tim Kermode who worked at that time for the Environment Agency as Area Flood Risk Manager of the Hampshire and Isle of Wight (IOW) Area. The presentation was given on 13th June 2006 as part of the LIFE3 Technical Conference titled 'Wetland Restoration at a Catchment Scale'. This presentation is furthermore the source of Fig. 1.1 in Chapter 1. The original pdf file was available at `www.newforestlife.org.uk/life3/PDFs/TimKermodeEA.pdf`, but the website was shut down in 2019. It is unclear whether the presentation was still available at that time. Fortunately, it was archived by the Wayback Machine of the Internet Archive foundation in 2009 under `https://web.archive.org/web/20091211162712/http://www.newforestlife.org.uk/life3/PDFs/TimKermodeEA.pdf`. It was last accessed by me on: 28.05.2024.

The map used in the presentation by Tim Kermode, and therefore also in Fig. 1.1, originates from a report titled 'Flooding at Lymington, Hampshire - Pre-feasibility Study - Volume 1, Factual Report'. The report was produced by Halcrow Water on behalf of the Environment Agency and published in May 2000. According to the Environment Agency, a physical copy of this report still exists within their paper storage archives. A scan of the official document provided to me by the Environment Agency is shown in Fig. A.1.

The sections concerning the flooding of Lymington in the presentation and scans of the original documents are included in my dissertation to preserve them with permission of the Environment Agency.

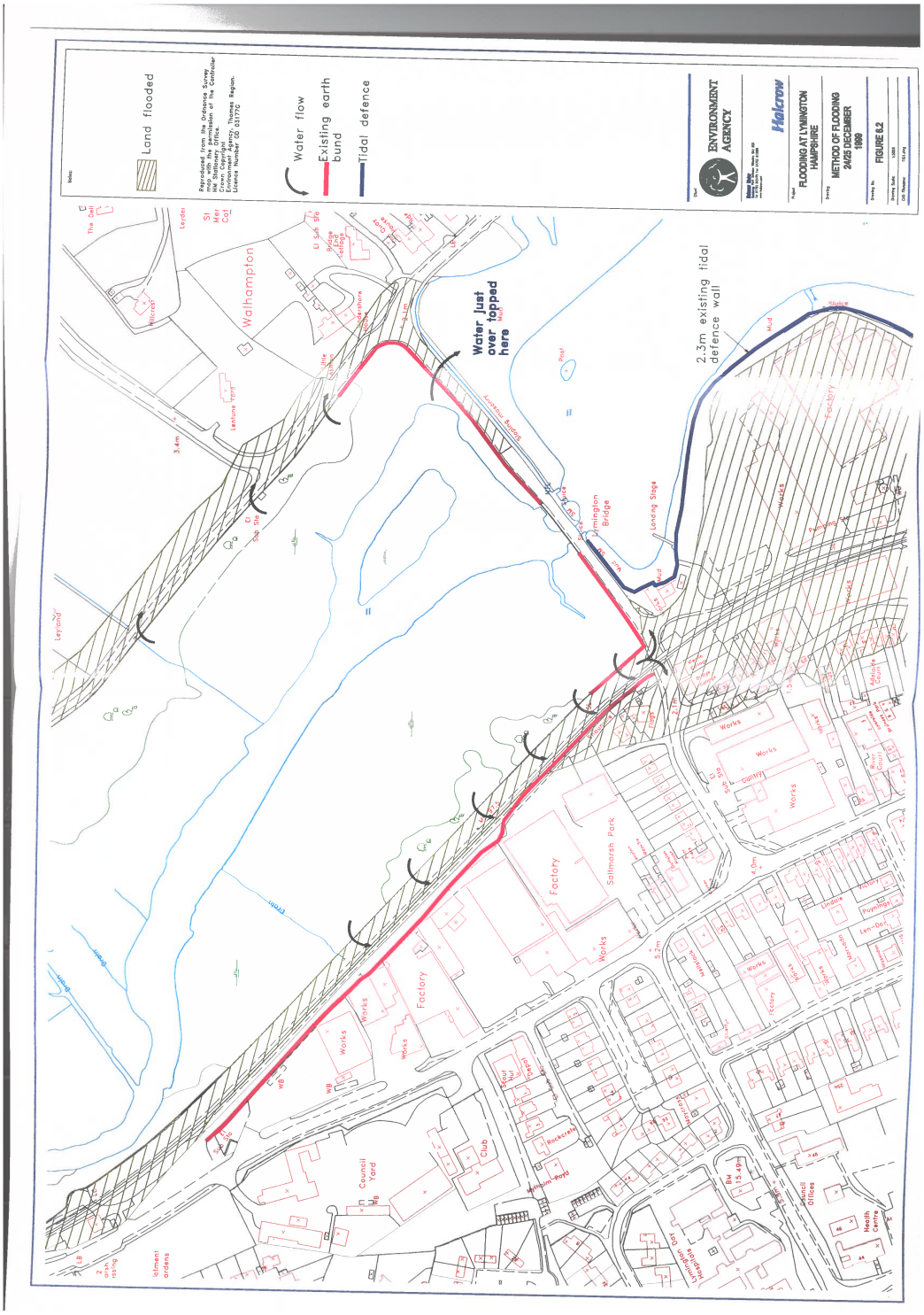

Figure A.1: Original document on the flooding of Lymington in December 1999, scanned and provided by the Environment Agency. Source: Flooding at Lymington, Hampshire - Pre-feasibility Study - Volume 1, Factual Report. Produced by Halcrow Water and published in May 2000. Contains public sector information licensed under the Open Government Licence v3.0.

New Forest Life
PARTNERSHIP

Environment Agency

Tim Kermode

Area Flood Risk Manager

Hampshire and IOW Area

Integrating Wetland Restoration and Flood Risk Management

NATURA 2000 · ENGLISH NATURE · Forestry Commission England · Hampshire County Council · THE NATIONAL TRUST · RSPB

New Forest Life
PARTNERSHIP

Environment Agency

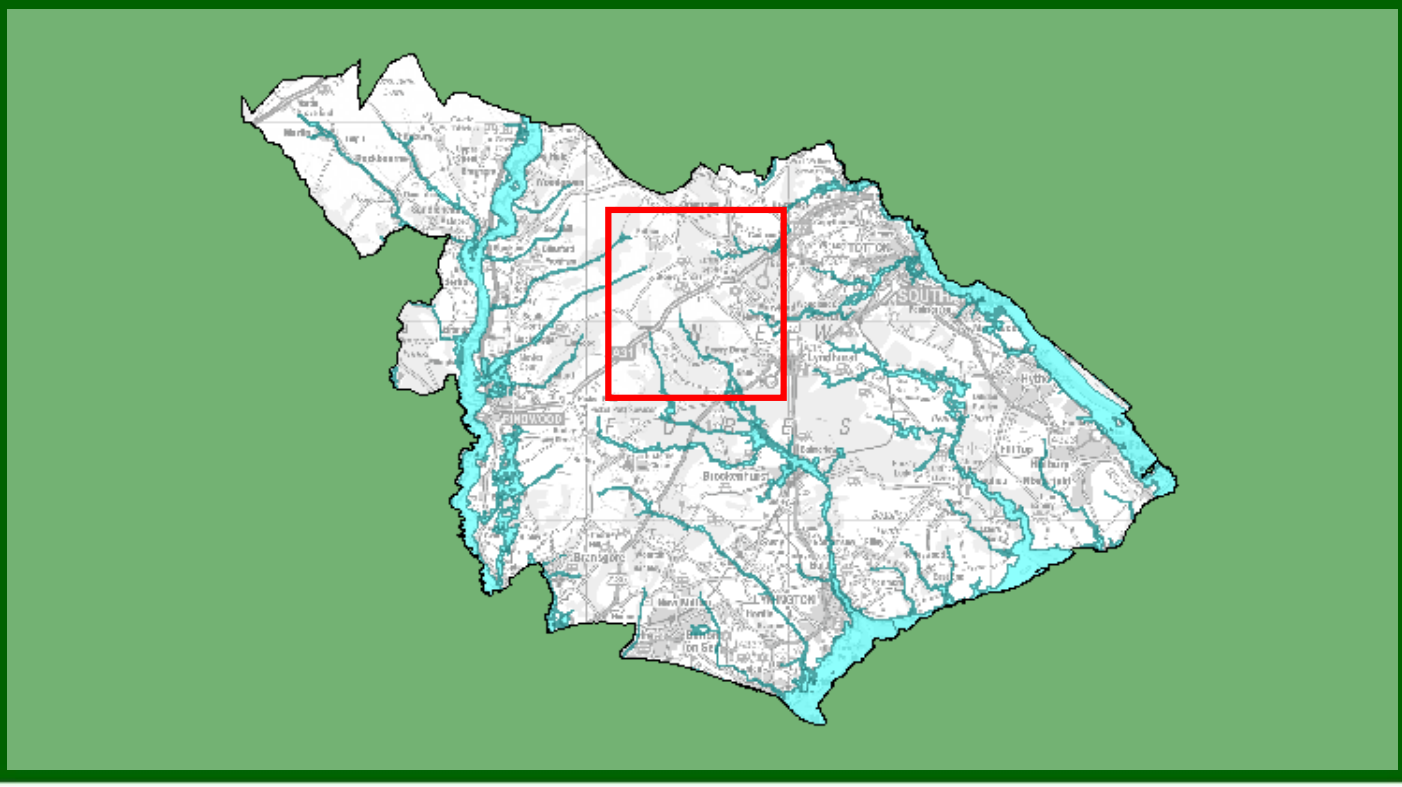

Life

New Forest Life

PARTNERSHIP

Environment Agency

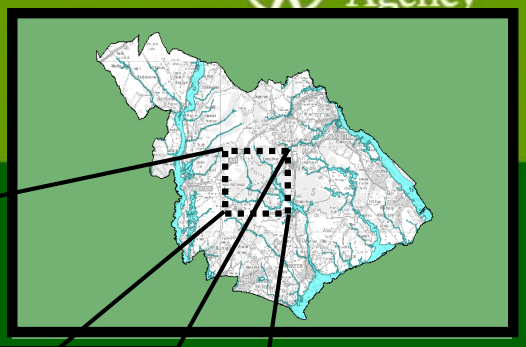

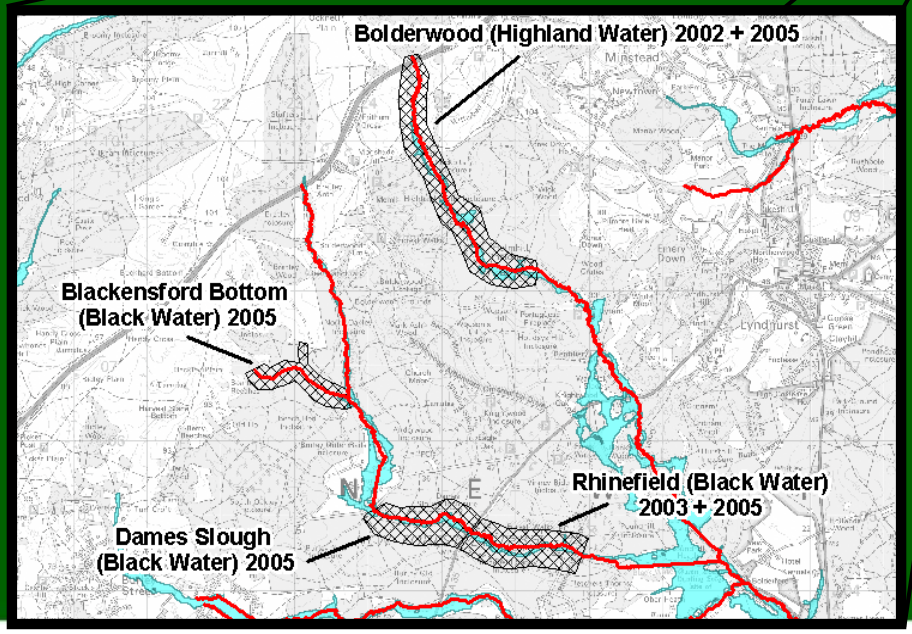

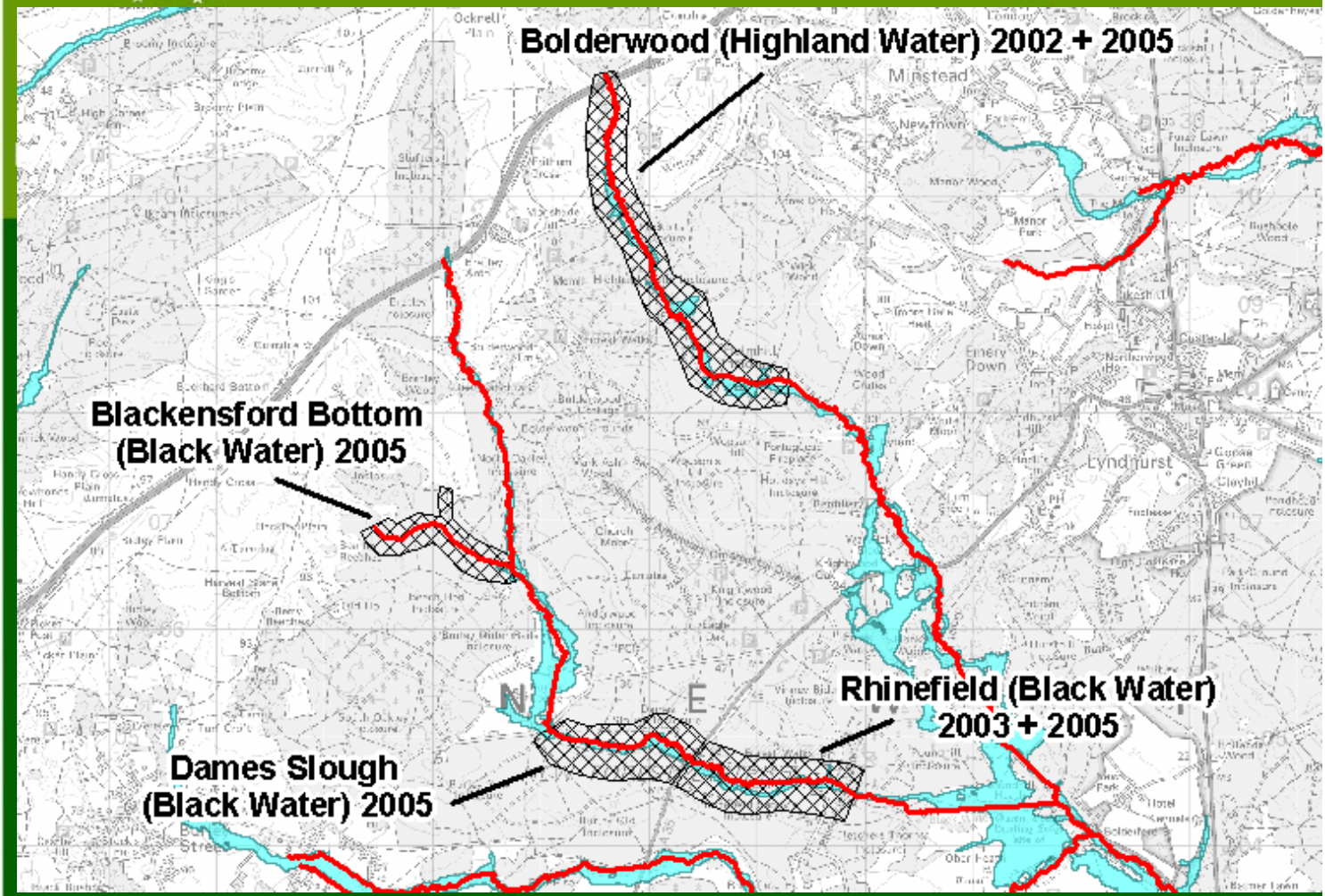

New Forest Life PARTNERSHIP

Environment Agency

What is the Problem?

- All significant Forest Rivers flow through towns and villages before reaching the sea
- Most rivers are “tide-locked”
- Flooding 1999 Lymington, Keyhaven, Brockenhurst, Beaulieu, Marchwood Hythe

New Forest Life PARTNERSHIP

Environment Agency

Life

New Forest Life
PARTNERSHIP

Environment Agency

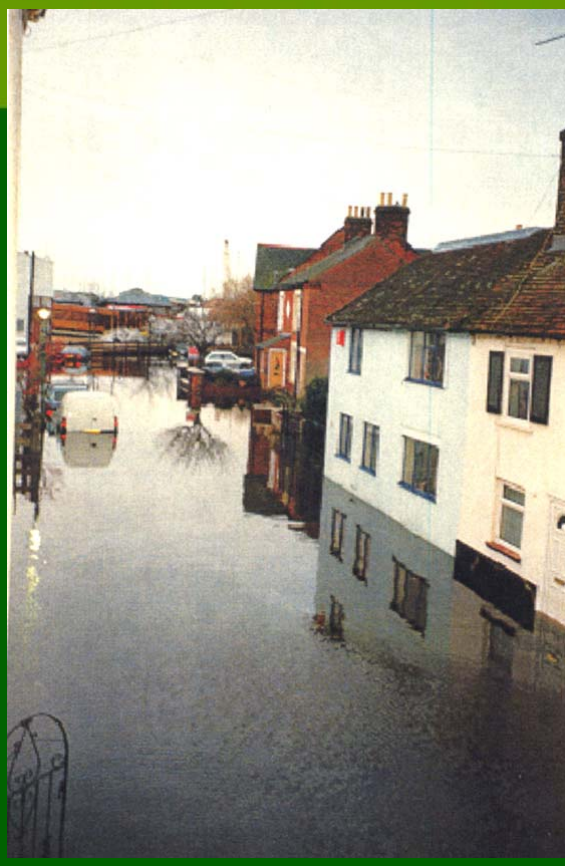

Life

New Forest Life
PARTNERSHIP

Environment Agency

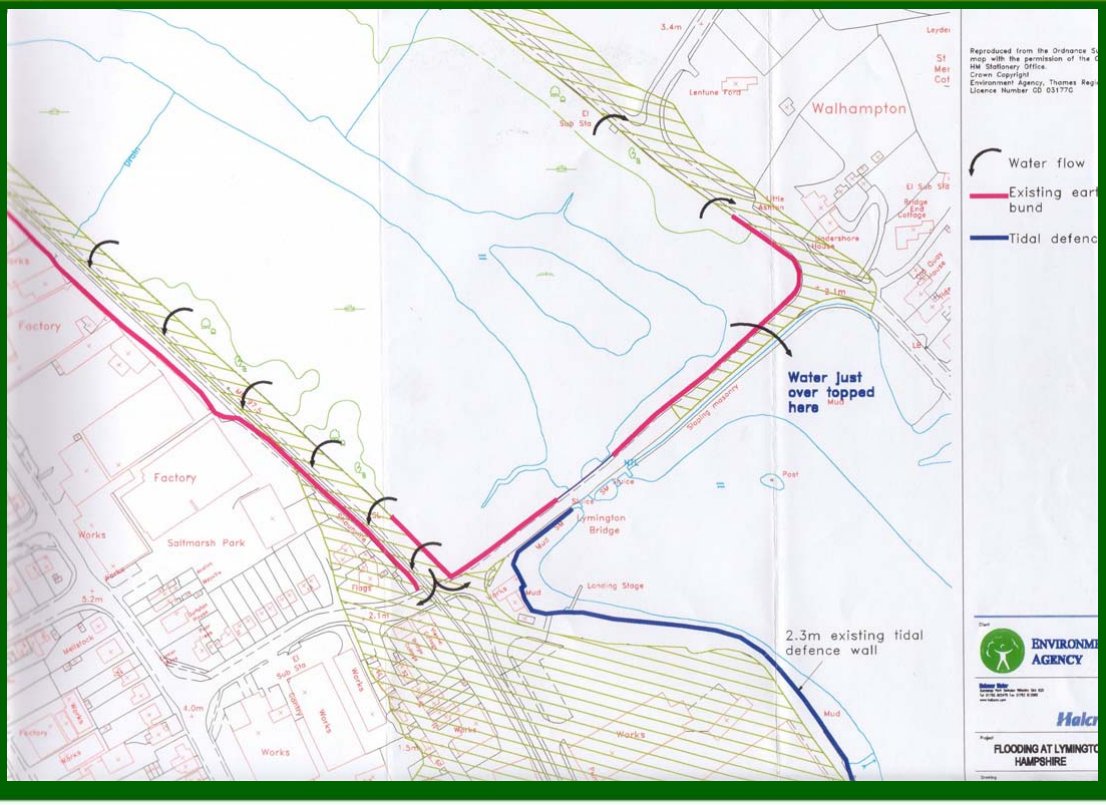

Environment Agency Southern Region, Hants & IoW Area

Final Report of Flood event 24th December to 26th December 1999

Neil O'Connell
June 2000

Executive summary

Over the Christmas period 1999 the area experienced intense rainfall and exceptionally high surge Spring Tides causing a number of locations to flood. In total 145 properties are known to have flooded in 17 locations. Many more properties experienced external flooding i.e. garages, gardens and sheds, which caused damage to vehicles and household goods. In additional a rail link was disrupted as well as numerous roads becoming dangerous and impassable.

The majority of the flooding was caused by the rivers' peak flows coinciding with the rising tide in their estuary's and preventing the normal outflow into the sea. However, there were also some instances of separate tidal and fluvial flooding incidents. The speed and intensity of the peak run off was enhanced because all the area's catchments were fully saturated.

The Area Incident Room was opened at various times over the holiday period to co-ordinate the operational response as well as liasing with the public and partner authorities. Agency staff were deployed across the area to monitor and undertake operations as required.

Introduction

This report has been written as a resource for the Environment Agency. The report covers the flooding events of December 1999, giving particular detail to the meteorological conditions at the time, descriptions of all the individual flood events and plans of the flooded properties. The report has been broken down into two key areas, Hampshire and the Isle of Wight. These areas are then divided down into smaller locations where the flood events occurred.

Shortly after each flood event, effected residents were asked to complete a sheet detailing the effects of the flood on their property. It was this information that was used to compile the plans of the flooded properties.

Meteorological Conditions

Approximately 40 to 60mm of rain fell in two distinct periods during 23rd & 24th December across the county. A further 14 to 20mm of rain was recorded during 26th December in two bands.

An unusually high High Water occurred on the night of 24th December at about midnight of nearly 2.85m Above Ordnance Datum (AOD) at Southampton compared with a predicted tide of 2.61m AOD, ie a surge of +0.24m. The highest recorded HW since 26th November 1924 occurred at about 13:15 on 26th December of 2.90m AOD, compared to a predicted tide of 1.96m AOD, i.e. a surge of +0.94m. Storm Tide Warning Service's surge prediction was a tide of 2.63m AOD, i.e. actual tide level was nearly 300mm on top of that forecast. *(STWS reported that the ports where they have gauges verified their forecast as being very accurate. Southampton is not a calibration port & is not currently modelled accurately due to the unusual tidal patterns.)*

The atmospheric pressure declined from 1015mb on the morning of the 23rd December to a low of 978mb on the evening of the 24th December. During 25th December the pressure then rose again to 994mb around midday falling to a low of 977mb around midnight. These low pressure systems added significant surges on the tides and contributed to the high rain falls. The surge at Lymington was about 900mm on the midnight tide of 24th December. Cowes and Ryde experienced a surge of 500mm on 24th whilst on 26th the surge was recorded at 770mm. At Southampton the 26th surge was 940mm. Refer to appendices one for raw data.

1.2.2 Lymington

- Rainfall at Brockenhurst between 22nd and 24th December was 60.40mm, however, the majority fell in two bands on 24th of 18.2mm (am) and 26.0mm (pm), total 44.2mm on the day. See below.

Date	Time	Length of period	Rainfall within period	Return period
24-12-99	01:24-06:09	4hrs 45mins	18.2mm	1 year
24-12-99	12:39-19:54	7hr 15mins	26.0mm	<1 year
24-12-99	01:24-19:54	18hrs 30mins	44mm	3.5 years

- The predicted tide was 1.09m (AOD); the actual recorded level was 1.99m AOD. High Water was at midnight and the second high water, (300mm lower), occurred approximately 2 hours later with ebb tide starting 3 hours after HW. This coincided with the rising river level although the peak river flow occurred after the second HW, Brockenhurst weir gauge peaked at about 2:15am, 25th Dec. (The Toll Bridge river gauge was not operational, however, the tidal gauge was working.)
- Flooding occurred due to the river overtopping upstream of the Toll Bridge on the Lymington side and flowing on to the railway. Water flowed towards the town along the railway until reaching a low point at the level crossing. Floodwater then found its way in to low points in the adjacent area, as a result Bridge Street, Waterloo Road and Webbs Chicken Factory were affected. It is estimated up to 25 houses and 4 commercial properties had water inside their properties. Depth of water seems to have been over 1m in places.
- The high tide prevented the floodwaters from the New Forest from discharging out to sea which effectively tide locked the fluvial flow in the reed bed area. EA staff confirmed that both gates were fully open around 1:30 to 2:00am (time of opening has not been recorded). Sewer surcharging was also evident and, due to the exceptionally high tide, contributed to the flooding.
- The new tidal defences prevented major flooding from the high surge tide. Bath Road, King's Saltern Rd and around into Quay Road/Street would otherwise have flooded in addition to Bridge Street and Waterloo Road.
- The high tide was the same level as in 1989 when the old defences were breached with widespread flooding of more than 50 homes and 10 commercial properties. The new defences therefore worked well in preventing more flooding.
- If the Toll Gates had not been constructed, the high tide was at a level that it would have still backed up the high river flow and is likely to have caused similar flooding upstream of the Toll Bridge. The new tidal gates, constructed about 4 years ago, at the Toll Bridge will have allowed more water out of the river than the older gates.
- EA Direct Workforce assisted the Fire Brigade and New Forest District Council staff by redeploying sandbags originally intended for the tidal defences to the affected area.

- The Agency's consultant has modelled the river upstream of the Toll Bridge and is investigating the flooding mechanism. Currently the return period for the event is estimated at 1 in 50 years as a combined fluvial and tidal event with a river flow return period of 1 in 20 years. An assessment of costs and benefits to justify raising any low points is also being made. Early indications are that the cost of works to provide a 1 in 200 year standard is +£170k giving possible benefits of £350k. Currently these figures would yield a high enough MAFF priority score to meet their funding threshold. However, these figures are subject to uncertainty and the resulting MAFF score may not meet their funding threshold in practice.
- For further information refer to consultant report 'Flooding at Lymington' (Halcrow Water) May 2000.

Summary of Warnings Issued

- Lower Test and Blackwater had Red warning.
- River Lymington, upper & lower fluvial Wallington and Monks Brook had Amber warnings.
- All Tidal areas had Amber warnings.
- Yellow warnings were also issued in advance of the above in some cases.
- River and Tidal Warnings issued during the 24th as situation developed.
- Further Tidal warnings issued for 26th, Amber for Hayling Island and all others Yellow.

Conclusions

A combination of very heavy rainfall and high tides increased by the low pressure that passed over the south between the 23rd and the 26th resulted in extensive flooding throughout the south.

The majority of the flooding was caused by the rivers' peak flows coinciding with these rising tide in their estuary's and preventing the normal outflow into the sea. However, there were also some instances of separate tidal and fluvial flooding incidents. The speed and intensity of the peak run off was enhanced because all the area's catchments were fully saturated.

In all 10 significant flood events occurred in Hampshire with a further 7 on the Isle of Wight. Based on property damage, the worst effected areas were Monkton Mead, Ryde on the Isle of Wight, Totton near Southampton and Lymington. All these areas had in excess of 30 properties damaged. In total across all 17 areas 289 properties were effected. The ratio between flooding inside and outside of these properties is approximately 1:1. So for every property flooded on the outside one would be flooded on the inside.

It should be noted that not every household effected by the flooding completed an information sheet, hence these figures are based solely on the data collected.

In additional a rail link was disrupted as well as numerous roads becoming dangerous and impassable.

The Area Incident Room was opened at various times over the holiday period to co-ordinate the operational response as well as liasing with the public and partner authorities. Agency staff were deployed across the area to monitor and undertake operations as required.

LIST OF FREE AND OPEN-SOURCE SOFTWARE PACKAGES

This list contains references to the free and open-source software packages used in the creation of this dissertation, where the software had references available. This dissertation would not have been possible without your amazing work. Citations are displayed as intended by the software authors.

Akiba, T., Sano, S., Yanase, T., Ohta, T. and Koyama, M. (2019). 'Optuna: A Next-generation Hyperparameter Optimization Framework'. In: *Proceedings of the 25th ACM SIGKDD International Conference on Knowledge Discovery & Data Mining*. KDD '19. Anchorage, AK, USA: Association for Computing Machinery, pp. 2623–2631. ISBN: 9781450362016. DOI: 10.1145/3292500.3330701.

Ansel, J., Yang, E., He, H., Gimelshein, N., Jain, A., Voznesensky, M., Bao, B., Bell, P., Berard, D., Burovski, E., Chauhan, G., Chourdia, A., Constable, W., Desmaison, A., DeVito, Z., Ellison, E., Feng, W., Gong, J., Gschwind, M., Hirsh, B., Huang, S., Kalambarkar, K., Kirsch, L., Lazos, M., Lezcano, M., Liang, Y., Liang, J., Lu, Y., Luk, C. K., Maher, B., Pan, Y., Puhrsch, C., Reso, M., Saroufim, M., Siraichi, M. Y., Suk, H., Zhang, S., Suo, M., Tillet, P., Zhao, X., Wang, E., Zhou, K., Zou, R., Wang, X., Mathews, A., Wen, W., Chanan, G., Wu, P. and Chintala, S. (2024). 'PyTorch 2: Faster Machine Learning Through Dynamic Python Bytecode Transformation and Graph Compilation'. In: *Proceedings of the 29th ACM International Conference on Architectural Support for Programming Languages and Operating Systems, Volume 2*. ASPLOS '24. New York, NY, USA: Association for Computing Machinery, pp. 929–947. DOI: 10.1145/3620665.3640366.

Bayer, M. (2012). 'SQLAlchemy'. In: *The Architecture of Open Source Applications Volume II: Structure, Scale, and a Few More Fearless Hacks*. Ed. by A. Brown and G. Wilson. Mountain View. aosabook.org. URL: https://aosabook.org/en/sqlalchemy.html (visited on 14th March 2024).

Clark, A. (2015). *Pillow (PIL Fork) Documentation*. readthedocs. URL: https://buildmedia.readthedocs.org/media/pdf/pillow/latest/pillow.pdf (visited on 14th March 2024).

Falcon, W. and The PyTorch Lightning team (2023). *PyTorch Lightning*. Version 2.1.3. Zenodo. DOI: 10.5281/zenodo.10419201.

Gillies, S., van der Wel, C., Van den Bossche, J., Taves, M. W., Arnott, J., Ward, B. C. et al. (2022). *Shapely*. Version 2.0.0. DOI: 10.5281/zenodo.7428463.

Hagberg, A. A., Schult, D. A. and Swart, P. J. (2008). 'Exploring Network Structure, Dynamics, and Function using NetworkX'. In: *Proceedings of the 7th Python in Science Conference*. Ed. by G. Varoquaux, T. Vaught and J. Millman. Pasadena, CA USA, pp. 11–15.

Harris, C. R., Millman, K. J., van der Walt, S. J., Gommers, R., Virtanen, P., Cournapeau, D., Wieser, E., Taylor, J., Berg, S., Smith, N. J., Kern, R., Picus,

M., Hoyer, S., van Kerkwijk, M. H., Brett, M., Haldane, A., del Río, J. F., Wiebe, M., Peterson, P., Gérard-Marchant, P., Sheppard, K., Reddy, T., Weckesser, W., Abbasi, H., Gohlke, C. and Oliphant, T. E. (2020). 'Array programming with NumPy'. In: *Nature* 585.7825, pp. 357–362. DOI: 10.1038/s41586-020-2649-2.

Hoyer, S. and Hamman, J. (2017). 'xarray: N-D labeled arrays and datasets in Python'. In: *Journal of Open Research Software* 5.1. Ubiquity Press. DOI: 10.5334/jors.148.

Hunter, J. D. (2007). 'Matplotlib: A 2D graphics environment'. In: *Computing in Science & Engineering* 9.3. IEEE COMPUTER SOC, pp. 90–95. DOI: 10.1109/MCSE.2007.55.

Lamport, L. (1986). *LATEX: A Document Preparation System, Adison*. Wesley Publishing Co., Reading. Ma.

Met Office (2010). *Cartopy: a cartographic python library with a Matplotlib interface*. Exetger, Devon. URL: https://scitools.org.uk/cartopy/docs/latest/ (visited on 14th March 2024).

Meurer, A., Smith, C. P., Paprocki, M., Čertík, O., Kirpichev, S. B., Rocklin, M., Kumar, A., Ivanov, S., Moore, J. K., Singh, S., Rathnayake, T., Vig, S., Granger, B. E., Muller, R. P., Bonazzi, F., Gupta, H., Vats, S., Johansson, F., Pedregosa, F., Curry, M. J., Terrel, A. R., Roučka, Š., Saboo, A., Fernando, I., Kulal, S., Cimrman, R. and Scopatz, A. (2017). 'SymPy: symbolic computing in Python'. In: *PeerJ Computer Science* 3, e103. DOI: 10.7717/peerj-cs.103.

Nicki Skafte Detlefsen, Jiri Borovec, Justus Schock, Ananya Harsh, Teddy Koker, Luca Di Liello, Daniel Stancl, Changsheng Quan, Maxim Grechkin and William Falcon (2022). *TorchMetrics - Measuring Reproducibility in PyTorch*. Apache-2.0. DOI: 10.21105/joss.04101. URL: https://github.com/Lightning-AI/torchmetrics.

Pedregosa, F., Varoquaux, G., Gramfort, A., Michel, V., Thirion, B., Grisel, O., Blondel, M., Prettenhofer, P., Weiss, R., Dubourg, V., Vanderplas, J., Passos, A., Cournapeau, D., Brucher, M., Perrot, M. and Duchesnay, É. (2011). 'Scikit-learn: Machine Learning in Python'. In: *Journal of Machine Learning Research* 12.85, pp. 2825–2830. URL: http://jmlr.org/papers/v12/pedregosa11a.html (visited on 14th March 2024).

Rew, R. and Davis, G. (1990). 'NetCDF: An Interface for Scientific Data Access'. In: *IEEE Computer Graphics and Applications* 10.4, pp. 76–82.

Schlawack, H., Tvrtkovic, T., Euresti, D., Armstrong, C., Altendorf, K., Cournapeau, D., wouter bolsterlee, Scherfke, S., Stephens, A., Botelho, A., Glyph, Belmonte, J., Oreman, J., Grainger, T., Gates, T., Ford, A., Ganssle, P., paul fisher, Chan, A., Bodrov, A., Freeland, A., Dombrova, C., Macon, G., Bullock, M., Pate, R., Loria, S., Seligmann, T., Iyer, V. and Silva, W. J. (2023). *python-attrs/attrs: 22.1.0*. Version 22.1.0. Publisher: Zenodo. DOI: 10.5281/zenodo.6925130.

The Manim Community Developers (2023). *Manim - Mathematical Animation Framework*. Version v0.18.0. MIT License. URL: https://www.manim.community/ (visited on 25th April 2024).

The mpmath development team (2023). *mpmath: a Python library for arbitrary-precision floating-point arithmetic (version 1.3.0)*. URL: https://mpmath.org/ (visited on 14th March 2024).

The pandas development team (2024). *pandas-dev/pandas: Pandas*. Version v2.2.1. Zenodo. DOI: 10.5281/zenodo.10697587.

TorchVision maintainers and contributors (2016). *TorchVision: PyTorch's Computer Vision library*. BSD-3-Clause. URL: https://github.com/pytorch/vision (visited on 14th March 2024).

Van Rossum, G. and Drake, F. L. (2009). *Python 3 Reference Manual*. Scotts Valley, CA: CreateSpace. ISBN: 1441412697.

Virtanen, P., Gommers, R., Oliphant, T. E., Haberland, M., Reddy, T., Cournapeau, D., Burovski, E., Peterson, P., Weckesser, W., Bright, J., van der Walt, S. J., Brett, M., Wilson, J., Millman, K. J., Mayorov, N., Nelson, A. R. J., Jones, E., Kern, R., Larson, E., Carey, C. J., Polat, İ., Feng, Y., Moore, E. W., VanderPlas, J., Laxalde, D., Perktold, J., Cimrman, R., Henriksen, I., Quintero, E. A., Harris, C. R., Archibald, A. M., Ribeiro, A. H., Pedregosa, F., van Mulbregt, P. and SciPy 1.0 Contributors (2020). 'SciPy 1.0: Fundamental Algorithms for Scientific Computing in Python'. In: *Nature Methods* 17, pp. 261–272. DOI: 10.1038/s41592-019-0686-2.

BIBLIOGRAPHY

AghaKouchak, A., Chiang, F., Huning, L. S., Love, C. A., Mallakpour, I., Mazdiyasni, O., Moftakhari, H., Papalexiou, S. M., Ragno, E. and Sadegh, M. (2020). 'Climate Extremes and Compound Hazards in a Warming World'. In: *Annual Review of Earth and Planetary Sciences* 48, pp. 519–548. DOI: 10.1146/annurev-earth-071719-055228.

Ai, P., Yuan, D. and Xiong, C. (2018). 'Copula-Based Joint Probability Analysis of Compound Floods from Rainstorm and Typhoon Surge: A Case Study of Jiangsu Coastal Areas, China'. In: *Sustainability* 10.7, p. 2232. DOI: 10.3390/su10072232.

Allen, R. G., Pereira, L. S., Raes, D. and Smith, M. (1998). *Crop evapotranspiration-Guidelines for computing crop water requirements-FAO Irrigation and drainage paper 56*. Vol. 300. 9. FAO - Food and Agriculture Organization of the United Nations, p. D05109. ISBN: 92-5-104219-5.

Arns, A., Wahl, T., Dangendorf, S. and Jensen, J. (2015). 'The impact of sea level rise on storm surge water levels in the northern part of the German Bight'. In: *Coastal Engineering* 96, pp. 118–131. DOI: 10.1016/j.coastaleng.2014.12.002.

Arrighi, C., Pregnolato, M., Dawson, R. J. and Castelli, F. (2019). 'Preparedness against mobility disruption by floods'. In: *Science of The Total Environment* 654, pp. 1010–1022. DOI: 10.1016/j.scitotenv.2018.11.191.

Banfi, F. and De Michele, C. (2022). 'Compound flood hazard at Lake Como, Italy, is driven by temporal clustering of rainfall events'. In: *Communications Earth & Environment* 3.1, p. 234. DOI: 10.1038/s43247-022-00557-9.

Ben Daoued, A., Hamdi, Y., Mouhous-Voyneau, N. and Sergent, P. (2020). 'Modeling dependence and coincidence of storm surges and high tide: methodology, discussion and recommendations based on a simplified case study in Le Havre (France)'. In: *Natural Hazards and Earth System Sciences* 20.12, pp. 3387–3398. DOI: 10.5194/nhess-20-3387-2020.

Bennett, W. G., Karunarathna, H., Xuan, Y., Kusuma, M. S. B., Farid, M., Kuntoro, A. A., Rahayu, H. P., Kombaitan, B., Septiadi, D., Kesuma, T. N. A., Haigh, R. and Amaratunga, D. (2023). 'Modelling compound flooding: a case study from Jakarta, Indonesia'. In: *Natural Hazards* 118.1, pp. 277–305. DOI: 10.1007/s11069-023-06001-1.

Benninghoff, M. and Winter, C. (2019). 'Recent morphologic evolution of the German Wadden Sea'. In: *Scientific Reports* 9.1, p. 9293. DOI: 10.1038/s41598-019-45683-1.

Bermúdez, M., Farfán, J. F., Willems, P. and Cea, L. (2021). 'Assessing the Effects of Climate Change on Compound Flooding in Coastal River Areas'. In: *Water Resources Research* 57.10, e2020WR029321. DOI: 10.1029/2020WR029321.

Bevacqua, E., Maraun, D., Vousdoukas, M. I., Voukouvalas, E., Vrac, M., Mentaschi, L. and Widmann, M. (2019). 'Higher probability of compound flooding from precipitation and storm surge in Europe under anthropogenic climate change'. In: *Science Advances* 5.9, eaaw5531. DOI: 10.1126/sciadv.aaw5531.

Bevacqua, E., Vousdoukas, M. I., Zappa, G., Hodges, K., Shepherd, T. G., Maraun, D., Mentaschi, L. and Feyen, L. (2020). 'More meteorological events that drive compound coastal flooding are projected under climate change'. In: *Communications Earth & Environment* 1.1, p. 47. DOI: 10.1038/s43247-020-00044-z.

Bezak, N., Panagos, P., Liakos, L. and Mikoš, M. (2023). 'Brief communication: A first hydrological investigation of extreme August 2023 floods in Slovenia, Europe'. In: *Natural Hazards and Earth System Sciences* 23.12, pp. 3885–3893. DOI: 10.5194/nhess-23-3885-2023.

Bi, D., Dix, M., Marsland, S., O'Farrell, S., Sullivan, A., Bodman, R., Law, R., Harman, I., Srbinovsky, J., Rashid, H. A., Dobrohotoff, P., Mackallah, C., Yan, H., Hirst, A., Savita, A., Dias, F. B., Woodhouse, M., Fiedler, R. and Heerdegen, A. (2020). 'Configuration and spin-up of ACCESS-CM2, the new generation Australian Community Climate and Earth System Simulator Coupled Model'. In: *Journal of Southern Hemisphere Earth Systems Science* 70.1, pp. 225–251. DOI: 10.1071/ES19040.

Bilskie, M. V. and Hagen, S. C. (2018). 'Defining Flood Zone Transitions in Low-Gradient Coastal Regions'. In: *Geophysical Research Letters* 45.6, pp. 2761–2770. DOI: 10.1002/2018GL077524.

Blöschl, G., Hall, J., Parajka, J., Perdigão, R. A. P., Merz, B., Arheimer, B., Aronica, G. T., Bilibashi, A., Bonacci, O., Borga, M., Čanjevac, I., Castellarin, A., Chirico, G. B., Claps, P., Fiala, K., Frolova, N., Gorbachova, L., Gül, A., Hannaford, J., Harrigan, S., Kireeva, M., Kiss, A., Kjeldsen, T. R., Kohnová, S., Koskela, J. J., Ledvinka, O., Macdonald, N., Mavrova-Guirguinova, M., Mediero, L., Merz, R., Molnar, P., Montanari, A., Murphy, C., Osuch, M., Ovcharuk, V., Radevski, I., Rogger, M., Salinas, J. L., Sauquet, E., Šraj, M., Szolgay, J., Viglione, A., Volpi, E., Wilson, D., Zaimi, K. and Živković, N. (2017). 'Changing climate shifts timing of European floods'. In: *Science* 357.6351, pp. 588–590. DOI: 10.1126/science.aan2506.

Bollmeyer, C., Keller, J. D., Ohlwein, C., Wahl, S., Crewell, S., Friederichs, P., Hense, A., Keune, J., Kneifel, S., Pscheidt, I., Redl, S. and Steinke, S. (2015). 'Towards a high-resolution regional reanalysis for the European CORDEX domain'. In: *Quarterly Journal of the Royal Meteorological Society* 141.686, pp. 1–15. DOI: 10.1002/qj.2486.

Bormann, H., Kebschull, J. and Spiekermann, J. (2023). 'Quantifizierung der Auswirkungen des Meeresspiegelanstiegs auf die Entwässerungskapazitäten an der Nordseeküste'. In: *Wasser und Abfall* 25.9, pp. 24–31. DOI: 10.1007/s35152-023-1457-z.

Boucher, O., Servonnat, J., Albright, A. L., Aumont, O., Balkanski, Y., Bastrikov, V., Bekki, S., Bonnet, R., Bony, S., Bopp, L., Braconnot, P., Brockmann, P., Cadule, P.,

Caubel, A., Cheruy, F., Codron, F., Cozic, A., Cugnet, D., D'Andrea, F., Davini, P., Lavergne, C. d., Denvil, S., Deshayes, J., Devilliers, M., Ducharne, A., Dufresne, J.-L., Dupont, E., Éthé, C., Fairhead, L., Falletti, L., Flavoni, S., Foujols, M.-A., Gardoll, S., Gastineau, G., Ghattas, J., Grandpeix, J.-Y., Guenet, B., Lionel, G. E., Guilyardi, E., Guimberteau, M., Hauglustaine, D., Hourdin, F., Idelkadi, A., Joussaume, S., Kageyama, M., Khodri, M., Krinner, G., Lebas, N., Levavasseur, G., Lévy, C., Li, L., Lott, F., Lurton, T., Luyssaert, S., Madec, G., Madeleine, J.-B., Maignan, F., Marchand, M., Marti, O., Mellul, L., Meurdesoif, Y., Mignot, J., Musat, I., Ottlé, C., Peylin, P., Planton, Y., Polcher, J., Rio, C., Rochetin, N., Rousset, C., Sepulchre, P., Sima, A., Swingedouw, D., Thiéblemont, R., Traore, A. K., Vancoppenolle, M., Vial, J., Vialard, J., Viovy, N. and Vuichard, N. (2020). 'Presentation and Evaluation of the IPSL-CM6A-LR Climate Model'. In: *Journal of Advances in Modeling Earth Systems* 12.7, e2019MS002010. DOI: 10.1029/2019MS002010.

Bouwer, L. M., Vermaat, J. E. and Aerts, J. C. J. H. (2006). 'Winter atmospheric circulation and river discharge in northwest Europe'. In: *Geophysical Research Letters* 33.6, pp. 2–5. ISSN: 0094-8276. DOI: 10.1029/2005GL025548.

Bray, S. N. and McCuen, R. H. (2014). 'Importance of the Assumption of Independence or Dependence among Multiple Flood Sources'. In: *Journal of Hydrologic Engineering* 19.6, pp. 1194–1202. DOI: 10.1061/(ASCE)HE.1943-5584.0000901.

Brunner, M. I. and Slater, L. J. (2022). 'Extreme floods in Europe: going beyond observations using reforecast ensemble pooling'. In: *Hydrology and Earth System Sciences* 26.2, pp. 469–482. DOI: 10.5194/hess-26-469-2022.

Bundesamt für Seeschifffahrt und Hydrographie (2022). *Report on the oceanographic conditions at site N-7.2*. file name: N-07-02_oceanography_report_EN.pdf. URL: https://pinta.bsh.de/N-7.2?tab=daten (visited on 19th April 2022).

Cahynová, M. and Huth, R. (2016). 'Atmospheric circulation influence on climatic trends in Europe: an analysis of circulation type classifications from the COST733 catalogue'. In: *International Journal of Climatology* 36.7, pp. 2743–2760. DOI: 10.1002/joc.4003.

Camus, P., Haigh, I. D., Nasr, A. A., Wahl, T., Darby, S. E. and Nicholls, R. J. (2021). 'Regional analysis of multivariate compound coastal flooding potential around Europe and environs: sensitivity analysis and spatial patterns'. In: *Natural Hazards and Earth System Science* 21.7, pp. 2021–2040. DOI: 10.5194/nhess-21-2021-2021.

Camus, P., Haigh, I. D., Wahl, T., Nasr, A. A., Méndez, F. J., Darby, S. E. and Nicholls, R. J. (2022). 'Daily synoptic conditions associated with occurrences of compound events in estuaries along North Atlantic coastlines'. In: *International Journal of Climatology* 42.11, pp. 5694–5713. DOI: 10.1002/joc.7556.

Čepienė, E., Dailidytė, L., Stonevičius, E. and Dailidienė, I. (2022). 'Sea Level Rise Impact on Compound Coastal River Flood Risk in Klaipėda City (Baltic Coast, Lithuania)'. In: *Water* 14.3, p. 414. DOI: 10.3390/w14030414.

Chattopadhyay, A., Hassanzadeh, P. and Pasha, S. (2020). 'Predicting clustered weather patterns: A test case for applications of convolutional neural networks to

spatio-temporal climate data'. In: *Scientific Reports* 10.1, p. 1317. ISSN: 2045-2322. DOI: 10.1038/s41598-020-57897-9.

Chen, W.-B. and Liu, W.-C. (2014). 'Modeling Flood Inundation Induced by River Flow and Storm Surges over a River Basin'. In: *Water* 6.10, pp. 3182–3199. DOI: 10.3390/w6103182.

Cherchi, A., Fogli, P. G., Lovato, T., Peano, D., Iovino, D., Gualdi, S., Masina, S., Scoccimarro, E., Materia, S., Bellucci, A. and Navarra, A. (2019). 'Global Mean Climate and Main Patterns of Variability in the CMCC-CM2 Coupled Model'. In: *Journal of Advances in Modeling Earth Systems* 11.1, pp. 185–209. DOI: 10.1029/2018MS001369.

Clarke, B. J., Otto, F. E. L. and Jones, R. G. (2021). 'Inventories of extreme weather events and impacts: Implications for loss and damage from and adaptation to climate extremes'. In: *Climate Risk Management* 32, p. 100285. ISSN: 2212-0963. DOI: 10.1016/j.crm.2021.100285.

Cornes, R. C., van der Schrier, G., van den Besselaar, E. J. M. and Jones, P. D. (2018). 'An Ensemble Version of the E-OBS Temperature and Precipitation Data Sets'. In: *Journal of Geophysical Research: Atmospheres* 123.17, pp. 9391–9409. DOI: 10.1029/2017JD028200.

Cortés Arbués, I., Chatzivasileiadis, T., Ivanova, O., Storm, S., Bosello, F. and Filatova, T. (2024). 'Distribution of economic damages due to climate-driven sea-level rise across European regions and sectors'. In: *Scientific Reports* 14.1, p. 126. DOI: 10.1038/s41598-023-48136-y.

Couasnon, A. A. O., Eilander, D., Muis, S., Veldkamp, T. I. E., Haigh, I. D., Wahl, T., Winsemius, H. C. and Ward, P. J. (2020). 'Measuring compound flood potential from river discharge and storm surge extremes at the global scale'. In: *Natural Hazards and Earth System Sciences* 20.2, pp. 489–504. DOI: 10.5194/nhess-20-489-2020.

Couasnon, A. A. O. (2023). 'The role of (in) dependence in flood risk assessments'. PhD thesis. Vrije Universiteit Amsterdam. DOI: 10.5463/thesis.176.

Daewel, U. and Schrum, C. (2013). 'Simulating long-term dynamics of the coupled North Sea and Baltic Sea ecosystem with ECOSMO II: Model description and validation'. In: *Journal of Marine Systems* 119, pp. 30–49. DOI: 10.1016/j.jmarsys.2013.03.008.

Danabasoglu, G., Lamarque, J.-F., Bacmeister, J., Bailey, D. A., DuVivier, A. K., Edwards, J., Emmons, L. K., Fasullo, J., Garcia, R., Gettelman, A., Hannay, C., Holland, M. M., Large, W. G., Lauritzen, P. H., Lawrence, D. M., Lenaerts, J. T. M., Lindsay, K., Lipscomb, W. H., Mills, M. J., Neale, R., Oleson, K. W., Otto-Bliesner, B., Phillips, A. S., Sacks, W., Tilmes, S., van Kampenhout, L., Vertenstein, M., Bertini, A., Dennis, J., Deser, C., Fischer, C., Fox-Kemper, B., Kay, J. E., Kinnison, D., Kushner, P. J., Larson, V. E., Long, M. C., Mickelson, S., Moore, J. K., Nienhouse, E., Polvani, L., Rasch, P. J. and Strand, W. G. (2020). 'The

Community Earth System Model Version 2 (CESM2)'. In: *Journal of Advances in Modeling Earth Systems* 12.2, e2019MS001916. DOI: 10.1029/2019MS001916.

Davenport, F. V., Burke, M. and Diffenbaugh, N. S. (2021). 'Contribution of historical precipitation change to US flood damages'. In: *Proceedings of the National Academy of Sciences* 118.4. pp. e2017524118. DOI: 10.1073/pnas.2017524118.

Davies, H. C. (1976). 'A lateral boundary formulation for multi-level prediction models'. In: *Quarterly Journal of the Royal Meteorological Society* 102.432, pp. 405–418. DOI: 10.1002/qj.49710243210.

Davison, M., Currie, I. and Ogley, B. (1993). *The Hampshire and Isle of Wight Weather Book*. Froglets Publications Ltd. ISBN: 1872337201.

De Bruijn, K. M., Diermanse, F. L. M. and Beckers, J. V. L. (2014). 'An advanced method for flood risk analysis in river deltas, applied to societal flood fatality risk in the Netherlands'. In: *Natural Hazards and Earth System Sciences* 14.10, pp. 2767–2781. DOI: 10.5194/nhess-14-2767-2014.

de Ruiter, M. C., Couasnon, A. A. O., van den Homberg, M. J. C., Daniell, J. E., Gill, J. C. and Ward, P. J. (2020). 'Why We Can No Longer Ignore Consecutive Disasters'. In: *Earth's Future* 8.3, e2019EF001425. DOI: 10.1029/2019EF001425.

De Sherbinin, A., Schiller, A. and Pulsipher, A. (2007). 'The vulnerability of global cities to climate hazards'. In: *Environment and Urbanization* 19.1, pp. 39–64. DOI: 10.1177/0956247807076725.

Del-Rosal-Salido, J., Folgueras, P., Bermudez, M., Ortega-Sanchez, M. and Losada, M. A. (2021). 'Flood management challenges in transitional environments: Assessing the effects of sea-level rise on compound flooding in the 21st century'. In: *Coastal Engineering* 167, p. 103872. DOI: 10.1016/j.coastaleng.2021.103872.

Demuzere, M., Werner, M., Van Lipzig, N. P. M. and Roeckner, E. (2009). 'An analysis of present and future ECHAM5 pressure fields using a classification of circulation patterns'. In: *International Journal of Climatology* 29.12, pp. 1796–1810. DOI: 10.1002/joc.1821.

Deng, Z., Wang, B., Xu, Y., Xu, T., Liu, C. and Zhu, Z. (2019). 'Multi-Scale Convolutional Neural Network With Time-Cognition for Multi-Step Short-Term Load Forecasting'. In: *IEEE Access* 7, pp. 88058–88071. DOI: 10.1109/ACCESS.2019.2926137.

Di Sante, F., Coppola, E. and Giorgi, F. (2021). 'Projections of river floods in Europe using EURO-CORDEX, CMIP5 and CMIP6 simulations'. In: *International Journal of Climatology* 41.5, pp. 3203–3221. DOI: 10.1002/joc.7014.

Dietz, M. (2019). 'Veränderungen der Großwetterlagen Mitteleuropas und ihr Einfluss auf die Hochwassergefahr an großen Flüssen in Deutschland'. MA thesis. Albert-Ludwigs-Universität Freiburg.

Döscher, R., Acosta, M., Alessandri, A., Anthoni, P., Arneth, A., Arsouze, T., Bergmann, T., Bernadello, R., Bousetta, S., Caron, L.-P., Carver, G., Castrillo, M., Catalano, F., Cvijanovic, I., Davini, P., Dekker, E., Doblas-Reyes, F. J., Docquier,

D., Echevarria, P., Fladrich, U., Fuentes-Franco, R., Gröger, M., v. Hardenberg, J., Hieronymus, J., Karami, M. P., Keskinen, J.-P., Koenigk, T., Makkonen, R., Massonnet, F., Ménégoz, M., Miller, P. A., Moreno-Chamarro, E., Nieradzik, L., van Noije, T., Nolan, P., O'Donnell, D., Ollinaho, P., van den Oord, G., Ortega, P., Prims, O. T., Ramos, A., Reerink, T., Rousset, C., Ruprich-Robert, Y., Sager, P. L., Schmith, T., Schrödner, R., Serva, F., Sicardi, V., Madsen, M. S., Smith, B., Tian, T., Tourigny, E., Uotila, P., Vancoppenolle, M., Wang, S., Wårlind, D., Willén, U., Wyser, K., Yang, S., Yepes-Arbós, X. and Zhang, Q. (2022). 'The EC-Earth3 Earth system model for the Coupled Model Intercomparison Project 6'. In: *Geoscientific Model Development* 15.7, pp. 2973–3020. DOI: 10.5194/gmd-15-2973-2022.

Douben, K.-J. (2006). 'Characteristics of river floods and flooding: a global overview, 1985–2003'. In: *Irrigation and Drainage* 55.S1, S9–S21. DOI: 10.1002/ird.239.

Dykstra, S. L. and Dzwonkowski, B. (2021). 'The Role of Intensifying Precipitation on Coastal River Flooding and Compound River-Storm Surge Events, Northeast Gulf of Mexico'. In: *Water Resources Research* 57.11, e2020WR029363. DOI: 10.1029/2020WR029363.

Eilander, D., Couasnon, A. A. O., Ikeuchi, H., Muis, S., Yamazaki, D., Winsemius, H. C. and Ward, P. J. (2020). 'The effect of surge on riverine flood hazard and impact in deltas globally'. In: *Environmental Research Letters* 15.10, p. 104007. DOI: 10.1088/1748-9326/ab8ca6.

Engeland, K., Hisdal, H. and Frigessi, A. (2004). 'Practical Extreme Value Modelling of Hydrological Floods and Droughts: A Case Study'. In: *Extremes* 7.1, pp. 5–30. DOI: 10.1007/s10687-004-4727-5.

European Centre for Medium-Range Weather Forecasts (2014). *ERA-20C Project (ECMWF Atmospheric Reanalysis of the 20th Century)*. Boulder CO. DOI: 10.5065/D6VQ30QG.

European Commission and Directorate-General for European Civil Protection and Humanitarian Aid Operations (ECHO) (2021). *Overview of natural and man-made disaster risks the European Union may face : 2020 edition*. Publications Office. DOI: 10.2795/19072.

European Environment Agency (2024). *European climate risk assessment - Full Report*. Note: The 'Full report' and 'Executive summary' share the same doi. Publications Office of the European Union. DOI: 10.2800/204249.

European Union (2007). *Directive 2007/60/EC of the European Parliament and of the Council of 23 October 2007 on the assessment and management of flood risks*. URL: https://eur-lex.europa.eu/eli/dir/2007/60 (visited on 18th March 2024).

Fan, H., Murrell, T., Wang, H., Alwala, K. V., Li, Y., Li, Y., Xiong, B., Ravi, N., Li, M., Yang, H., Malik, J., Girshick, R., Feiszli, M., Adcock, A., Lo, W.-Y. and Feichtenhofer, C. (2021). 'PyTorchVideo: A Deep Learning Library for Video Understanding'. In: *Proceedings of the 29th ACM International Conference on Multimedia*. DOI: 10.48550/arXiv.2111.09887.

Fang, J., Wahl, T., Fang, J., Sun, X., Kong, F. and Liu, M. (2021). 'Compound flood potential from storm surge and heavy precipitation in coastal China: dependence, drivers, and impacts'. In: *Hydrology and Earth System Sciences* 25.8, pp. 4403–4416. DOI: 10.5194/hess-25-4403-2021.

Feser, F., Barcikowska, M., Krueger, O., Schenk, F., Weisse, R. and Xia, L. (2015). 'Storminess over the North Atlantic and northwestern Europe-A review'. In: *Quarterly Journal of the Royal Meteorological Society* 141.687, pp. 350–382. DOI: 10.1002/qj.2364.

Feyen, L., Ciscar Martinez, J. C., Gosling, S., Ibarreta Ruiz, D. and Soria Ramirez, A. (2020). *Climate change impacts and adaptation in Europe. JRC PESETA IV final report*. Tech. rep. Joint Research Centre (Seville site). DOI: 10.2760/171121.

Fox-Kemper, B., Hewitt, H. T., Xiao, C., Adalgeirsdottir, G., Drijfhout, S. S., Edwards, T. L., Golledge, N. R., Hemer, M., Kopp, R. E., Krinner, G., Mix, A., Notz, D., Nowicki, S., Nurhati, I. S., Ruiz, L., Sallée, J.-B., Slangen, A. B. A. and Yu, Y. (2021). 'Ocean, Cryosphere and Sea Level Change'. In: *Climate Change 2021: The Physical Science Basis. Contribution of Working Group I to the Sixth Assessment Report of the Intergovernmental Panel on Climate Change*. Cambridge, United Kingdom and New York, NY, USA: Cambridge University Press. Chap. 9, pp. 1211–1362. DOI: 10.1017/9781009157896.011.

Galiatsatou, P., Anagnostopoulou, C. and Prinos, P. (2016). 'Modeling nonstationary extreme wave heights in present and future climates of Greek Seas'. In: *Water Science and Engineering* 9.1, pp. 21–32. DOI: 10.1016/j.wse.2016.03.001.

Ganguli, P. and Merz, B. (2019). 'Trends in Compound Flooding in Northwestern Europe During 1901–2014'. In: *Geophysical Research Letters* 46.19, pp. 10810–10820. DOI: 10.1029/2019GL084220.

Ganguli, P., Paprotny, D., Hasan, M., Güntner, A. and Merz, B. (2020). 'Projected Changes in Compound Flood Hazard From Riverine and Coastal Floods in Northwestern Europe'. In: *Earth's Future* 8.11, e2020EF001752. DOI: 10.1029/2020EF001752.

Garner, G. G., Hermans, T., Kopp, R. E., Slangen, A. B. A., Edwards, T. L., Levermann, A., Nowikci, S., Palmer, M. D., Smith, C., Fox-Kemper, B., Hewitt, H. T., Xiao, C., Aðalgeirsdóttir, G., Drijfhout, S. S., Edwards, T. L., Golledge, N. R., Hemer, M., Krinner, G., Mix, A., Notz, D., Nowicki, S., Nurhati, I. S., Ruiz, L., Sallée, J.-B., Yu, Y., Hua, L., Palmer, T. and Pearson, B. (2021). *IPCC AR6 Sea Level Projections*. Version 20210809. DOI: 10.5281/zenodo.5914710. (Visited on 12th July 2022).

Gaslikova, L., Grabemann, I. and Groll, N. (2013). 'Changes in North Sea storm surge conditions for four transient future climate realizations'. In: *Natural Hazards* 66, pp. 1501–1518. DOI: 10.1007/s11069-012-0279-1.

Gerstengarbe, F.-W., Werner, P. C. and Rüge, U. (1999). *Katalog der Grosswetterlagen Europas (1881-1998) nach Paul Hess und Helmuth Brezowsky*. Potsdam-Institut

für Klimafolgenforschung. URL: https://www.pik-potsdam.de/en/output/publications/pikreports/.files/pr119.pdf (visited on 26th May 2023).

Gettelman, A., Mills, M. J., Kinnison, D. E., Garcia, R. R., Smith, A. K., Marsh, D. R., Tilmes, S., Vitt, F., Bardeen, C. G., McInerny, J., Liu, H.-L., Solomon, S. C., Polvani, L. M., Emmons, L. K., Lamarque, J.-F., Richter, J. H., Glanville, A. S., Bacmeister, J. T., Phillips, A. S., Neale, R. B., Simpson, I. R., DuVivier, A. K., Hodzic, A. and Randel, W. J. (2019). 'The Whole Atmosphere Community Climate Model Version 6 (WACCM6)'. In: *Journal of Geophysical Research: Atmospheres* 124.23, pp. 12380–12403. DOI: 10.1029/2019JD030943.

Geyer, B. (2014). 'High-resolution atmospheric reconstruction for Europe 1948–2012: coastDat2'. In: *Earth System Science Data* 6.1, pp. 147–164. DOI: 10.5194/essd-6-147-2014.

Giorgetta, M. A., Jungclaus, J., Reick, C. H., Legutke, S., Bader, J., Böttinger, M., Brovkin, V., Crueger, T., Esch, M., Fieg, K., Glushak, K., Gayler, V., Haak, H., Hollweg, H.-D., Ilyina, T., Kinne, S., Kornblueh, L., Matei, D., Mauritsen, T., Mikolajewicz, U., Mueller, W., Notz, D., Pithan, F., Raddatz, T., Rast, S., Redler, R., Roeckner, E., Schmidt, H., Schnur, R., Segschneider, J., Six, K. D., Stockhause, M., Timmreck, C., Wegner, J., Widmann, H., Wieners, K.-H., Claussen, M., Marotzke, J. and Stevens, B. (2013). 'Climate and carbon cycle changes from 1850 to 2100 in MPI-ESM simulations for the Coupled Model Intercomparison Project phase 5'. In: *Journal of Advances in Modeling Earth Systems* 5.3, pp. 572–597. DOI: 10.1002/jame.20038.

Giorgi, F., Jones, C. and Asrar, G. R. (2009). 'Addressing climate information needs at the regional level: the CORDEX framework'. In: *World Meteorological Organization (WMO) Bulletin* 58.3, p. 175. ISSN: 0042-9767. URL: https://library.wmo.int/idurl/4/58817 (visited on 29th May 2024).

Gonzalez, P. L. M., Brayshaw, D. J. and Zappa, G. (2019). 'The contribution of North Atlantic atmospheric circulation shifts to future wind speed projections for wind power over Europe'. In: *Climate Dynamics* 53.7, pp. 4095–4113. DOI: 10.1007/s00382-019-04776-3.

Grabau, J. (1987). 'Klimaschwankungen und Großwetterlagen in Mitteleuropa seit 1881'. In: *Geographica Helvetica* 42.1, pp. 35–40. DOI: 10.5194/gh-42-35-1987.

Gumbel, E. J. (1958). *Statistics of extremes*. Columbia university press. DOI: 10.7312/gumb92958.

Hagemann, S., Stacke, T. and Ho-Hagemann, H. T. M. (2020). 'High Resolution Discharge Simulations Over Europe and the Baltic Sea Catchment'. In: *Frontiers in Earth Science* 8, p. 12. DOI: 10.3389/feart.2020.00012.

Hagemann, S. and Stacke, T. (2021). *Forcing for HD Model from HydroPy and subsequent HD Model river runoff over Europe based on EOBS22 and ERA5 data*. DOI: 10.26050/WDCC/EOBS_ERA5-River_Runoff.

Hagemann, S. and Ho-Hagemann, H. T. M. (2021). *The Hydrological Discharge Model - a river runoff component for offline and coupled model applications*. DOI: 10.5281/zenodo.4893099.

Hagemann, S. and Stacke, T. (2023). 'Complementing ERA5 and E-OBS with high-resolution river discharge over Europe'. In: *Oceanologia* 65.1, pp. 230–248. DOI: 10.1016/j.oceano.2022.07.003.

Haigh, I. D., Wadey, M. P., Wahl, T., Ozsoy, O., Nicholls, R. J., Brown, J. M., Horsburgh, K. and Gouldby, B. (2016). 'Spatial and temporal analysis of extreme sea level and storm surge events around the coastline of the UK'. In: *Scientific Data* 3.1, p. 160107. DOI: 10.1038/sdata.2016.107.

Hajima, T., Watanabe, M., Yamamoto, A., Tatebe, H., Noguchi, M. A., Abe, M., Ohgaito, R., Ito, A., Yamazaki, D., Okajima, H., Ito, A., Takata, K., Ogochi, K., Watanabe, S. and Kawamiya, M. (2020). 'Development of the MIROC-ES2L Earth system model and the evaluation of biogeochemical processes and feedbacks'. In: *Geoscientific Model Development* 13.5, pp. 2197–2244. DOI: 10.5194/gmd-13-2197-2020.

Ham, Y.-G., Kim, J.-H. and Luo, J.-J. (2019). 'Deep learning for multi-year ENSO forecasts'. In: *Nature* 573.7775, pp. 568–572. DOI: 10.1038/s41586-019-1559-7.

Hansen, F., Belušić, D., Wyser, K. and Koenigk, T. (2023). 'Future changes of circulation types and their effects on surface air temperature and precipitation in the SMHI large ensemble'. In: *Climate Dynamics* 61.5, pp. 2921–2936. DOI: 10.1007/s00382-023-06704-y.

Hao, Z., Singh, V. P. and Hao, F. (2018). 'Compound Extremes in Hydroclimatology: A Review'. In: *Water* 10.6, p. 718. DOI: 10.3390/w10060718.

Harley, M. (2017). 'Coastal storm definition'. In: *Coastal Storms*. John Wiley & Sons, Ltd. Chap. 1, pp. 1–21. DOI: 10.1002/9781118937099.ch1.

Harris, C. R., Millman, K. J., van der Walt, S. J., Gommers, R., Virtanen, P., Cournapeau, D., Wieser, E., Taylor, J., Berg, S., Smith, N. J., Kern, R., Picus, M., Hoyer, S., van Kerkwijk, M. H., Brett, M., Haldane, A., del Río, J. F., Wiebe, M., Peterson, P., Gérard-Marchant, P., Sheppard, K., Reddy, T., Weckesser, W., Abbasi, H., Gohlke, C. and Oliphant, T. E. (2020). 'Array programming with NumPy'. In: *Nature* 585.7825, pp. 357–362. DOI: 10.1038/s41586-020-2649-2.

Harrison, L. M., Coulthard, T. J., Robins, P. E. and Lewis, M. J. (2022). 'Sensitivity of Estuaries to Compound Flooding'. In: *Estuaries and Coasts* 45.5, pp. 1250–1269. DOI: 10.1007/s12237-021-00996-1.

Hattermann, F. F., Huang, S. and Koch, H. (2015). 'Climate change impacts on hydrology and water resources'. In: *Meteorologische Zeitschrift* 24.2, pp. 201–211. DOI: 10.1127/metz/2014/0575.

Hausfather, Z. and Peters, G. P. (2020). 'Emissions–the 'business as usual' story is misleading'. In: *Nature* 577, pp. 618–620. DOI: 10.1038/d41586-020-00177-3.

He, K., Zhang, X., Ren, S. and Sun, J. (2016). 'Deep Residual Learning for Image Recognition'. In: *2016 IEEE Conference on Computer Vision and Pattern Recognition (CVPR)*, pp. 770–778. DOI: 10.1109/CVPR.2016.90.

Heinrich, P., Hagemann, S., Weisse, R., Schrum, C., Daewel, U. and Gaslikova, L. (2023a). 'Compound flood events: analysing the joint occurrence of extreme river discharge events and storm surges in northern and central Europe'. In: *Natural Hazards and Earth System Sciences* 23.5, pp. 1967–1985. DOI: 10.5194/nhess-23-1967-2023.

Heinrich, P., Hagemann, S., Weisse, R. and Gaslikova, L. (2023b). 'Changes in compound flood event frequency in northern and central Europe under climate change'. In: *Frontiers in Climate* 5, p. 1227613. DOI: 10.3389/fclim.2023.1227613.

Heinrich, P., Hagemann, S. and Weisse, R. (2024). 'Automated Classification of Atmospheric Circulation Types for Compound Flood Risk Assessment: CMIP6 Model Analysis Utilising a Deep Learning Ensemble'. In: *Theoretical and Applied Climatology* 0. "Preprint", pp. 1–47. DOI: 10.21203/rs.3.rs-4017900/v1.

Heinrich, P. (2024). *Convolutional Neural Meteorology Network (CNMN)*. Version 1.0.0. DOI: 10.5281/zenodo.10959809.

Hendry, A., Haigh, I. D., Nicholls, R. J., Winter, H., Neal, R., Wahl, T., Joly-Laugel, A. and Darby, S. E. (2019). 'Assessing the characteristics and drivers of compound flooding events around the UK coast'. In: *Hydrology and Earth System Sciences* 23.7, pp. 3117–3139. DOI: 10.5194/hess-23-3117-2019.

Hendry, A. (2021). 'Compound Flooding in the UK: Past, Present and Future Co-occurring Extreme Flooding Hazard Sources'. PhD thesis. University of Southampton. URL: https://eprints.soton.ac.uk/id/eprint/452419 (visited on 27th February 2024).

Herrera-Lormendez, P., John, A., Douville, H. and Matschullat, J. (2023). 'Projected changes in synoptic circulations over Europe and their implications for summer precipitation: A CMIP6 perspective'. In: *International Journal of Climatology* 43.7, pp. 3373–3390. DOI: 10.1002/joc.8033.

Hersbach, H., Bell, B., Berrisford, P., Hirahara, S., Horányi, A., Muñoz-Sabater, J., Nicolas, J., Peubey, C., Radu, R., Schepers, D., Simmons, A., Soci, C., Abdalla, S., Abellan, X., Balsamo, G., Bechtold, P., Biavati, G., Bidlot, J., Bonavita, M., De Giovanna, D., Dahlgren, P., Dee, D., Diamantakis, M., Dragani, R., Flemming, J., Forbes, R., Fuentes, M., Geer, A., Haimberger, L., Healy, S., J. Robin, J., Hólm, E., Janisková, M., Keeley, S., Laloyaux, P., Lopez, P., Lupu, C., Radnoti, G., de Patricia, d., Rozum, I., Vamborg, F., Villaume, S. and Thépaut, J.-N. (2020). 'The ERA5 global reanalysis'. In: *Quarterly Journal of the Royal Meteorological Society* 146.730, pp. 1999–2049. DOI: 10.1002/qj.3803.

Hess, P. and Brezowsky, H. (1969). *Katalog der Grosswetterlagen Europas*. ISSN: 0072-4130. Dt. Wetterdienst.

Howard, T., Lowe, J. and Horsburgh, K. (2010). 'Interpreting Century-Scale Changes in Southern North Sea Storm Surge Climate Derived from Coupled Model Simulations'. In: *Journal of Climate* 23.23, pp. 6234–6247. DOI: 10.1175/2010JCLI3520.1.

Hoy, A., Sepp, M. and Matschullat, J. (2013). 'Atmospheric circulation variability in Europe and northern Asia (1901 to 2010)'. In: *Theoretical and Applied Climatology* 113.1, pp. 105–126. DOI: 10.1007/s00704-012-0770-3.

Hoy, A., Schucknecht, A., Sepp, M. and Matschullat, J. (2014). 'Large-scale synoptic types and their impact on European precipitation'. In: *Theoretical and Applied Climatology* 116, pp. 19–35. DOI: 10.1007/s00704-013-0897-x.

Hu, P., Zhang, Q., Shi, P., Chen, B. and Fang, J. (2018). 'Flood-induced mortality across the globe: Spatiotemporal pattern and influencing factors'. In: *Science of the Total Environment* 643, pp. 171–182. DOI: 10.1016/j.scitotenv.2018.06.197.

Huang, W., Ye, F., Zhang, Y. J., Park, K., Du, J., Moghimi, S., Myers, E., Pe'eri, S., Calzada, J. R., Yu, H. C., Nunez, K. and Liu, Z. (2021). 'Compounding factors for extreme flooding around Galveston Bay during Hurricane Harvey'. In: *Ocean Modelling* 158, p. 101735. DOI: 10.1016/j.ocemod.2020.101735.

Huang, L., Qin, J., Zhou, Y., Zhu, F., Liu, L. and Shao, L. (2023). 'Normalization Techniques in Training DNNs: Methodology, Analysis and Application'. In: *IEEE Transactions on Pattern Analysis and Machine Intelligence* 45.8, pp. 10173–10196. DOI: 10.1109/TPAMI.2023.3250241.

Huguenin, M. F., Fischer, E. M., Kotlarski, S., Scherrer, S. C., Schwierz, C. and Knutti, R. (2020). 'Lack of Change in the Projected Frequency and Persistence of Atmospheric Circulation Types Over Central Europe'. In: *Geophysical Research Letters* 47.9, e2019GL086132. DOI: 10.1029/2019GL086132.

Ikeuchi, H., Hirabayashi, Y., Yamazaki, D., Muis, S., Ward, P. J., Winsemius, H. C., Verlaan, M. and Kanae, S. (2017). 'Compound simulation of fluvial floods and storm surges in a global coupled river-coast flood model: Model development and its application to 2007 Cyclone Sidr in Bangladesh'. In: *Journal of Advances in Modeling Earth Systems* 9.4, pp. 1847–1862. DOI: 10.1002/2017MS000943.

Interreg North Sea Programme (2021). *Interreg North Sea Programme 2021-2027*. URL: https://www.interregnorthsea.eu/sites/default/files/2022-11/Interreg_North_Sea_Programme_2021-2027.pdf (visited on 29th January 2024).

IPCC (2023). *Climate Change 2021: The Physical Science Basis. Contribution of Working Group I to the Sixth Assessment Report of the Intergovernmental Panel on Climate Change*. Cambridge University Press. DOI: 10.1017/9781009157896.

Islam, M. A., Kowal, M., Jia, S., Derpanis, K. G. and Bruce, N. D. B. (2021). 'Global Pooling, More Than Meets the Eye: Position Information Is Encoded Channel-Wise in CNNs'. In: *Proceedings of the IEEE/CVF International Conference on Computer Vision (ICCV)*, pp. 793–801. DOI: 10.48550/arXiv.2108.07884.

Jaagus, J., Briede, A., Rimkus, E. and Remm, K. (2010). 'Precipitation pattern in the Baltic countries under the influence of large-scale atmospheric circulation and

local landscape factors'. In: *International Journal of Climatology* 30.5, pp. 705–720. DOI: 10.1002/joc.1929.

Jacob, D., Bärring, L., Christensen, O. B., Christensen, J. H., de Castro, M., Déqué, M., Giorgi, F., Hagemann, S., Hirschi, M., Jones, R., Kjellström, E., Lenderink, G., Rockel, B., Sánchez, E., Schär, C., Seneviratne, S. I., Somot, S., van Ulden, A. and van den Hurk, B. (2007). 'An inter-comparison of regional climate models for Europe: model performance in present-day climate'. In: *Climatic Change* 81.1, pp. 31–52. DOI: 10.1007/s10584-006-9213-4.

Jacob, D., Elizalde, A., Haensler, A., Hagemann, S., Kumar, P., Podzun, R., Rechid, D., Remedio, A. R., Saeed, F., Sieck, K., Teichmann, C. and Wilhelm, C. (2012). 'Assessing the Transferability of the Regional Climate Model REMO to Different COordinated Regional Climate Downscaling EXperiment (CORDEX) Regions'. In: *Atmosphere* 3.1, pp. 181–199. DOI: 10.3390/atmos3010181.

Jacob, D., Petersen, J., Eggert, B., Alias, A., Christensen, O. B., Bouwer, L. M., Braun, A., Colette, A., Déqué, M., Georgievski, G., Georgopoulou, E., Gobiet, A., Menut, L., Nikulin, G., Haensler, A., Hempelmann, N., Jones, C., Keuler, K., Kovats, S., Kröner, N., Kotlarski, S., Kriegsmann, A., Martin, E., van Meijgaard, E., Moseley, C., Pfeifer, S., Preuschmann, S., Radermacher, C., Radtke, K., Rechid, D., Rounsevell, M., Samuelsson, P., Somot, S., Soussana, J.-F., Teichmann, C., Valentini, R., Vautard, R., Weber, B. and Yiou, P. (2014). 'EURO-CORDEX: new high-resolution climate change projections for European impact research'. In: *Regional Environmental Change* 14.2, pp. 563–578. DOI: 10.1007/s10113-013-0499-2.

James, P. M. (2006). 'An assessment of European synoptic variability in Hadley Centre Global Environmental models based on an objective classification of weather regimes'. In: *Climate Dynamics* 27, pp. 215–231. DOI: 10.1007/s00382-006-0133-9.

James, P. M. (2007). 'An objective classification method for Hess and Brezowsky Grosswetterlagen over Europe'. In: *Theoretical and Applied Climatology* 88.1, pp. 17–42. DOI: 10.1007/s00704-006-0239-3.

Jane, R., Wahl, T., Santos, V. M., Misra, S. K. and White, K. D. (2022). 'Assessing the Potential for Compound Storm Surge and Extreme River Discharge Events at the Catchment Scale with Statistical Models: Sensitivity Analysis and Recommendations for Best Practice'. In: *Journal of Hydrologic Engineering* 27.3, p. 04022001. DOI: 10.1061/(ASCE)HE.1943-5584.0002154.

Jaruskova, D. and Hanek, M. (2006). 'Peaks over threshold method in comparison with block-maxima method for estimating high return levels of several Northern Moravia precipitation and discharges series'. In: *Journal of Hydrology and Hydromechanics/Vodohospodarsky Casopis* 54.4, pp. 309–319.

Jiang, D., Lin, W. and Raghavan, N. (2020). 'A Novel Framework for Semiconductor Manufacturing Final Test Yield Classification Using Machine Learning Techniques'. In: *IEEE Access* 8, pp. 197885–197895. DOI: 10.1109/ACCESS.2020.3034680.

Joe, H. (2014). *Dependence modeling with copulas*. CRC press. ISBN: 9781032477374.

Jolliffe, B. (2007). '500 residents still at risk from flooding'. In: *Bournemouth Daily Echo*. URL: https://www.bournemouthecho.co.uk/news/1244792.500-residents-still-at-risk-from-flooding/ (visited on 28th May 2024).

Jones, C. D., Hughes, J. K., Bellouin, N., Hardiman, S. C., Jones, G. S., Knight, J., Liddicoat, S., O'Connor, F. M., Andres, R. J., Bell, C., Boo, K.-O., Bozzo, A., Butchart, N., Cadule, P., Corbin, K. D., Doutriaux-Boucher, M., Friedlingstein, P., Gornall, J., Gray, L., Halloran, P. R., Hurtt, G., Ingram, W. J., Lamarque, J.-F., Law, R. M., Meinshausen, M., Osprey, S., Palin, E. J., Parsons Chini, L., Raddatz, T., Sanderson, M. G., Sellar, A. A., Schurer, A., Valdes, P., Wood, N., Woodward, S., Yoshioka, M. and Zerroukat, M. (2011). 'The HadGEM2-ES implementation of CMIP5 centennial simulations'. In: *Geoscientific Model Development* 4.3, pp. 543–570. DOI: 10.5194/gmd-4-543-2011.

Jonkman, S. N. (2005). 'Global perspectives on loss of human life caused by floods'. In: *Natural Hazards* 34.2, pp. 151–175. DOI: 10.1007/s11069-004-8891-3.

Juarez, B., Stockton, S. A., Serafin, K. A. and Valle-Levinson, A. (2022). 'Compound flooding in a subtropical estuary caused by Hurricane Irma 2017'. In: *Geophysical Research Letters* 49.18, e2022GL099360. DOI: 10.1029/2022GL099360.

Kalnay, E., Kanamitsu, M., Kistler, R., Collins, W., Deaven, D., Gandin, L., Iredell, M., Saha, S., White, G., Woollen, J., Zhu, Y., Chelliah, M., Ebisuzaki, W., Higgins, W., Janowiak, J., Mo, K. C., Ropelewski, C., Wang, J., Leetmaa, A., Reynolds, R., Jenne, R. and Joseph, D. (1996). 'The NCEP/NCAR 40-year reanalysis project'. In: *Bulletin of the American Meteorological Society* 77.3, pp. 437–472. DOI: 10.1175/1520-0477(1996)077<0437:TNYRP>2.0.CO;2.

Kapitza, H. (2008). 'MOPS - A Morphodynamical Prediction System on Cluster Computers'. In: *International Conference on High Performance Computing for Computational Science*. Springer, pp. 63–68. DOI: 10.1007/978-3-540-92859-1_8.

Kawamiya, M., Hajima, T., Tachiiri, K., Watanabe, S. and Yokohata, T. (2020). 'Two decades of Earth system modeling with an emphasis on Model for Interdisciplinary Research on Climate (MIROC)'. In: *Progress in Earth and Planetary Science* 7.1, p. 64. DOI: 10.1186/s40645-020-00369-5.

Kew, S. F., Selten, F. M., Lenderink, G. and Hazeleger, W. (2013). 'The simultaneous occurrence of surge and discharge extremes for the Rhine delta'. In: *Natural Hazards and Earth System Sciences* 13.8, pp. 2017–2029. DOI: 10.5194/nhess-13-2017-2013.

Khanal, S., Ridder, N. N., De Vries, H., Terink, W. and Van den Hurk, B. (2019a). 'Storm Surge and Extreme River Discharge: A Compound Event Analysis Using Ensemble Impact Modeling'. In: *Frontiers in Earth Science* 7, p. 224. DOI: 10.3389/feart.2019.00224.

Khanal, S., Lutz, A. F., Immerzeel, W. W., Vries, H. d., Wanders, N. and van den Hurk, B. (2019b). 'The Impact of Meteorological and Hydrological Memory on

Compound Peak Flows in the Rhine River Basin'. In: *Atmosphere* 10.4, p. 171. DOI: 10.3390/atmos10040171.

Khanam, M., Sofia, G., Koukoula, M., Lazin, R., Nikolopoulos, E. I., Shen, X. and Anagnostou, E. N. (2021). 'Impact of compound flood event on coastal critical infrastructures considering current and future climate'. In: *Natural Hazards and Earth System Sciences* 21.2, pp. 587–605. DOI: 10.5194/nhess-21-587-2021.

Khatun, A., Ganguli, P., Bisht, D. S., Chatterjee, C. and Sahoo, B. (2022). 'Understanding the impacts of predecessor rain events on flood hazard in a changing climate'. In: *Hydrological Processes* 36.2, e14500. DOI: 10.1002/hyp.14500.

Kingma, D. P. and Ba, J. (2014). 'Adam: A Method for Stochastic Optimization'. In: *arXiv preprint arXiv:1412.6980* 0.0, pp. 1–15. DOI: 10.48550/arXiv.1412.6980.

Kjellström, E., Nikulin, G., Strandberg, G., Christensen, O. B., Jacob, D., Keuler, K., Lenderink, G., van Meijgaard, E., Schär, C., Somot, S., Sørland, S. L., Teichmann, C. and Vautard, R. (2018). 'European climate change at global mean temperature increases of 1.5 and 2 C above pre-industrial conditions as simulated by the EURO-CORDEX regional climate models'. In: *Earth System Dynamics* 9.2, pp. 459–478. DOI: 10.5194/esd-9-459-2018.

Klein Tank, A., Wijngaard, J., Können, G., Böhm, R., Demarée, G., Gocheva, A., Mileta, M., Pashiardis, S., Hejkrlik, L., Kern-Hansen, C., Heino, R., Bessemoulin, P., Müller-Westermeier, G., Tzanakou, M., Szalai, S., Pálsdóttir, T., Fitzgerald, D., Rubin, S., Capaldo, M., Maugeri, M., Leitass, A., Bukantis, A., Aberfeld, R., van Engelen, A. F. V., Forland, E., Mietus, M., Coelho, F., Mares, C., Razuvaev, V., E., N., Cegnar, T., Antonio López, J., Dahlström, B., Moberg, A., Kirchhofer, W., Ceylan, A., Pachaliuk, O., Alexander, L. V. and Petrovic, P. (2002). 'Daily dataset of 20th-century surface air temperature and precipitation series for the European Climate Assessment'. In: *International Journal of Climatology* 22.12, pp. 1441–1453. DOI: 10.1002/joc.773.

Klerk, W.-J., Winsemius, H. C., Van Verseveld, W. J., Bakker, A. M. R. and Diermanse, F. L. M. (2015). 'The co-incidence of storm surges and extreme discharges within the Rhine–Meuse Delta'. In: *Environmental Research Letters* 10.3, p. 035005. DOI: 10.1088/1748-9326/10/3/035005.

Klok, E. J. and Klein Tank, A. M. G. (2009). 'Updated and extended European dataset of daily climate observations'. In: *International Journal of Climatology* 29.8, pp. 1182–1191. DOI: 10.1002/joc.1779.

Kopp, R. E., Garner, G. G., Hermans, T. H. J., Jha, S., Kumar, P., Reedy, A., Slangen, A. B. A., Turilli, M., Edwards, T. L., Gregory, J. M., Koubbe, G., Levermann, A., Merzky, A., Nowicki, S., Palmer, M. D. and Smith, C. (2023). 'The Framework for Assessing Changes To Sea-level (FACTS) v1. 0: a platform for characterizing parametric and structural uncertainty in future global, relative, and extreme sea-level change'. In: *Geoscientific Model Development* 16.24, pp. 7461–7489. DOI: 10.5194/gmd-16-7461-2023.

Kreibich, H., Bubeck, P., Van Vliet, M. and De Moel, H. (2015). 'A review of damage-reducing measures to manage fluvial flood risks in a changing climate'. In: *Mitigation and Adaptation Strategies for Global Change* 20, pp. 967–989. DOI: 10.1007/s11027-014-9629-5.

Krizhevsky, A., Sutskever, I. and Hinton, G. E. (2017). 'ImageNet Classification with Deep Convolutional Neural Networks'. In: *Commun. ACM* 60.6, pp. 84–90. ISSN: 0001-0782. DOI: 10.1145/3065386.

Kruczkiewicz, A., Cian, F., Monasterolo, I., Di Baldassarre, G., Caldas, A., Royz, M., Glasscoe, M., Ranger, N. and van Aalst, M. (2022). 'Multiform flood risk in a rapidly changing world: what we do not do, what we should and why it matters'. In: *Environmental Research Letters* 17.8, p. 081001. DOI: 10.1088/1748-9326/ac7ed9.

Kumbier, K., Carvalho, R. C., Vafeidis, A. T. and Woodroffe, C. D. (2018). 'Investigating compound flooding in an estuary using hydrodynamic modelling: a case study from the Shoalhaven River, Australia'. In: *Natural Hazards and Earth System Sciences* 18.2, pp. 463–477. DOI: 10.5194/nhess-18-463-2018.

Kupfer, S., Santamaria-Aguilar, S., Van Niekerk, L., Lück-Vogel, M. and Vafeidis, A. T. (2022). 'Investigating the interaction of waves and river discharge during compound flooding at Breede Estuary, South Africa'. In: *Natural Hazards and Earth System Sciences* 22.1, pp. 187–205. DOI: 10.5194/nhess-22-187-2022.

Lai, Y., Li, J., Gu, X., Liu, C. and Chen, Y. D. (2021). 'Global Compound Floods from Precipitation and Storm Surge: Hazards and the Roles of Cyclones'. In: *Journal of Climate* 34.20, pp. 8319–8339. DOI: 10.1175/JCLI-D-21-0050.1.

Lee, J., Kim, J., Sun, M.-A., Kim, B.-H., Moon, H., Sung, H. M., Kim, J. and Byun, Y.-H. (2020a). 'Evaluation of the Korea Meteorological Administration Advanced Community Earth-System model (K-ACE)'. In: *Asia-Pacific Journal of Atmospheric Sciences* 56, pp. 381–395. DOI: 10.1007/s13143-019-00144-7.

Lee, W.-L., Wang, Y.-C., Shiu, C.-J., Tsai, I.-c., Tu, C.-Y., Lan, Y.-Y., Chen, J.-P., Pan, H.-L. and Hsu, H.-H. (2020b). 'Taiwan Earth System Model Version 1: description and evaluation of mean state'. In: *Geoscientific Model Development* 13.9, pp. 3887–3904. DOI: 10.5194/gmd-13-3887-2020.

Leonard, M., Westra, S., Phatak, A., Lambert, M., van den Hurk, B., McInnes, K., Risbey, J., Schuster, S., Jakob, D. and Stafford-Smith, M. (2014). 'A compound event framework for understanding extreme impacts'. In: *Wiley Interdisciplinary Reviews: Climate Change* 5.1, pp. 113–128. DOI: 10.1002/wcc.252.

Li, L., Yu, Y., Tang, Y., Lin, P., Xie, J., Song, M., Dong, L., Zhou, T., Liu, L., Wang, L., Pu, Y., Chen, X., Chen, L., Xie, Z., Liu, H., Zhang, L., Huang, X., Feng, T., Zheng, W., Xia, K., Liu, H., Liu, J., Wang, Y., Wang, L., Jia, B., Xie, F., Wang, B., Zhao, S., Yu, Z., Zhao, B. and Wei, J. (2020). 'The Flexible Global Ocean-Atmosphere-Land System Model Grid-Point Version 3 (FGOALS-g3): Description and Evaluation'. In: *Journal of Advances in Modeling Earth Systems* 12.9, e2019MS002012. DOI: 10.1029/2019MS002012.

Li, J., Han, Y., Zhang, M., Li, G. and Zhang, B. (2022). 'Multi-scale residual network model combined with Global Average Pooling for action recognition'. In: *Multimedia Tools and Applications* 81.1, pp. 1375–1393. DOI: 10.1007/s11042-021-11435-5.

Lian, J. J., Xu, K. and Ma, C. (2013). 'Joint impact of rainfall and tidal level on flood risk in a coastal city with a complex river network: a case study of Fuzhou City, China'. In: *Hydrology and Earth System Sciences* 17.2, pp. 679–689. DOI: 10.5194/hess-17-679-2013.

Liang, B., Shao, Z., Li, H., Shao, M. and Lee, D. (2019). 'An automated threshold selection method based on the characteristic of extrapolated significant wave heights'. In: *Coastal Engineering* 144, pp. 22–32. ISSN: 0378-3839. DOI: 10.1016/j.coastaleng.2018.12.001.

Lin, M., Chen, Q. and Yan, S. (2013). 'Network in Network'. In: *arXiv preprint arXiv:1312.4400* 0.0, pp. 1–10. DOI: 10.48550/arXiv.1312.4400.

Liu, Y., Racah, E., Correa, J., Khosrowshahi, A., Lavers, D., Kunkel, K., Wehner, M. and Collins, W. (2016). 'Application of Deep Convolutional Neural Networks for Detecting Extreme Weather in Climate Datasets'. In: *arXiv preprint arXiv:1605.01156* 0.0, pp. 1–8. DOI: 10.48550/arXiv.1605.01156.

Liu, Z., Mao, H., Wu, C.-Y., Feichtenhofer, C., Darrell, T. and Xie, S. (2022a). 'A ConvNet for the 2020s'. In: *2022 IEEE/CVF Conference on Computer Vision and Pattern Recognition (CVPR)*, pp. 11976–11986. DOI: 10.1109/CVPR52688.2022.01167.

Liu, X., Meinke, I. and Weisse, R. (2022b). 'Still normal? Near-real-time evaluation of storm surge events in the context of climate change'. In: *Natural Hazards and Earth System Sciences* 22.1, pp. 97–116. DOI: 10.5194/nhess-22-97-2022.

Longobardi, A. and Villani, P. (2023). 'Baseflow index characterization in typical temperate to dry climates: conceptual analysis and simulation experiment to assess the relative role of climate forcing features and catchment geological settings'. In: *Hydrology Research* 54.2, pp. 136–148. DOI: 10.2166/nh.2023.026.

Luferov, V. and Fedotova, E. (2020). 'A Deep Learning Approach to Recognition of the Atmospheric Circulation Regimes'. In: *Progress in Computer Recognition Systems*. Springer, pp. 195–204. DOI: 10.1007/978-3-030-19738-4_20.

Lyard, F., Lefevre, F., Letellier, T. and Francis, O. (2006). 'Modelling the global ocean tides: modern insights from FES2004'. In: *Ocean Dynamics* 56.5, pp. 394–415. DOI: 10.1007/s10236-006-0086-x.

Martin, G. M., Ringer, M. A., Pope, V. D., Jones, A., Dearden, C. and Hinton, T. J. (2006). 'The physical properties of the atmosphere in the new Hadley Centre Global Environmental Model (HadGEM1). Part I: Model description and global climatology'. In: *Journal of Climate* 19.7, pp. 1274–1301. DOI: 10.1175/JCLI3636.1.

Masson-Delmotte, V., Zhai, P., Pirani, A., Connors, S., Péan, C., Berger, S., Caud, N., Chen, Y., Goldfarb, L., Gomis, M., Huang, M., Leitzell, K., Lonnoy, E., Matthews, J., Maycock, T. K., Waterfield, T., Yelekçi, O., Yu, R. and Zhou, B. (2021). 'Climate

Change 2021: The Physical Science Basis. Contribution of Working Group I to the Sixth Assessment Report of the Intergovernmental Panel on Climate Change'. In: *Cambridge University Press*, pp. 3–32. DOI: 10.1017/9781009157896.001.

Mauritsen, T., Bader, J., Becker, T., Behrens, J., Bittner, M., Brokopf, R., Brovkin, V., Claussen, M., Crueger, T., Esch, M., Fast, I., Fiedler, S., Fläschner, D., Gayler, V., Giorgetta, M., Goll, D. S., Haak, H., Hagemann, S., Hedemann, C., Hohenegger, C., Ilyina, T., Jahns, T., Jimenéz-de-la-Cuesta, D., Jungclaus, J., Kleinen, T., Kloster, S., Kracher, D., Kinne, S., Kleberg, D., Lasslop, G., Kornblueh, L., Marotzke, J., Matei, D., Meraner, K., Mikolajewicz, U., Modali, K., Möbis, B., Müller, W. A., Nabel, J. E. M. S., Nam, C. C. W., Notz, D., Nyawira, S.-S., Paulsen, H., Peters, K., Pincus, R., Pohlmann, H., Pongratz, J., Popp, M., Raddatz, T. J., Rast, S., Redler, R., Reick, C. H., Rohrschneider, T., Schemann, V., Schmidt, H., Schnur, R., Schulzweida, U., Six, K. D., Stein, L., Stemmler, I., Stevens, B., von Storch, J.-S., Tian, F., Voigt, A., Vrese, P., Wieners, K.-H., Wilkenskjeld, S., Winkler, A. and Roeckner, E. (2019). 'Developments in the MPI-M Earth System Model version 1.2 (MPI-ESM1. 2) and its response to increasing CO2'. In: *Journal of Advances in Modeling Earth Systems* 11.4, pp. 998–1038. DOI: 10.1029/2018MS001400.

McEvoy, S., Haasnoot, M. and Biesbroek, R. (2021). 'How are European countries planning for sea level rise?' In: *Ocean & Coastal Management* 203, p. 105512. DOI: 10.1016/j.ocecoaman.2020.105512.

McGranahan, G., Balk, D. and Anderson, B. (2007). 'The rising tide: assessing the risks of climate change and human settlements in low elevation coastal zones'. In: *Environment and Urbanization* 19.1, pp. 17–37. DOI: 10.1177/0956247807076960.

Meinshausen, M., Nicholls, Z. R. J., Lewis, J., Gidden, M. J., Vogel, E., Freund, M., Beyerle, U., Gessner, C., Nauels, A., Bauer, N., Canadell, J. G., Daniel, J. S., John, A., Krummel, P. B., Luderer, G., Meinshausen, N., Montzka, S. A., Rayner, P. J., Reimann, S., Smith, S. J., van den Berg, M., Velders, G. J. M., Vollmer, M. K. and Wang, R. H. J. (2020). 'The shared socio-economic pathway (SSP) greenhouse gas concentrations and their extensions to 2500'. In: *Geoscientific Model Development* 13.8, pp. 3571–3605. DOI: 10.5194/gmd-13-3571-2020.

Mittermeier, M., Weigert, M., Rügamer, D., Küchenhoff, H. and Ludwig, R. (2022). 'A deep learning based classification of atmospheric circulation types over Europe: projection of future changes in a CMIP6 large ensemble'. In: *Environmental Research Letters* 17.8, p. 084021. DOI: 10.1088/1748-9326/ac8068.

Moftakhari, H. R., Salvadori, G., AghaKouchak, A., Sanders, B. F. and Matthew, R. A. (2017). 'Compounding effects of sea level rise and fluvial flooding'. In: *Proceedings of the National Academy of Sciences* 114.37, pp. 9785–9790. DOI: 10.1073/pnas.1620325114.

Moftakhari, H. R., Schubert, J. E., AghaKouchak, A., Matthew, R. A. and Sanders, B. F. (2019). 'Linking statistical and hydrodynamic modeling for compound flood hazard assessment in tidal channels and estuaries'. In: *Advances in Water Resources* 128, pp. 28–38. DOI: 10.1016/j.advwatres.2019.04.009.

Mohr, S., Ehret, U., Kunz, M., Ludwig, P., Caldas-Alvarez, A., Daniell, J. E., Ehmele, F., Feldmann, H., Franca, M. J., Gattke, C., Hundhausen, M., Knippertz, P., Küpfer, K., Mühr, B., Pinto, J. G., Quinting, J., Schäfer, A. M., Scheibel, M., Seidel, F. and Wisotzky, C. (2023). 'A multi-disciplinary analysis of the exceptional flood event of July 2021 in central Europe. Part 1: Event description and analysis'. In: *Natural Hazards and Earth System Sciences* 23.2, pp. 525–551. DOI: 10.5194/nhess-23-525-2023.

Moss, R. H., Edmonds, J. A., Hibbard, K. A., Manning, M. R., Rose, S. K., Van Vuuren, D. P., Carter, T. R., Emori, S., Kainuma, M., Kram, T., Meehl, G. A., Mitchell, J. F. B., Nakicenovic, N., Riahi, K., Smith, S. J., Stouffer, R. J., Thomson, A. M., Weyant, J. P. and Wilbanks, T. J. (2010). 'The next generation of scenarios for climate change research and assessment'. In: *Nature* 463.7282, pp. 747–756. DOI: 10.1038/nature08823.

Müller, W. A., Jungclaus, J. H., Mauritsen, T., Baehr, J., Bittner, M., Budich, R., Bunzel, F., Esch, M., Ghosh, R., Haak, H., Ilyina, T., Kleine, T., Kornblueh, L., Li, H., Modali, K., Notz, D., Pohlmann, H., Roeckner, E., Stemmler, I., Tian, F. and Marotzke, J. (2018). 'A Higher-resolution Version of the Max Planck Institute Earth System Model (MPI-ESM1.2-HR)'. In: *Journal of Advances in Modeling Earth Systems* 10.7, pp. 1383–1413. DOI: 10.1029/2017MS001217.

Nasr, A. A., Wahl, T., Rashid, M. M., Camus, P. and Haigh, I. D. (2021). 'Assessing the dependence structure between oceanographic, fluvial, and pluvial flooding drivers along the United States coastline'. In: *Hydrology and Earth System Sciences* 25.12, pp. 6203–6222. DOI: 10.5194/hess-25-6203-2021.

Neal, R., Dankers, R., Saulter, A., Lane, A., Millard, J., Robbins, G. and Price, D. (2018). 'Use of probabilistic medium-to long-range weather-pattern forecasts for identifying periods with an increased likelihood of coastal flooding around the UK'. In: *Meteorological Applications* 25.4, pp. 534–547. DOI: 10.1002/met.1719.

Nearing, G., Cohen, D., Dube, V., Gauch, M., Gilon, O., Harrigan, S., Hassidim, A., Klotz, D., Kratzert, F., Metzger, A., Nevo, S., Pappenberger, F., Prudhomme, C., Shalev, G., Shenzis, S., Tekalign, T. Y., Weitzner, D. and Matias, Y. (2024). 'Global prediction of extreme floods in ungauged watersheds'. In: *Nature* 627.8004, pp. 559–563. ISSN: 1476-4687. DOI: 10.1038/s41586-024-07145-1.

Neumann, B., Vafeidis, A. T., Zimmermann, J. and Nicholls, R. J. (2015). 'Future Coastal Population Growth and Exposure to Sea-Level Rise and Coastal Flooding - A Global Assessment'. In: *PLOS ONE* 10.3, pp. 1–34. DOI: 10.1371/journal.pone.0118571.

O'Connell, N. (2000). *Final Report of Flood event 24th December to 26th December 1999*. Tech. rep. Environment Agency Southern Region, Hants & IoW Area.

Olbert, A. I., Moradian, S., Nash, S., Comer, J., Kazmierczak, B., Falconer, R. A. and Hartnett, M. (2023). 'Combined statistical and hydrodynamic modelling of compound flooding in coastal areas-Methodology and application'. In: *Journal of Hydrology* 620, p. 129383. DOI: 10.1016/j.jhydrol.2023.129383.

Olonscheck, D., Suarez-Gutierrez, L., Milinski, S., Beobide-Arsuaga, G., Baehr, J., Fröb, F., Ilyina, T., Kadow, C., Krieger, D., Li, H., Marotzke, J., Plésiat, É., Schupfner, M., Wachsmann, F., Wallberg, L., Wieners, K.-H. and Brune, S. (2023). 'The New Max Planck Institute Grand Ensemble With CMIP6 Forcing and High-Frequency Model Output'. In: *Journal of Advances in Modeling Earth Systems* 15.10, e2023MS003790. DOI: 10.1029/2023MS003790.

Osman, M. B., Coats, S., Das, S. B., McConnell, J. R. and Chellman, N. (2021). 'North Atlantic jet stream projections in the context of the past 1,250 years'. In: *Proceedings of the National Academy of Sciences* 118.38, e2104105118. DOI: 10.1073/pnas.2104105118.

Otero, N., Sillmann, J. and Butler, T. (2018). 'Assessment of an extended version of the Jenkinson–Collison classification on CMIP5 models over Europe'. In: *Climate Dynamics* 50.5-6, pp. 1559–1579. DOI: 10.1007/s00382-017-3705-y.

Ozturk, T., Matte, D. and Christensen, J. H. (2022). 'Robustness of future atmospheric circulation changes over the EURO-CORDEX domain'. In: *Climate Dynamics* 59.5, pp. 1799–1814. DOI: 10.1007/s00382-021-06069-0.

Pachauri, R. K., Allen, M. R., Barros, V. R., Broome, J., Cramer, W., Christ, R., Church, J. A., Clarke, L., Dahe, Q., Dasgupta, P., Dubash, N. K., Edenhofer, O., Elgizouli, I., Field, C. B., Forster, P., Friedlingstein, P., Fuglestvedt, J., Gomez-Echeverri, L., Hallegatte, S., Hegerl, G., Howden, M., Jiang, K., Cisneroz, B. J., Kattsov, V., Lee, H., Mach, K. J., Marotzke, J., Mastrandrea, M. D., Meyer, L., Minx, J., Mulugetta, Y., O'Brien, K., Oppenheimer, M., Pereira, J. J., Pichs-Madruga, R., Plattner, G.-K., Pörtner, H.-O., Power, S. B., Preston, B., Ravindranath, N. H., Reisinger, A., Riahi, K., Rusticucci, M., Scholes, R., Seyboth, K., Sokona, Y., Stavins, R., Stocker, T. F., Tschakert, P., van Vuuren, D. and van Ypserle, J.-P. (2014). *Climate Change 2014: Synthesis Report. Contribution of Working Groups I, II and III to the Fifth Assessment Report of the Intergovernmental Panel on Climate Change*. Geneva, Switzerland: IPCC, p. 151.

Pant, R., Thacker, S., Hall, J. W., Alderson, D. and Barr, S. (2018). 'Critical infrastructure impact assessment due to flood exposure'. In: *Journal of Flood Risk Management* 11.1, pp. 22–33. DOI: 10.1111/jfr3.12288.

Paprotny, D., Vousdoukas, M. I., Morales-Nápoles, O., Jonkman, S. N. and Feyen, L. (2018a). 'Compound flood potential in Europe'. In: *Hydrology and Earth System Sciences Discussions*, pp. 1–34. DOI: 10.5194/hess-2018-132.

Paprotny, D., Morales-Nápoles, O. and Jonkman, S. N. (2018b). 'HANZE: a pan-European database of exposure to natural hazards and damaging historical floods since 1870'. In: *Earth System Science Data* 10.1, pp. 565–581. DOI: 10.5194/essd-10-565-2018.

Paprotny, D., Vousdoukas, M. I., Morales-Nápoles, O., Jonkman, S. N. and Feyen, L. (2020). 'Pan-European hydrodynamic models and their ability to identify compound floods'. In: *Natural Hazards* 101, pp. 933–957. DOI: 10.1007/s11069-020-03902-3.

Pasquier, U., He, Y., Hooton, S., Goulden, M. and Hiscock, K. M. (2019). 'An integrated 1D–2D hydraulic modelling approach to assess the sensitivity of a coastal region to compound flooding hazard under climate change'. In: *Natural Hazards* 98.3, pp. 915–937. DOI: 10.1007/s11069-018-3462-1.

Petrik, R. and Geyer, B. (2021). *coastDat3 COSMO-CLM MERRA2*. DOI: 10.26050/WDCC/coastDat3_COSMO-CLM_MERRA2.

Pfahl, S., O'Gorman, P. A. and Fischer, E. M. (2017). 'Understanding the regional pattern of projected future changes in extreme precipitation'. In: *Nature Climate Change* 7.6, pp. 423–427. DOI: 10.1038/nclimate3287.

Pickands III, J. (1975). 'Statistical Inference Using Extreme Order Statistics'. In: *The Annals of Statistics* 3 (1), pp. 119–131. DOI: 10.1214/aos/1176343003.

Poschlod, B., Zscheischler, J., Sillmann, J., Wood, R. R. and Ludwig, R. (2020). 'Climate change effects on hydrometeorological compound events over southern Norway'. In: *Weather and Climate Extremes* 28, p. 100253. DOI: 10.1016/j.wace.2020.100253.

Prabhat, Kashinath, K., Mudigonda, M., Kim, S., Kapp-Schwoerer, L., Graubner, A., Karaismailoglu, E., von Kleist, L., Kurth, T., Greiner, A., Mahesh, A., Yang, K., Colby, L., Chen, J., Lou, A., Chandran, S., Toms, B., Chapman, W., Dagon, K., Shields, C. A., O'Brien, T., Wehner, M. and Collins, W. (2021). 'ClimateNet: an expert-labeled open dataset and deep learning architecture for enabling high-precision analyses of extreme weather'. In: *Geoscientific Model Development* 14.1, pp. 107–124. DOI: 10.5194/gmd-14-107-2021.

Rajczak, J. and Schär, C. (2017). 'Projections of Future Precipitation Extremes Over Europe: A Multimodel Assessment of Climate Simulations'. In: *Journal of Geophysical Research: Atmospheres* 122.20, pp. 10, 773–10, 800. DOI: 10.1002/2017JD027176.

Rakovec, O. and Kumar, R. (2022). *Mesoscale Hydrologic Model based historical streamflow simulation over Europe at 1/16 degree*. DOI: 10.26050/WDCC/mHMbassimEur.

Remedio, A. R., Teichmann, C., Buntemeyer, L., Sieck, K., Weber, T., Rechid, D., Hoffmann, P., Nam, C., Kotova, L. and Jacob, D. (2019). 'Evaluation of New COR-DEX Simulations Using an Updated Köppen–Trewartha Climate Classification'. In: *Atmosphere* 10.11, p. 726. DOI: 10.3390/atmos10110726.

Riahi, K., Van Vuuren, D. P., Kriegler, E., Edmonds, J., O'Neill, B. C., Fujimori, S., Bauer, N., Calvin, K., Dellink, R., Fricko, O., Lutza, W., Popp, A., Cuaresma, J. C., K.C., S., Leimbach, M., Jiange, L., Kramb, T., Rao, S., Emmerling, J., Ebi, K., Hasegawaf, T., Havlik, P., Humpenöderc, F., Silvai, L. A. D., Smith, S., Stehfest, E., Bosetti, V., Eomd, J., Gernaat, D., Masuif, T., Rogelj, J., Streflerc, J., Drouet, L., Kreya, V., Ludererc, G., Harmsen, M., Takahashif, K., Baumstarkc, L., Doelmanb, J. C., Kainuma, M., Klimont, Z., Marangonii, G., Lotze-Campenc, H., Obersteinera, M., Tabeau, A. and Tavoni, M. (2017). 'The Shared Socioeconomic Pathways and their energy, land use, and greenhouse gas emissions implications: An overview'.

In: *Global Environmental Change* 42, pp. 153–168. DOI: 10.1016/j.gloenvcha.2016.05.009.

Ridder, N. N., Vries, H. d. and Drijfhout, S. (2018). 'The role of atmospheric rivers in compound events consisting of heavy precipitation and high storm surges along the Dutch coast'. In: *Natural Hazards and Earth System Sciences* 18.12, pp. 3311–3326. DOI: 10.5194/nhess-18-3311-2018.

Ridder, N. N., Pitman, A. J., Westra, S., Ukkola, A., Do, H. X., Bador, M., Hirsch, A. L., Evans, J. P., Di Luca, A. and Zscheischler, J. (2020). 'Global hotspots for the occurrence of compound events'. In: *Nature Communications* 11.1, p. 5956. DOI: 10.1038/s41467-020-19639-3.

Ridder, N. N., Ukkola, A. M., Pitman, A. J. and Perkins-Kirkpatrick, S. E. (2022). 'Increased occurrence of high impact compound events under climate change'. In: *npj Climate and Atmospheric Science* 5.1, p. 3. DOI: 10.1038/s41612-021-00224-4.

Rivoire, P., Martius, O. and Naveau, P. (2021). 'A Comparison of Moderate and Extreme ERA-5 Daily Precipitation With Two Observational Data Sets'. In: *Earth and Space Science* 8.4, e2020EA001633. DOI: 10.1029/2020EA001633.

Robins, P. E., Lewis, M. J., Elnahrawi, M., Lyddon, C., Dickson, N. and Coulthard, T. J. (2021). 'Compound Flooding: Dependence at Sub-daily Scales Between Extreme Storm Surge and Fluvial Flow'. In: *Frontiers in Built Environment* 7, p. 116. DOI: 10.3389/fbuil.2021.727294.

Rockel, B., Will, A. and Hense, A. (2008). 'The regional climate model COSMO-CLM (CCLM)'. In: *Meteorologische Zeitschrift* 17.4, pp. 347–348. DOI: 10.1127/0941-2948/2008/0309.

Rodrigues do Amaral, F., Gratiot, N., Pellarin, T. and Tu, T. A. (2023). 'Assessing typhoon-induced compound flood drivers: a case study in Ho Chi Minh City, Vietnam'. In: *Natural Hazards and Earth System Sciences* 23.11, pp. 3379–3405. DOI: 10.5194/nhess-23-3379-2023.

Rohrer, M., Croci-Maspoli, M. and Appenzeller, C. (2017). 'Climate change and circulation types in the Alpine region'. In: *Meteorologische Zeitschrift* 26.1, pp. 83–92. DOI: 10.1127/metz/2016/0681.

Ruocco, A. C., Nicholls, R. J., Haigh, I. D. and Wadey, M. P. (2011). 'Reconstructing coastal flood occurrence combining sea level and media sources: a case study of the Solent, UK since 1935'. In: *Natural Hazards* 59, pp. 1773–1796. DOI: 10.1007/s11069-011-9868-7.

Russakovsky, O., Deng, J., Su, H., Krause, J., Satheesh, S., Ma, S., Huang, Z., Karpathy, A., Khosla, A., Bernstein, M., Berg, A. C. and Fei-Fei, L. (2015). 'ImageNet Large Scale Visual Recognition Challenge'. In: *International Journal of Computer Vision* 115.3, pp. 211–252. DOI: 10.1007/s11263-015-0816-y.

Sadegh, M., Moftakhari, H., Gupta, H. V., Ragno, E., Mazdiyasni, O., Sanders, B., Matthew, R. and AghaKouchak, A. (2018). 'Multihazard Scenarios for Analysis of

Compound Extreme Events'. In: *Geophysical Research Letters* 45.11, pp. 5470–5480. DOI: 10.1029/2018GL077317.

Santiago-Collazo, F. L., Bilskie, M. V. and Hagen, S. C. (2019). 'A comprehensive review of compound inundation models in low-gradient coastal watersheds'. In: *Environmental Modelling & Software* 119, pp. 166–181. DOI: 10.1016/j.envsoft.2019.06.002.

Santos, V. M., Wahl, T., Jane, R., Misra, S. K. and White, K. D. (2021a). 'Assessing compound flooding potential with multivariate statistical models in a complex estuarine system under data constraints'. In: *Journal of Flood Risk Management* 14.4, e12749. DOI: 10.1111/jfr3.12749.

Santos, V. M., Casas-Prat, M., Poschlod, B., Ragno, E., Van Den Hurk, B., Hao, Z., Kalmár, T., Zhu, L. and Najafi, H. (2021b). 'Statistical modelling and climate variability of compound surge and precipitation events in a managed water system: a case study in the Netherlands'. In: *Hydrology and Earth System Sciences* 25.6, pp. 3595–3615. DOI: 10.5194/hess-25-3595-2021.

Sayol, J. M. and Marcos, M. (2018). 'Assessing Flood Risk Under Sea Level Rise and Extreme Sea Levels Scenarios: Application to the Ebro Delta (Spain)'. In: *Journal of Geophysical Research: Oceans* 123.2, pp. 794–811. DOI: 10.1002/2017JC013355.

Schrum, C. and Backhaus, J. O. (1999). 'Sensitivity of atmosphere–ocean heat exchange and heat content in the North Sea and the Baltic Sea'. In: *Tellus A: Dynamic Meteorology and Oceanography* 51.4, pp. 526–549. DOI: 10.3402/tellusa.v51i4.13825.

Séférian, R., Nabat, P., Michou, M., Saint-Martin, D., Voldoire, A., Colin, J., Decharme, B., Delire, C., Berthet, S., Chevallier, M., Sénési, S., Franchisteguy, L., Vial, J., Mallet, M., Joetzjer, E., Geoffroy, O., Guérémy, J.-F., Moine, M.-P., Msadek, R., Ribes, A., Rocher, M., Roehrig, R., Salas-y-Mélia, D., Sanchez, E., Terray, L., Valcke, S., Waldman, R., Aumont, O., Bopp, L., Deshayes, J., Éthé, C. and Madec, G. (2019). 'Evaluation of CNRM Earth System Model, CNRM-ESM2-1: Role of Earth System Processes in Present-Day and Future Climate'. In: *Journal of Advances in Modeling Earth Systems* 11.12, pp. 4182–4227. DOI: 10.1029/2019MS001791.

Seland, Ø., Bentsen, M., Olivié, D., Toniazzo, T., Gjermundsen, A., Graff, L. S., Debernard, J. B., Gupta, A. K., He, Y.-C., Kirkevåg, A., Schwinger, J., Tjiputra, J., Aas, K. S., Bethke, I., Fan, Y., Griesfeller, J., Grini, A., Guo, C., Ilicak, M., Karset, I. H. H., Landgren, O., Liakka, J., Moseid, K. O., Nummelin, A., Spensberger, C., Tang, H., Zhang, Z., Heinze, C., Iversen, T. and Schulz, M. (2020). 'Overview of the Norwegian Earth System Model (NorESM2) and key climate response of CMIP6 DECK, historical, and scenario simulations'. In: *Geoscientific Model Development* 13.12, pp. 6165–6200. DOI: 10.5194/gmd-13-6165-2020.

Seneviratne, S. I., Nicholls, N., Easterling, D., Goodess, C. M., Kanae, S., Kossin, J., Luo, Y., Marengo, J., McInnes, K., Rahimi, M., Reichstein, M., Sorteberg, A., Vera, C. and Zhang, X. (2012). 'Changes in climate extremes and their impacts on the natural physical environment'. In: *Managing the risks of extreme events and disasters to advance climate change adaptation : Special Report of the Intergovernmental Panel on*

Climate Change. Cambridge: Cambridge University Press. Chap. 3, pp. 109–230. ISBN: 978-1-107-02506-6. DOI: 10.7916/d8-6nbt-s431.

Serinaldi, F. (2013). 'An uncertain journey around the tails of multivariate hydrological distributions'. In: *Water Resources Research* 49.10, pp. 6527–6547. DOI: 10.1002/wrcr.20531.

Serinaldi, F., Bárdossy, A. and Kilsby, C. G. (2015). 'Upper tail dependence in rainfall extremes: would we know it if we saw it?' In: *Stochastic Environmental Research and Risk Assessment* 29.4, pp. 1211–1233. DOI: 10.1007/s00477-014-0946-8.

Simonyan, K. and Zisserman, A. (2014). 'Very Deep Convolutional Networks for Large-Scale Image Recognition'. In: *arXiv preprint arXiv:1409.1556* 0.0, pp. 1–14. DOI: 10.48550/arXiv.1409.1556.

Solari, S., Egüen, M., Polo, M. J. and Losada, M. A. (2017). 'Peaks Over Threshold (POT): A methodology for automatic threshold estimation using goodness of fit p-value'. In: *Water Resources Research* 53.4, pp. 2833–2849. DOI: 10.1002/2016WR019426.

Stacke, T. and Hagemann, S. (2021). 'HydroPy (v1. 0): A new global hydrology model written in Python'. In: *Geoscientific Model Development* 14.12, pp. 7795–7816. DOI: 10.5194/gmd-14-7795-2021.

Sterl, A., van den Brink, H., de Vries, H., Haarsma, R. and van Meijgaard, E. (2009). 'An ensemble study of extreme storm surge related water levels in the North Sea in a changing climate'. In: *Ocean Science* 5.3, pp. 369–378. DOI: 10.5194/os-5-369-2009.

Stryhal, J. and Huth, R. (2019). 'Trends in winter circulation over the British Isles and central Europe in twenty-first century projections by 25 CMIP5 GCMs'. In: *Climate Dynamics* 52.1-2, pp. 1063–1075. DOI: 10.1007/s00382-018-4178-3.

Svensson, C. and Jones, D. A. (2002). 'Dependence between extreme sea surge, river flow and precipitation in eastern Britain'. In: *International Journal of Climatology* 22.10, pp. 1149–1168. DOI: 10.1002/joc.794.

Svensson, C. and Jones, D. A. (2004). 'Dependence between sea surge, river flow and precipitation in south and west Britain'. In: *Hydrology and Earth System Sciences* 8.5, pp. 973–992. DOI: 10.5194/hess-8-973-2004.

Swapna, P., Roxy, M. K., Aparna, K., Kulkarni, K., Prajeesh, A. G., Ashok, K., Krishnan, R., Moorthi, S., Kumar, A. and Goswami, B. N. (2015). 'The IITM Earth System Model: Transformation of a Seasonal Prediction Model to a Long-Term Climate Model'. In: *Bulletin of the American Meteorological Society* 96.8, pp. 1351–1367. DOI: 10.1175/BAMS-D-13-00276.1.

Swart, N. C., Cole, J. N. S., Kharin, V. V., Lazare, M., Scinocca, J. F., Gillett, N. P., Anstey, J., Arora, V., Christian, J. R., Hanna, S., Jiao, Y., Lee, W. G., Majaess, F., Saenko, O. A., Seiler, C., Seinen, C., Shao, A., Sigmond, M., Solheim, L., van Salzen, K., Yang, D. and Winter, B. (2019). 'The Canadian Earth System Model

version 5 (CanESM5.0.3)'. In: *Geoscientific Model Development* 12.11, pp. 4823–4873. DOI: 10.5194/gmd-12-4823-2019.

Tang, Y., Rumbold, S., Ellis, R., Kelley, D., Mulcahy, J., Sellar, A., Walton, J. and Jones, C. (2019). *MOHC UKESM1.0-LL model output prepared for CMIP6 CMIP*. DOI: 10.22033/ESGF/CMIP6.1569.

Tatebe, H., Ogura, T., Nitta, T., Komuro, Y., Ogochi, K., Takemura, T., Sudo, K., Sekiguchi, M., Abe, M., Saito, F., Chikira, M., Watanabe, S., Mori, M., Hirota, N., Kawatani, Y., Mochizuki, T., Yoshimura, K., Takata, K., O'ishi, R., Yamazaki, D., Suzuki, T., Kurogi, M., Kataoka, T., Watanabe, M. and Kimoto, M. (2019). 'Description and basic evaluation of simulated mean state, internal variability, and climate sensitivity in MIROC6'. In: *Geoscientific Model Development* 12.7, pp. 2727–2765. DOI: 10.5194/gmd-12-2727-2019.

Tebaldi, C., Debeire, K., Eyring, V., Fischer, E., Fyfe, J., Friedlingstein, P., Knutti, R., Lowe, J., O'Neill, B., Sanderson, B., van Vuuren, D., Riahi, K., Meinshausen, M., Nicholls, Z., Tokarska, K. B., Hurtt, G., Kriegler, E., Lamarque, J.-F., Meehl, G., Moss, R., Bauer, S. E., Boucher, O., Brovkin, V., Byun, Y.-H., Dix, M., Gualdi, S., Guo, H., John, J. G., Kharin, S., Kim, Y. H., Koshiro, T., Ma, L., Olivié, D., Panickal, S., Qiao, F., Rong, X., Rosenbloom, N., Schupfner, M., Séférian, R., Sellar, A., Semmler, T., Shi, X., Song, Z., Steger, C., Stouffer, R., Swart, N., Tachiiri, K., Tang, Q., Tatebe, H., Voldoire, A., Volodin, E., Wyser, K., Xin, X., Yang, S., Yu, Y. and Ziehn, T. (2021). 'Climate model projections from the Scenario Model Intercomparison Project (ScenarioMIP) of CMIP6'. In: *Earth System Dynamics* 12.1, pp. 253–293. DOI: 10.5194/esd-12-253-2021.

Thober, S., Kumar, R., Wanders, N., Marx, A., Pan, M., Rakovec, O., Samaniego, L., Sheffield, J., Wood, E. F. and Zink, M. (2018). 'Multi-model ensemble projections of European river floods and high flows at 1.5, 2, and 3 degrees global warming'. In: *Environmental Research Letters* 13.1, p. 014003. DOI: 10.1088/1748-9326/aa9e35.

Thornthwaite, C. W. (1948). 'An Approach toward a Rational Classification of Climate'. In: *Geographical Review* 38.1, pp. 55–94. DOI: 10.2307/210739.

Tilloy, A., Malamud, B. D., Winter, H. and Joly-Laugel, A. (2019). 'A review of quantification methodologies for multi-hazard interrelationships'. In: *Earth-Science Reviews* 196, p. 102881. DOI: 10.1016/j.earscirev.2019.102881.

Trigo, R. M., Ramos, C., Pereira, S. S., Ramos, A. M., Zêzere, J. L. and Liberato, M. L. R. (2016). 'The deadliest storm of the 20th century striking Portugal: Flood impacts and atmospheric circulation'. In: *Journal of Hydrology* 541, pp. 597–610. DOI: 10.1016/j.jhydrol.2015.10.036.

United Nations (2015). *PARIS AGREEMENT*. URL: https://treaties.un.org/doc/Treaties/2016/02/20160215%2006-03%20PM/Ch_XXVII-7-d.pdf (visited on 23rd November 2022).

United Nations Office for Disaster Risk Reduction (2020). *The human cost of disasters: an overview of the last 20 years (2000-2019)*. URL: https://www.undrr.org/

publication/human-cost-disasters-overview-last-20-years-2000-2019 (visited on 27th February 2024).

van den Hurk, B., van Meijgaard, E., de Valk, P., van Heeringen, K.-J. and Gooijer, J. (2015). 'Analysis of a compounding surge and precipitation event in the Netherlands'. In: *Environmental Research Letters* 10.3, p. 035001. DOI: 10.1088/1748-9326/10/3/035001.

Van Dingenen, R., Crippa, M., Anssens-Maenhout, G., Guizzardi, D. and Dentener, F. (2018). 'Global trends of methane emissions and their impacts on ozone concentrations'. In: *JRC Science for Policy Report*. DOI: 10.2760/73788.

Van Vuuren, D. P., Stehfest, E., den Elzen, M. G. J., Kram, T., van Vliet, J., Deetman, S., Isaac, M., Klein Goldewijk, K., Hof, A., Mendoza Beltran, A., Oostenrijk, R. and van Ruijven, B. (2011a). 'RCP2.6: exploring the possibility to keep global mean temperature increase below 2°C'. In: *Climatic Change* 109.1, pp. 95–116. DOI: 10.1007/s10584-011-0152-3.

Van Vuuren, D. P., Edmonds, J., Kainuma, M., Riahi, K., Thomson, A., Hibbard, K., Hurtt, G. C., Kram, T., Krey, V., Lamarque, J.-F., Masui, T., Meinshausen, M., Nakicenovic, N., Smith, S. J. and Rose, S. K. (2011b). 'The representative concentration pathways: an overview'. In: *Climatic Change* 109.1, pp. 5–31. DOI: 10.1007/s10584-011-0148-z.

Visser-Quinn, A., Beevers, L., Collet, L., Formetta, G., Smith, K., Wanders, N., Thober, S., Pan, M. and Kumar, R. (2019). 'Spatio-temporal analysis of compound hydro-hazard extremes across the UK'. In: *Advances in Water Resources* 130, pp. 77–90. DOI: 10.1016/j.advwatres.2019.05.019.

Voldoire, A., Saint-Martin, D., Sénési, S., Decharme, B., Alias, A., Chevallier, M., Colin, J., Guérémy, J.-F., Michou, M., Moine, M.-P., Nabat, P., Roehrig, R., Mélia, D. S. y., Séférian, R., Valcke, S., Beau, I., Belamari, S., Berthet, S., Cassou, C., Cattiaux, J., Deshayes, J., Douville, H., Ethé, C., Franchistéguy, L., Geoffroy, O., Lévy, C., Madec, G., Meurdesoif, Y., Msadek, R., Ribes, A., Sanchez-Gomez, E., Terray, L. and Waldman, R. (2019). 'Evaluation of CMIP6 DECK Experiments With CNRM-CM6-1'. In: *Journal of Advances in Modeling Earth Systems* 11.7, pp. 2177–2213. DOI: 10.1029/2019MS001683.

Volodin, E. M., Mortikov, E. V., Kostrykin, S. V., Galin, V. Y., Lykossov, V. N., Gritsun, A. S., Diansky, N. A., Gusev, A. V., Iakovlev, N. G., Shestakova, A. A. and Emelina, S. V. (2018). 'Simulation of the modern climate using the INM-CM48 climate model'. In: *Russian Journal of Numerical Analysis and Mathematical Modelling* 33.6, pp. 367–374. DOI: 10.1515/rnam-2018-0032.

von Storch, H., Langenberg, H. and Feser, F. (2000). 'A Spectral Nudging Technique for Dynamical Downscaling Purposes'. In: *Monthly Weather Review* 128.10, pp. 3664–3673. DOI: 10.1175/1520-0493(2000)128<3664:ASNTFD>2.0.CO;2.

Vousdoukas, M. I., Mentaschi, L., Voukouvalas, E., Bianchi, A., Dottori, F. and Feyen, L. (2018a). 'Climatic and socioeconomic controls of future coastal flood

risk in Europe'. In: *Nature Climate Change* 8.9, pp. 776–780. DOI: 10.1038/s41558-018-0260-4.

Vousdoukas, M. I., Mentaschi, L., Voukouvalas, E., Verlaan, M., Jevrejeva, S., Jackson, L. P. and Feyen, L. (2018b). 'Global probabilistic projections of extreme sea levels show intensification of coastal flood hazard'. In: *Nature Communications* 9.1, p. 2360. DOI: 10.1038/s41467-018-04692-w.

Vousdoukas, M. I., Mentaschi, L., Mongelli, I., Ciscar Martinez, J. C., Hinkel, J., Ward, P. j., Gosling, S. and Feyen, L. (2020a). 'Adapting to rising coastal flood risk in the EU under climate change'. In: *Publications Office of the the European Union: Luxembourg*. DOI: 10.2760/456870.

Vousdoukas, M. I., Mentaschi, L., Hinkel, J., Ward, P. J., Mongelli, I., Ciscar, J.-C. and Feyen, L. (2020b). 'Economic motivation for raising coastal flood defenses in Europe'. In: *Nature Communications* 11.1, p. 2119. DOI: 10.1038/s41467-020-15665-3.

Wahl, T., Jain, S., Bender, J., Meyers, S. D. and Luther, M. E. (2015). 'Increasing risk of compound flooding from storm surge and rainfall for major US cities'. In: *Nature Climate Change* 5.12, pp. 1093–1097. DOI: 10.1038/nclimate2736.

Wapler, K. and James, P. (2015). 'Thunderstorm occurrence and characteristics in Central Europe under different synoptic conditions'. In: *Atmospheric Research* 158-159, pp. 231–244. DOI: 10.1016/j.atmosres.2014.07.011.

Ward, P. J., Couasnon, A. A. O., Eilander, D., Haigh, I. D., Hendry, A., Muis, S., Veldkamp, T. I. E., Winsemius, H. C. and Wahl, T. (2018). 'Dependence between high sea-level and high river discharge increases flood hazard in global deltas and estuaries'. In: *Environmental Research Letters* 13.8, p. 084012. DOI: 10.1088/1748-9326/aad400.

Ward, P. J., Blauhut, V., Bloemendaal, N., Daniell, J. E., de Ruiter, M. C., Duncan, M. J., Emberson, R., Jenkins, S. F., Kirschbaum, D., Kunz, M., Mohr, S., Muis, S., Riddell, G. A., Schäfer, A., Stanley, T., Veldkamp, T. I. E. and Winsemius, H. C. (2020). 'Review article: Natural hazard risk assessments at the global scale'. In: *Natural Hazards and Earth System Sciences* 20.4, pp. 1069–1096. DOI: 10.5194/nhess-20-1069-2020.

Weisse, R., Bisling, P., Gaslikova, L., Geyer, B., Groll, N., Hortamani, M., Matthias, V., Maneke, M., Meinke, I., Meyer, E. M. I., Schwichtenberg, F., Stempinski, F., Wiese, F. and Wöckner-Kluwe, K. (2015). 'Climate services for marine applications in Europe'. In: *Earth Perspectives* 2.1, p. 3. DOI: 10.1186/s40322-015-0029-0.

Weisse, R., Dailidienė, I., Hünicke, B., Kahma, K., Madsen, K., Omstedt, A., Parnell, K., Schöne, T., Soomere, T., Zhang, W. and Zorita, E. (2021). 'Sea level dynamics and coastal erosion in the Baltic Sea region'. In: *Earth System Dynamics* 12.3, pp. 871–898. DOI: 10.5194/esd-12-871-2021.

Weisse, R., Gaslikova, L., Hagemann, S., Heinrich, P., Berkenbrink, C., Chen, J. J., Bormann, H., Kebschull, J., Ley, A., Massmann, G., Greskowiak, J., Thissen, L., Karrasch, L., Schoppe, A., Ratter, B. and Wessels, A. (2024). 'Zusammenwirken

von Naturgefahren im Klimawandel ist für die Nordseeküste zunehmend eine Herausforderung'. In: *Wasser und Abfall* 26.5, pp. 38–45. DOI: 10.1007/s35152-024-1854-y.

Wolf, J. (2009). 'Coastal flooding: impacts of coupled wave–surge–tide models'. In: *Natural Hazards* 49.2, pp. 241–260. DOI: 10.1007/s11069-008-9316-5.

Wong, P. P., Losada, I. J., Gattuso, J.-P., Hinkel, J., Khattabi, A., McInnes, K. L., Saito, Y. and Sallenger, A. (2014). 'Coastal systems and low-lying areas. In: Climate Change 2014: Impacts, Adaptation, and Vulnerability. Part A: Global and Sectoral Aspects. Contribution of Working Group II to the Fifth Assessment Report of the Intergovernmental Panel on Climate Change'. In: *Climate Change*, pp. 361–410. DOI: 10.1017/CBO9781107415379.010.

Wu, T., Lu, Y., Fang, Y., Xin, X., Li, L., Li, W., Jie, W., Zhang, J., Liu, Y., Zhang, L., Zhang, F., Zhang, Y., Wu, F., Li, J., Chu, M., Wang, Z., Shi, X., Liu, X., Wei, M., Huang, A., Zhang, Y. and Liu, X. (2019). 'The Beijing Climate Center Climate System Model (BCC-CSM): the main progress from CMIP5 to CMIP6'. In: *Geoscientific Model Development* 12.4, pp. 1573–1600. DOI: 10.5194/gmd-12-1573-2019.

Xu, H., Tian, Z., Sun, L., Ye, Q., Ragno, E., Bricker, J., Mao, G., Tan, J., Wang, J., Ke, Q., Wang, S. and Toumi, R. (2022). 'Compound flood impact of water level and rainfall during tropical cyclone periods in a coastal city: the case of Shanghai'. In: *Natural Hazards and Earth System Sciences* 22.7, pp. 2347–2358. DOI: 10.5194/nhess-22-2347-2022.

Xu, K., Wang, C. and Bin, L. (2023). 'Compound flood models in coastal areas: a review of methods and uncertainty analysis'. In: *Natural Hazards* 116.1, pp. 469–496. DOI: 10.1007/s11069-022-05683-3.

Yamashita, R., Nishio, M., Do, R. K. G. and Togashi, K. (2018). 'Convolutional neural networks: an overview and application in radiology'. In: *Insights into Imaging* 9, pp. 611–629. DOI: 10.1007/s13244-018-0639-9.

Yu, J., Wang, Z., Vasudevan, V., Yeung, L., Seyedhosseini, M. and Wu, Y. (2022). 'CoCa: Contrastive Captioners are Image-Text Foundation Models'. In: *arXiv preprint arXiv:2205.01917* 0.0, pp. 1–19. DOI: 10.48550/arXiv.2205.01917.

Yukimoto, S., Kawai, H., Koshiro, T., Oshima, N., Yoshida, K., Urakawa, S., Tsujino, H., Deushi, M., Tanaka, T., Hosaka, M., Yabu, S., Yoshimura, H., Shindo, E., Mizuta, R., Obata, A., Adachi, Y. and Ishii, M. (2019). 'The Meteorological Research Institute Earth System Model Version 2.0, MRI-ESM2.0: Description and Basic Evaluation of the Physical Component'. In: *Journal of the Meteorological Society of Japan. Ser. II* 97.5, pp. 931–965. DOI: 10.2151/jmsj.2019-051.

Zappa, G., Shaffrey, L. C., Hodges, K. I., Sansom, P. G. and Stephenson, D. B. (2013). 'A Multimodel Assessment of Future Projections of North Atlantic and European Extratropical Cyclones in the CMIP5 Climate Models'. In: *Journal of Climate* 26.16, pp. 5846–5862. DOI: 10.1175/JCLI-D-12-00573.1.

Zhang, X., Hegerl, G., Seneviratne, S., Stewart, R., Zwiers, F. and Alexander, L. (2014). 'WCRP Grand Challenge: Understanding and Predicting Weather and

Climate Extremes'. In: *WCRP White Paper*. URL: https://clivar.org/sites/default/files/documents/WCRP_extremes_July_10.pdf (visited on 15th March 2024).

Zheng, F., Westra, S., Leonard, M. and Sisson, S. A. (2014). 'Modeling dependence between extreme rainfall and storm surge to estimate coastal flooding risk'. In: *Water Resources Research* 50.3, pp. 2050–2071. DOI: 10.1002/2013WR014616.

Zheng, F., Westra, S. and Sisson, S. A. (2013). 'Quantifying the dependence between extreme rainfall and storm surge in the coastal zone'. In: *Journal of Hydrology* 505, pp. 172–187. ISSN: 0022-1694. DOI: 10.1016/j.jhydrol.2013.09.054.

Ziehn, T., Chamberlain, M. A., Law, R. M., Lenton, A., Bodman, R. W., Dix, M., Stevens, L., Wang, Y.-P. and Srbinovsky, J. (2020). 'The Australian Earth System Model: ACCESS-ESM1.5'. In: *Journal of Southern Hemisphere Earth Systems Science* 70.1, pp. 193–214. DOI: 10.1071/ES19035.

Zscheischler, J. and Seneviratne, S. I. (2017). 'Dependence of drivers affects risks associated with compound events'. In: *Science Advances* 3.6, e1700263. DOI: 10.1126/sciadv.1700263.

Zscheischler, J., Westra, S., van den Hurk, B. J. J. M., Seneviratne, S. I., Ward, P. J., Pitman, A., AghaKouchak, A., Bresch, D. N., Leonard, M., Wahl, T. and Zhang, X. (2018). 'Future climate risk from compound events'. In: *Nature Climate Change* 8.6, pp. 469–477. DOI: 10.1038/s41558-018-0156-3.

Zscheischler, J., Martius, O., Westra, S., Bevacqua, E., Raymond, C., Horton, R. M., van den Hurk, B. J. J. M., AghaKouchak, A., Jézéquel, A., Mahecha, M. D., Maraun, D., Ramos, A. M., Ridder, N. N., Thiery, W. and Vignotto, E. (2020). 'A typology of compound weather and climate events'. In: *Nature Reviews Earth & Environment* 1.7, pp. 333–347. DOI: 10.1038/s43017-020-0060-z.

EIDESSTATTLICHE VERSICHERUNG

Eidesstattliche Versicherung
Declaration on Oath

Hiermit erkläre ich an Eides statt, dass ich die vorliegende Dissertationsschrift selbst verfasst und keine anderen als die angegebenen Quellen und Hilfsmittel benutzt habe.

I hereby declare upon oath that I have written the present dissertation independently and have not used further resources and aids than those stated in the dissertation.

Geesthacht, 30th May 2024

Philipp Maximilian Heinrich